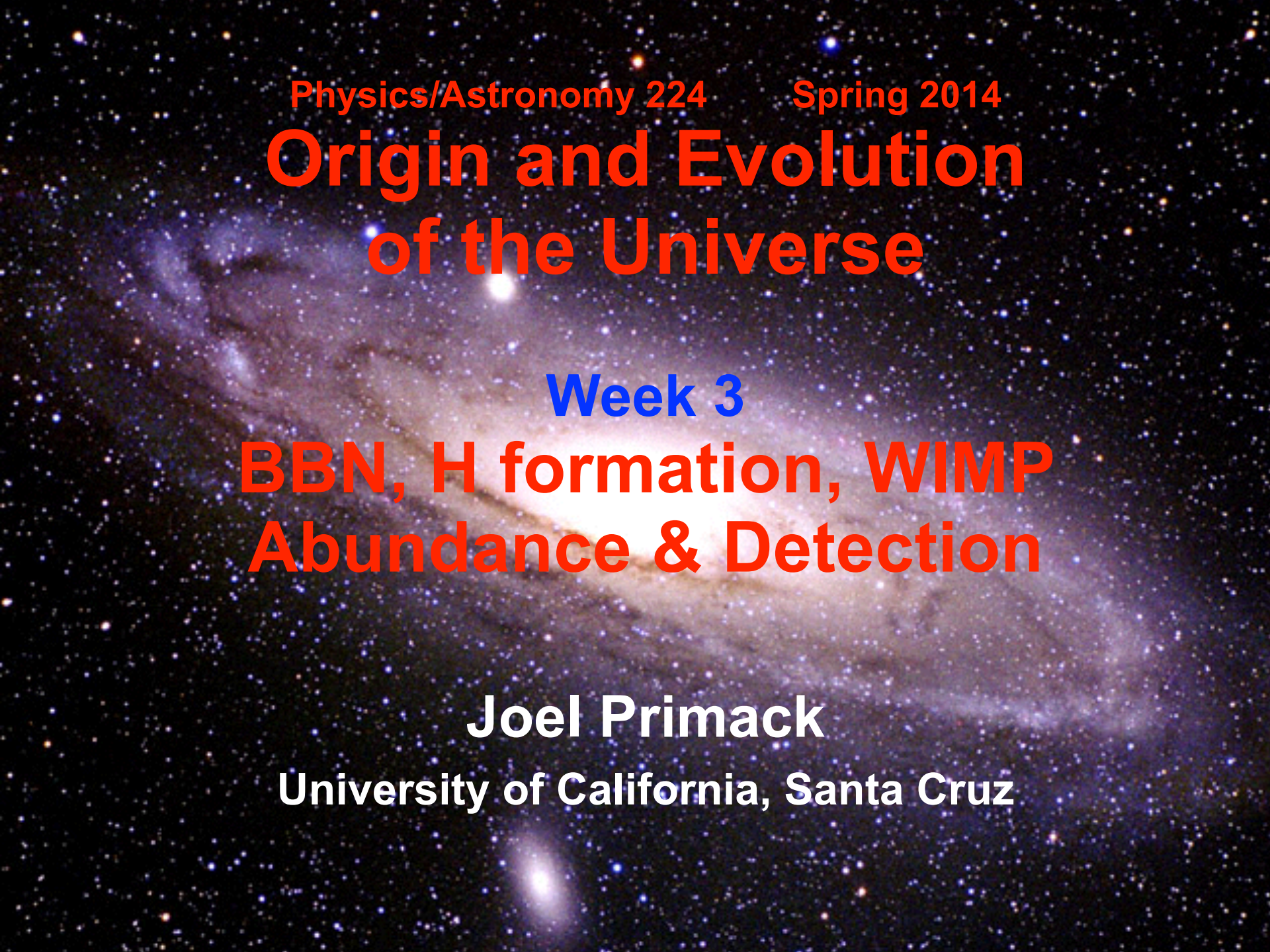

Physics/Astronomy 224 Spring 2014

Origin and Evolution of the Universe

Week 3

BBN, H formation, WIMP Abundance & Detection

Joel Primack

University of California, Santa Cruz

Big Bang Nucleosynthesis

BBN was conceived by Gamow in 1946 as an explanation for the formation of all the elements, but the absence of any stable nuclei with A=5,8 makes it impossible for BBN to proceed past Li. The formation of carbon and heavier elements occurs instead through the triple-α process in the centers of red giants (Burbidge[2], Fowler, & Hoyle 57). At the BBN baryon density of $2\times10^{-29}\ \Omega_b\ h^2\ (T/T_0)^3$ g cm^{-3} $\approx 2\times10^{-5}$ g cm^{-3}, the probability of the triple-α process is negligible even though $T \approx 10^9$K.

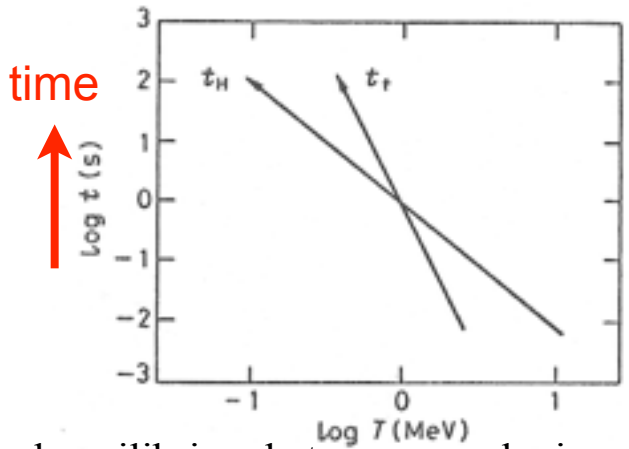

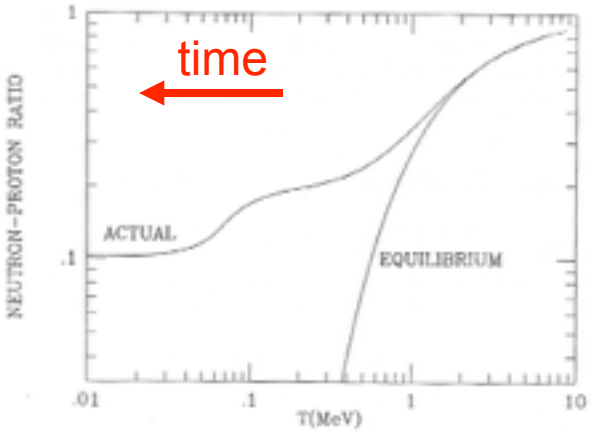

Kolb & Turner

Thermal equilibrium between n and p is maintained by weak interactions, which keeps $n/p = \exp(-Q/T)$ (where $Q = m_n - m_p = 1.293$ MeV) until about $t \approx 1$ s. But because the neutrino mean free time $t_\nu^{-1} \approx \sigma_\nu\, n_{e\pm} \approx (G_F T)^2 (T^3)$ is increasing as $t_\nu \propto T^{-5}$ (here the Fermi constant $G_F \approx 10^{-5}$ GeV^{-2}), while the horizon size is increasing only as $t_H \approx (G\rho)^{-1/2} \approx M_{Pl}\, T^{-2}$, these interactions freeze out when T drops below about 0.8 MeV. This leaves $n/(p+n) \approx 0.14$. The neutrons then decay with a mean lifetime 887 ± 2 s until they are mostly fused into D and then ^{4}He. The higher the baryon density, the higher the final abundance of ^{4}He and the lower the abundance of D that survives this fusion process. Since D/H is so sensitive to baryon density, David Schramm called deuterium the "baryometer." He and his colleagues also pointed out that since the horizon size increases more slowly with T^{-1} the larger the number of light neutrino species N_ν contributing to the energy density ρ, BBN predicted that $N_\nu \approx 3$ before N_ν was measured at accelerators by measuring the width of the Z^0 (Particle Data Group: $N_\nu = 2.984\pm0.008$).

The Early Universe

In the early universe after Cosmic Inflation and until about 45,000 years, the cosmic density is dominated by relativistic particles, initially mostly massive particles having energies much greater than their masses, then just e^+, e^-, neutrinos and photons, and after a few seconds when the e+ annihilate with all but a few e^-, just the neutrinos and photons. It is therefore essential to review the densities of such particles. (See Perkins Section 5.8.)

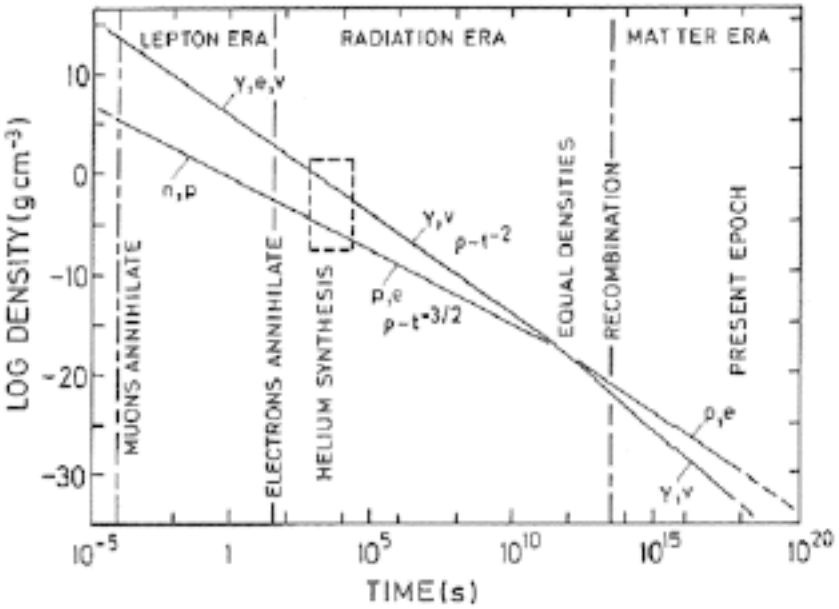

In the following slides, I summarize first the number and energy densities for the photons, and then more generally for fermions and bosons. The effective number of degrees of freedom $g^*(z)$ allows us to account for all the relativistic particles. There is an abrupt change in $g^*(z)$ at the quark-hadron phase transition at ~200 MeV. Above this temperature, quarks and gluons are free, representing a lot more possible states than just those available below ~200 MeV. Below this temperature there is an approximate time-temperature relation

$$T \approx 1 \text{ MeV } (t/\text{sec})^{-1/2} \ .$$

Thus T = 100 MeV corresponds roughly to $t \approx 10^{-4}$ s, and T = 100 keV to $t \approx 100$ s. "Freeze-out" is a key concept, describing going out of equilibrium when the relevant mean free path exceeds the Hubble length c/H.

Particles and Radiation in the Early Universe

The Friedmann equation says that $H^2 = (8\pi G/3)\,\rho$ in the early universe, where the Λ term is negligible and $\rho \propto g^* T^4$, so

$$H(t) = \left[\frac{4g^*\pi^3 G}{45\hbar^3 c^5}\right]^{1/2} (kT)^2$$

$$= \frac{\left(4\pi^3\, g^*/45\right)^{1/2}}{M_{PL}\hbar c^2} \times (kT)^2$$

$$= 1.66 g^{*1/2} \frac{(kT)^2}{M_{PL}\hbar c^2}$$

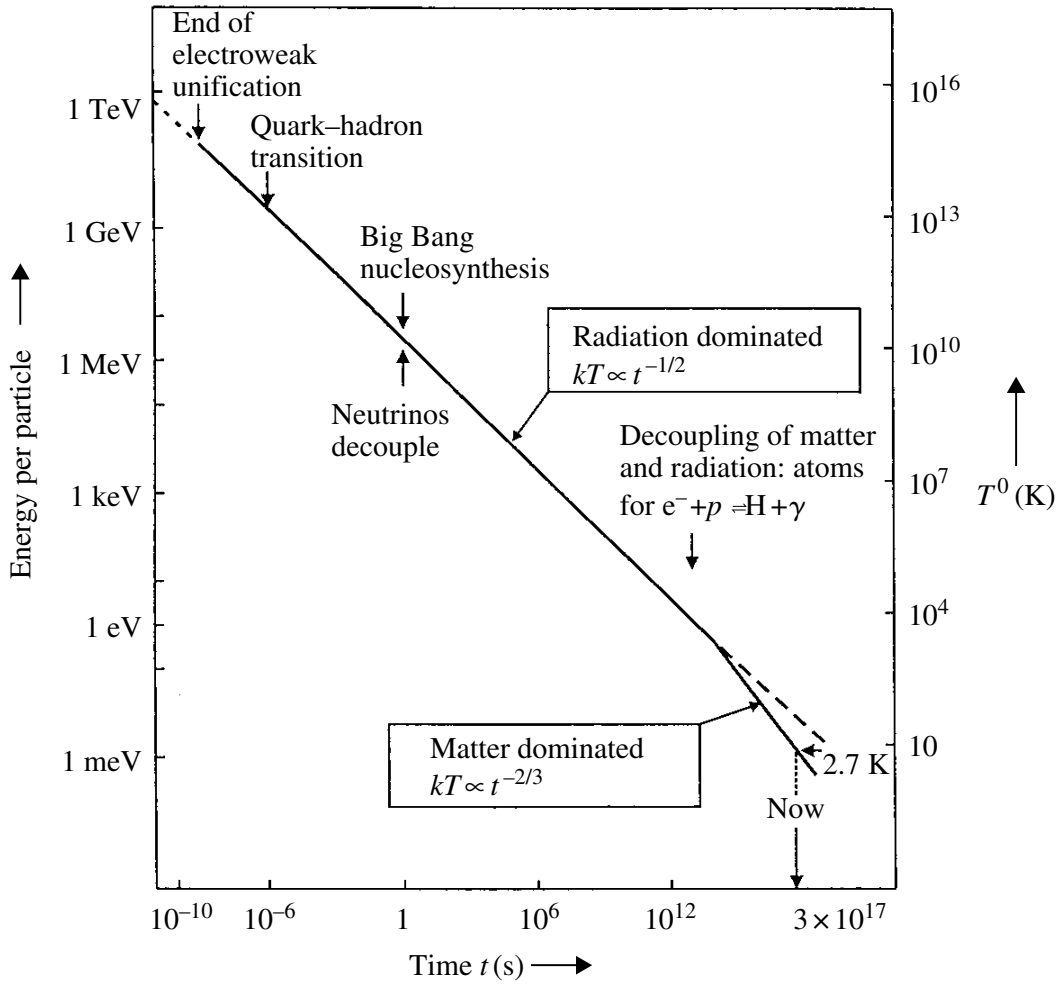

Here G was replaced by the Planck mass $M_{PL} = \left(\frac{\hbar c}{G}\right)^{1/2} = 1.2 \times 10^{19}\ \frac{\text{GeV}}{c^2}$

Particles and Radiation in the Early Universe

The Friedmann equation says that $H^2 = (8\pi G/3)\,\rho$ in the early universe, where the Λ term is negligible and $\rho \propto g^* T^4$, so

$$H(t) = \left[\frac{4g^*\pi^3 G}{45\hbar^3 c^5}\right]^{1/2} (kT)^2$$

$$= \frac{\left(4\pi^3 g^*/45\right)^{1/2}}{M_{PL}\hbar c^2} \times (kT)^2$$

$$= 1.66 g^{*1/2} \frac{(kT)^2}{M_{PL}\hbar c^2}$$

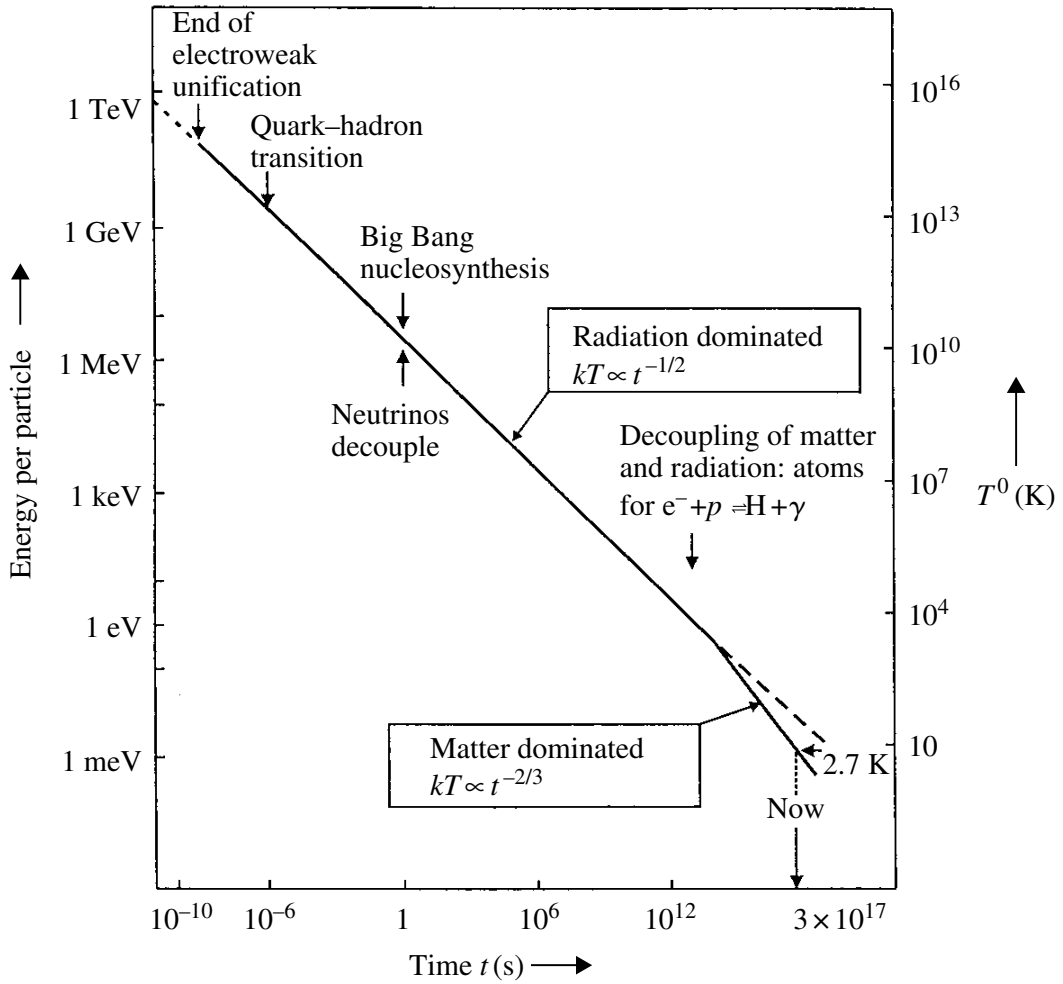

Here G was replaced by the Planck mass $M_{PL} = \left(\frac{\hbar c}{G}\right)^{1/2} = 1.2 \times 10^{19}\ \frac{\text{GeV}}{c^2}$

Note that in the radiation-dominated early universe,

$H(t) = 1/2t$ or $t = 1/2H(t)$

Cosmic Radiation: Photons

Photon energy density vs. time: $$\rho_r c^2 = \left(\frac{3c^2 / 32\pi G}{t^2} \right)$$

Photon energy density vs. Temperature: $$\rho_r c^2 = \frac{4\sigma T^4}{c} = \pi^4 (kT)^4 \left(\frac{g_\gamma / 2}{15\pi^2 \hbar^3 c^3} \right)$$

Early universe Temperature (in MeV) vs. time (in seconds): $$kT = \frac{\left[\left(45\hbar^3 c^5 / 16\pi^3 \mathrm{G} g_\gamma \right)^{1/4} \right]}{t^{1/2}} = 1.307 \ \frac{\mathrm{MeV}}{t^{1/2}}$$

Early universe Temperature (in Kelvin) vs. time (in seconds): $$T = 1.52 \times 10^{10} \frac{K}{t^{1/2}}.$$

Photon (Bose-Einstein) energy distribution: $$N(p)\mathrm{d}p = \frac{p^2 \mathrm{d}p}{\pi^2 \hbar^3 \left\{ \exp\left(E / kT\right) - 1 \right\}}$$

Photon number density today: $$N_\gamma = \left(\frac{2.404}{\pi^2} \right) \left(\frac{kT}{\hbar c} \right)^3 = 411 \left(\frac{T}{2.725} \right)^3 \ \mathrm{cm}^{-3}$$

$$N_\gamma = \frac{2\zeta(3)}{\pi^2} T^3 \ \text{with} \ 2\zeta(3)/\pi^2 \simeq 0.2436.$$

Photon energy density today: $\rho_r c^2 = 0.261 \ \mathrm{MeV\,m^{-3}}$ or $\Omega_\gamma(0) = 4.84 \times 10^{-5}$

Statistical Thermodynamics Integrals

The number density and mass-energy density of species i with mass m_i are given by

$$n_i = \frac{g_i}{2\pi^2}\left(\frac{kT_i}{\hbar c}\right)^3 I_i^{11}(\pm) \ , \quad \rho_i = \frac{g_i kT_i}{2\pi^2 c^2}\left(\frac{kT_i}{\hbar c}\right)^3 I_i^{21}(\pm) \ .$$

Here $\pm$ means to choose $+$ for Fermi-Dirac and $-$ for Bose-Einstein statistics, g_i is the number of spin states, and I_i^{mn} is defined by

$$I_i^{mn} \equiv \int_{\theta_i}^{\infty} \frac{x^m (x^2 - \theta_i^2)^{n/2}}{(e^x \pm 1)} dx \ ,$$

where $\theta_i \equiv kT_i/m_i c^2$. There are two important limiting cases,

Extreme Relativistic ($\theta_i >> 1$), for which

+ Fermi-Dirac

$$I^{11}(+) = \frac{3}{2}\zeta(3) = 1.803 \ , \quad I^{21}(+) = \frac{7\pi^4}{120}$$

− Bose-Einstein

$$I^{11}(-) = 2\zeta(3) = \frac{4}{3} I^{11}(+) \ , \quad I^{21}(-) = \frac{\pi^4}{15} = \frac{8}{7} I^{21}(+)$$

and **Non-Relativistic** ($\theta_i << 1$), for which

$$n_i = \frac{\rho_i}{m_i} = \frac{g_i}{(2\pi)^{3/2}}\left(\frac{kT_i}{\hbar c}\right)^3 \theta_i^{-3/2} e^{-\theta_i} \ .$$

Note that the Riemann zeta function $\zeta(3) = 1.2020569...$, and for positive integer n

$$\zeta(n) = \sum_{k=1}^{\infty} \frac{1}{k^n} = \prod_{\text{primes } p} \frac{1}{1 - p^{-n}} \ .$$

Neutrinos in the Early Universe

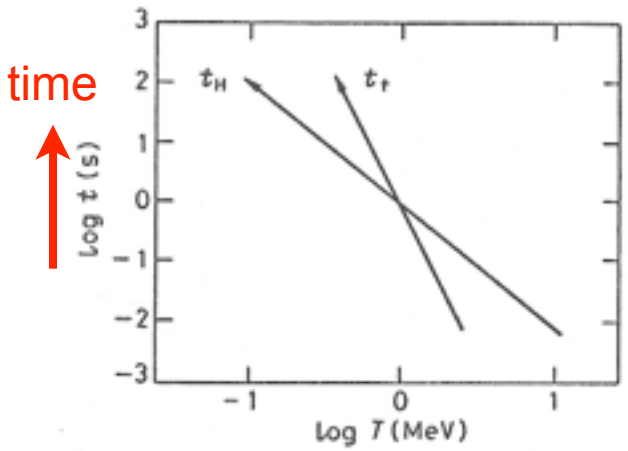

As we discussed, neutrino decoupling occurs at T ~ 1 MeV. After decoupling, the neutrino phase space distribution is

$f_\nu = [1+\exp(p_\nu c/T_\nu)]^{-1}$ (note: $\neq [1+\exp(E_\nu/T_\nu)]$ for NR neutrinos)

After e+e- annihilation, $T_\nu=(4/11)^{1/3}T_\gamma = 1.9K$. Proof :

Number densities of primordial particles

FermiDirac/BoseEinstein factor

$n_\gamma(T) = 2\,\zeta(3)\,\pi^{-2}\,T^3 = 400\ cm^{-3}\ (T/2.7K)^3$, $n_\nu(T) = (3/4)\ n_\gamma(T)$ including antineutrinos

Conservation of entropy s_I of interacting particles per comoving volume

$s_I = g_I(T)\ N_\gamma(T)$ = constant, where $N_\gamma = n_\gamma V$; we only include neutrinos for T>1 MeV.

Thus for T>1 MeV, $g_I = 2 + 4(7/8) + 6(7/8) = 43/4$ for γ, e+e-, and the three ν species, while for T< 1 MeV, $g_I = 2 + 4(7/8) = 11/2$. At e+e- annihilation, below about T=0.5 Mev, g_I drops to 2, so that $2N_{\gamma 0} = g_I(T<1\ MeV)\ N_\gamma(T<1\ MeV) = (11/2)\ N_\gamma(T<1\ MeV) = (11/2)(4/3)\ N_\nu(T<1\ MeV)$. Thus $n_{\nu 0} = (3/4)(4/11)\ n_{\gamma 0} = 109\ cm^{-3}\ (T/2.7K)^3$ for each of the three neutrino species, and $T_\nu = (4/11)^{1/3}\ T = 0.714\ T$

Particles and Radiation in the Early Universe

Fermi-Dirac energy distribution:

$$N(p)\mathrm{d}p = \frac{p^2\mathrm{d}p}{\pi^2\hbar^3\left\{\exp\left(E/kT\right)+1\right\}}\left(\frac{g_f}{2}\right)$$

Here $E^2=p^2+m^2$, and
g_f = number of spin states

Using these integrals one can find the energy and entropy densities for B-E and F-D distributions:

$$\mathrm{BE}: \quad \int \frac{x^3\mathrm{d}x}{(e^x-1)} = \frac{\pi^4}{15}; \quad \int \frac{x^2\mathrm{d}x}{(e^x-1)} = 2.404$$

$$\mathrm{FD}: \quad \int \frac{x^3\mathrm{d}x}{(e^x+1)} = \frac{7}{8}\times\frac{\pi^4}{15}; \quad \int \frac{x^2\mathrm{d}x}{(e^x+1)} = \frac{3}{4}\times 2.404$$

For the F-D distribution, the result for highly relativistic particles ($kT >> m$) is

$$\rho_f c^2 = \left(\frac{7}{8}\right)\pi^4\,(kT)^4\,\frac{(g_f/2)}{15\pi^2\hbar^3c^3}$$

For the B-E distribution, the result for photons ($g_\gamma = 2$) is

$$\rho_r c^2 = \frac{4\sigma T^4}{c} = \pi^4\,(kT)^4\left(\frac{g_\gamma/2}{15\pi^2\hbar^3c^3}\right)$$

For a mixture of highly relativistic fermions and bosons, replace g_γ by g^* including bosons and fermions

$$g^* = \sum g_b + \left(\frac{7}{8}\right)\sum g_f$$

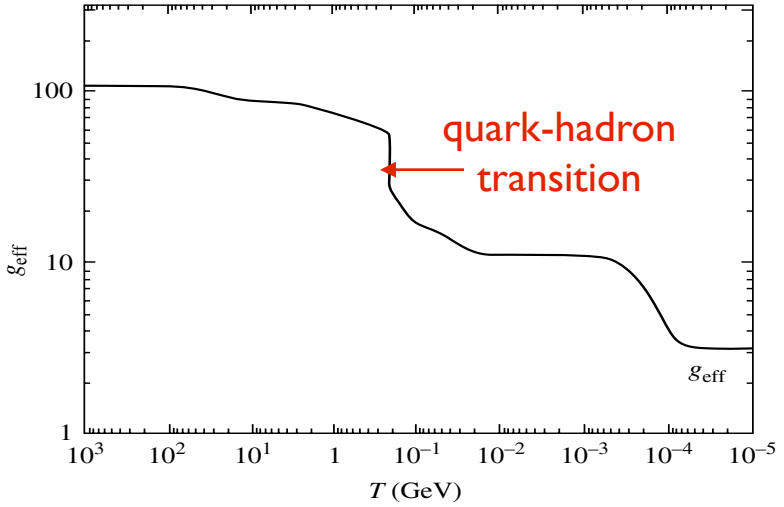

Boltzmann Equation

$$a^{-3}\frac{d\left(n_1 a^3\right)}{dt} = \int \frac{d^3p_1}{(2\pi)^3 2E_1}\int \frac{d^3p_2}{(2\pi)^3 2E_2}\int \frac{d^3p_3}{(2\pi)^3 2E_3}\int \frac{d^3p_4}{(2\pi)^3 2E_4}$$

Dodelson (3.1)

$$\times\,(2\pi)^4\delta^3(p_1+p_2-p_3-p_4)\delta(E_1+E_2-E_3-E_4)\,|\mathcal{M}|^2$$

$$\times\,\{f_3 f_4[1\pm f_1][1\pm f_2]-f_1 f_2[1\pm f_3][1\pm f_4]\}\,.$$

+ bosons
- fermions

In the absence of interactions (rhs=0) n_1 falls as a^{-3}

We will typically be interested in T>> E-μ (where μ is the chemical potential). In this limit, the exponential in the Fermi-Dirac or Bose-Einstein distributions is much larger than the ±1 in the denominator, so that

$$f(E)\rightarrow e^{\mu/T}e^{-E/T}$$

and the last line of the Boltzmann equation above simplifies to

$$f_3 f_4[1\pm f_1][1\pm f_2]-f_1 f_2[1\pm f_3][1\pm f_4]$$

$$\rightarrow\quad e^{-(E_1+E_2)/T}\left\{e^{(\mu_3+\mu_4)/T}-e^{(\mu_1+\mu_2)/T}\right\}.$$

The number densities are given by $n_i = g_i e^{\mu_i/T}\int\frac{d^3p}{(2\pi)^3}e^{-E_i/T}$. For our applications, i's are

Table 3.1. Reactions in This Chapter: $1+2\leftrightarrow 3+4$

	1	2	3	4
Neutron-Proton Ratio	n	ν_e or e^+	p	e^- or $\bar{\nu}_e$
Recombination	e	p	H	γ
Dark Matter Production	X	X	l	l

The equilibrium number densities are given by

$$n_i^{(0)} \equiv g_i \int \frac{d^3p}{(2\pi)^3} e^{-E_i/T} = \begin{cases} g_i \left(\frac{m_i T}{2\pi}\right)^{3/2} e^{-m_i/T} & m_i \gg T \\ g_i \frac{T^3}{\pi^2} & m_i \ll T \end{cases} . \tag{3.6}$$

With this defintion, $e^{\mu_i/T}$ can be rewritten as $n_i/n_i^{(0)}$, so the last line of Eq. (3.1) is equal to

$$e^{-(E_1+E_2)/T} \left\{ \frac{n_3 n_4}{n_3^{(0)} n_4^{(0)}} - \frac{n_1 n_2}{n_1^{(0)} n_2^{(0)}} \right\} . \tag{3.7}$$

With these approximations the Boltzmann equation now simplifies enormously. Define the thermally averaged cross section as

$$\langle \sigma v \rangle \equiv \frac{1}{n_1^{(0)} n_2^{(0)}} \int \frac{d^3p_1}{(2\pi)^3 2E_1} \int \frac{d^3p_2}{(2\pi)^3 2E_2} \int \frac{d^3p_3}{(2\pi)^3 2E_3} \int \frac{d^3p_4}{(2\pi)^3 2E_4} e^{-(E_1+E_2)/T}$$

$$\times (2\pi)^4 \delta^3(p_1 + p_2 - p_3 - p_4) \delta(E_1 + E_2 - E_3 - E_4) \left|\mathcal{M}\right|^2 . \tag{3.8}$$

Then, the Boltzmann equation becomes

$$a^{-3} \frac{d\left(n_1 a^3\right)}{dt} = n_1^{(0)} n_2^{(0)} \langle \sigma v \rangle \left\{ \frac{n_3 n_4}{n_3^{(0)} n_4^{(0)}} - \frac{n_1 n_2}{n_1^{(0)} n_2^{(0)}} \right\} . \tag{3.9}$$

If the reaction rate $n_2 \langle \sigma v \rangle$ is much smaller than the expansion rate (~ H), then the {} on the rhs must vanish. This is called *chemical equilibrium* in the context of the early universe, *nuclear statistical equilibrium* (NSE) in the context of Big Bang nucleosynthesis, and the *Saha equation* when discussing recombination of electrons and protons to form neutral hydrogen.

As the temperature of the universe cools to 1 MeV, the cosmic plasma consists of:

- **Relativistic particles in equilibrium: photons, electrons and positrons.** These are kept in close contact with each other by electromagnetic interactions such as $e^+e^- \leftrightarrow \gamma\gamma$. Besides a small difference due to fermion/boson statistics, these all have the same abundances.
- **Decoupled relativistic particles: neutrinos.** At temperatures a little above 1 MeV, the rate for processes such as $\nu e \leftrightarrow \nu e$ which keep neutrinos coupled to the rest of the plasma drops beneath the expansion rate. Neutrinos therefore share the same temperature as the other relativistic particles, and hence are roughly as abundant, but they do not couple to them.
- **Nonrelativistic particles: baryons.** If there had been no asymmetry in the initial number of baryons and anti-baryons, then both would be completely depleted by 1 MeV. However, such an asymmetry did exist: $(n_b - n_{\bar{b}})/s \sim 10^{-10}$ initially,[1] and this ratio remains constant throughout the expansion. By the time the temperature is of order 1 MeV, all anti-baryons have annihilated away (Exercise 12) so

$$\eta_b \equiv \frac{n_b}{n_\gamma} = 5.5 \times 10^{-10} \left(\frac{\Omega_b h^2}{0.020}\right). \tag{3.11}$$

There are thus many fewer baryons than relativistic particles when $T \sim$ MeV.

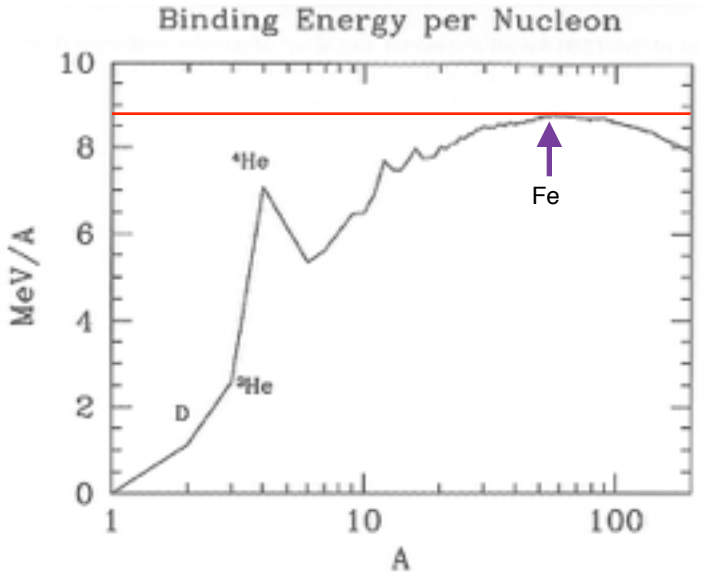

Figure 3.1. Binding energy of nuclei as a function of mass number. Iron has the highest binding energy, but among the light elements, ^{4}He is a crucial local maximum. Nucleosynthesis in the early universe essentially stops at ^{4}He because of the lack of tightly bound isotopes at $A = 5 - 8$. In the high-density environment of stars, three ^{4}He nuclei fuse to form ^{12}C, but the low baryon number precludes this process in the early universe.

Lightning Introduction to Nuclear Physics

A single proton is a hydrogen nucleus, referred to as ^{1}H or simply p; a proton and a neutron make up deuterium, ^{2}H or D; one proton and two neutrons make tritium, ^{3}H or T. Nuclei with two protons are helium; these can have one neutron (^{3}He) or two (^{4}He). Thus unique elements have a fixed number of protons, and isotopes of a given element have differing numbers of neutrons. The total number of neutrons and protons in the nucleus, the *atomic number*, is a superscript before the name of the element.

The total mass of a nucleus with Z protons and $A - Z$ neutrons differs slightly from the mass of the individual protons and neutrons alone. This difference is called the binding energy, defined as

$$B \equiv Zm_p + (A - Z)m_n - m \tag{3.12}$$

where m is the mass of the nucleus. For example, the mass of deuterium is 1875.62 MeV while the sum of the neutron and proton masses is 1877.84 MeV, so the binding energy of deuterium is 2.22 MeV. Nuclear binding energies are typically in the MeV range, which explains why Big Bang nucleosynthesis occurs at temperatures a bit less than 1 MeV even though nuclear masses are in the GeV range.

Neutrons and protons can interconvert via weak interactions:

$$p + \bar{e} \leftrightarrow n + e^+ \quad ; \quad p + e^- \leftrightarrow n + \nu \quad ; \quad n \leftrightarrow p + e^- + \bar{\nu} \tag{3.13}$$

where all the reactions can proceed in either direction. The light elements are built up via electromagnetic interactions. For example, deuterium forms from $p + n \to \mathrm{D} + \gamma$. Then, $\mathrm{D} + \mathrm{D} \to n + {}^3\mathrm{He}$, after which ${}^3\mathrm{He} + \mathrm{D} \to p + {}^4\mathrm{He}$ produces ^{4}He.

$$\frac{n_D}{n_n n_p} = \frac{n_D^{(0)}}{n_n^{(0)} n_p^{(0)}}. \tag{3.14}$$

The integrals on the right, as given in Eq. (3.6), lead to

$$\frac{n_D}{n_n n_p} = \frac{3}{4}\left(\frac{2\pi m_D}{m_n m_p T}\right)^{3/2} e^{[m_n + m_p - m_D]/T}, \tag{3.15}$$

the factor of 3/4 being due to the number of spin states (3 for D and 2 each for p and n). In the prefactor, m_D can be set to $2m_n = 2m_p$, but in the exponential the small difference between $m_n + m_p$ and m_D is important: indeed the argument of the exponential is by definition equal to the binding energy of deuterium, $B_D = 2.22$ MeV. Therefore, as long as equilibrium holds,

$$\frac{n_D}{n_n n_p} = \frac{3}{4}\left(\frac{4\pi}{m_p T}\right)^{3/2} e^{B_D/T}. \tag{3.16}$$

Both the neutron and proton density are proportional to the baryon density, so roughly,

$$\frac{n_D}{n_b} \sim \eta_b \left(\frac{T}{m_p}\right)^{3/2} e^{B_D/T}. \tag{3.17}$$

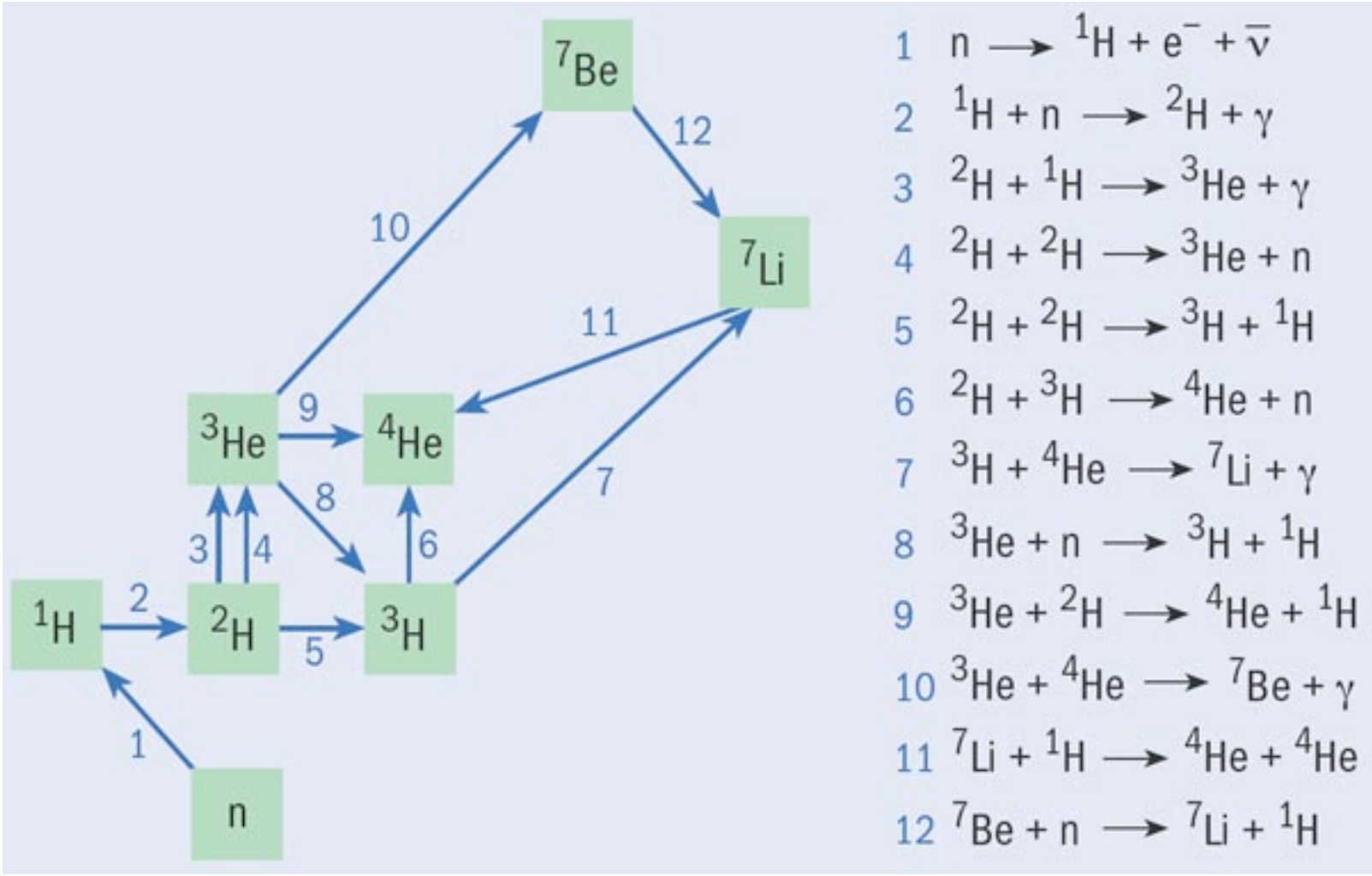

Deuterium nuclei (^{2}H) were produced by collisions between protons and neutrons, and further nuclear collisions led to every neutron grabbing a proton to form the most tightly bound type of light nucleus: ^{4}He. This process was complete after about five minutes, when the universe became too cold for nuclear reactions to continue. Tiny amounts of deuterium, ^{3}He, ^{7}Li, and ^{7}Be were produced as by-products, with the ^{7}Be undergoing beta decay to form ^{7}Li. Almost all of the protons that were not incorporated into ^{4}He nuclei remained as free particles, and this is why the universe is close to 25% ^{4}He and 75% H by mass. The other nuclei are less abundant by several orders of magnitude.

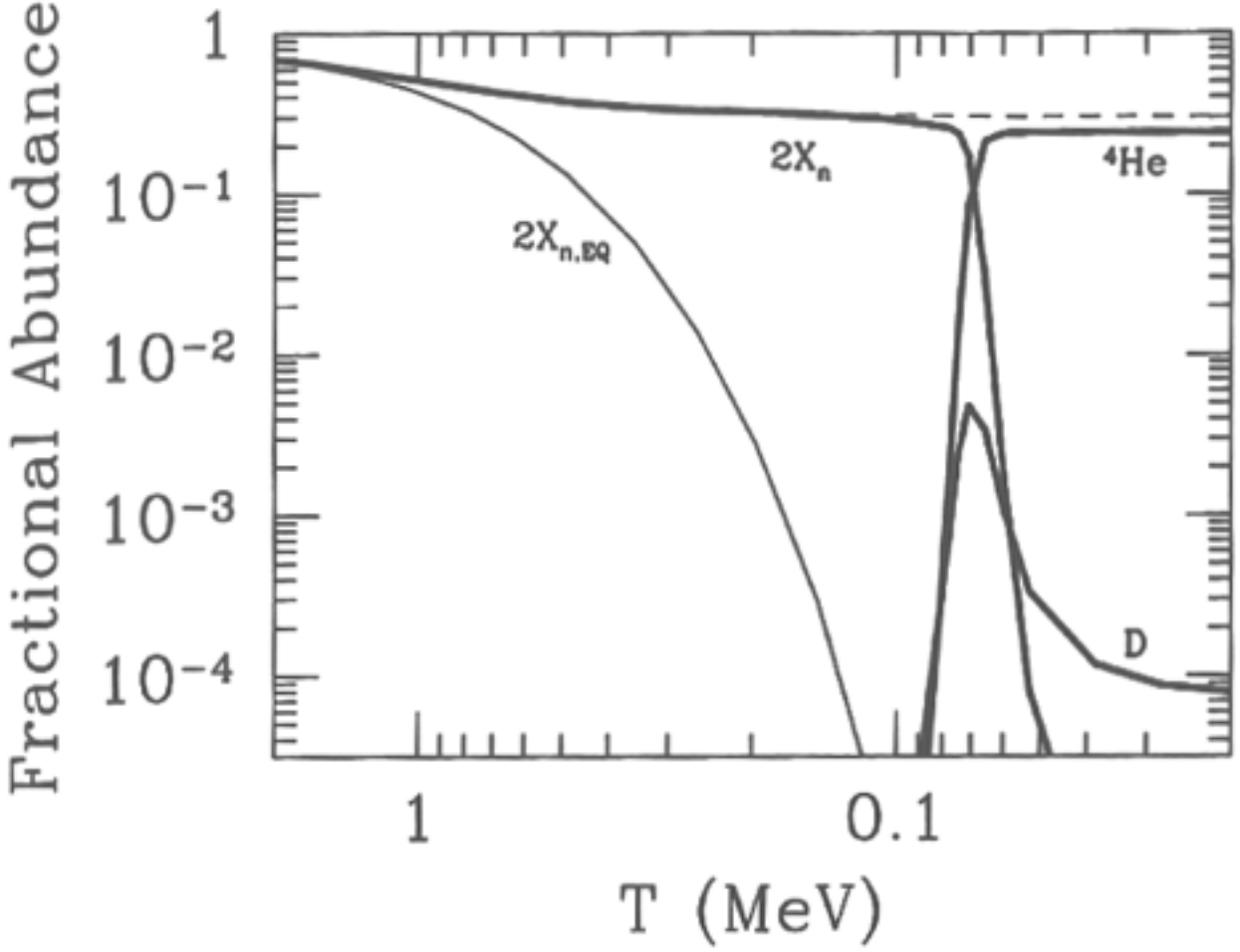

Figure 3.2. Evolution of light element abundances in the early universe. Heavy solid curves are results from Wagoner (1973) code; dashed curve is from integration of Eq. (3.27); light solid curve is twice the neutron equilibrium abundance. Note the good agreement of Eq. (3.27) and the exact result until the onset of neutron decay. Also note that the neutron abundance falls out of equilibrium at $T \sim$MeV.

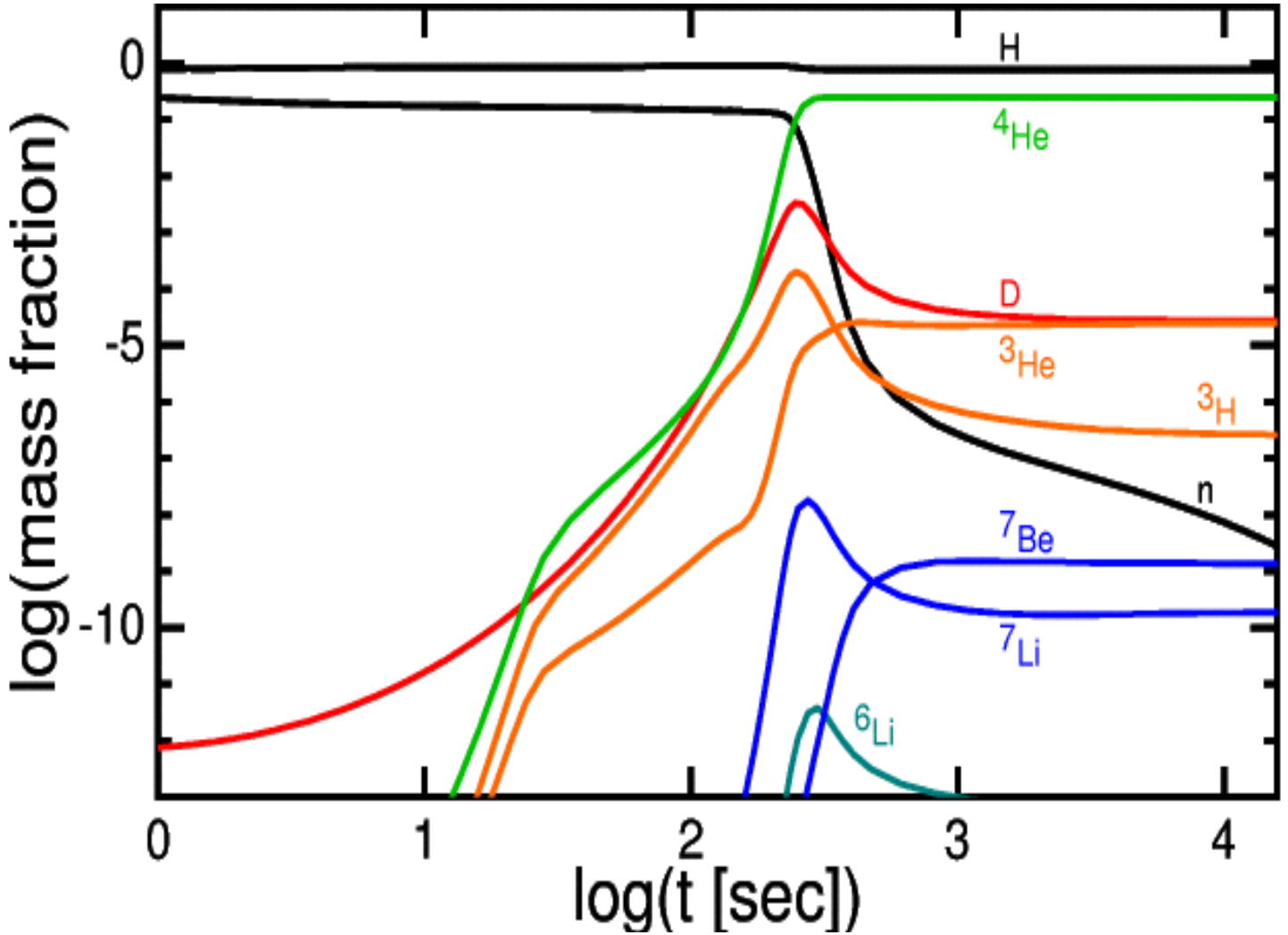

The detailed production of the lightest elements out of protons and neutrons during the first three minutes of the universe's history. The nuclear reactions occur rapidly when the temperature falls below a billion degrees Kelvin. Subsequently, the reactions are shut down, because of the rapidly falling temperature and density of matter in the expanding universe.

Ken Kawano's (1992) BBN code is available at
http://www-thphys.physics.ox.ac.uk/users/SubirSarkar/bbn.html

5 INDEPENDENT MEASURES AGREE: ATOMS ARE ONLY 4% OF THE COSMIC DENSITY

Galaxy Cluster in X-rays

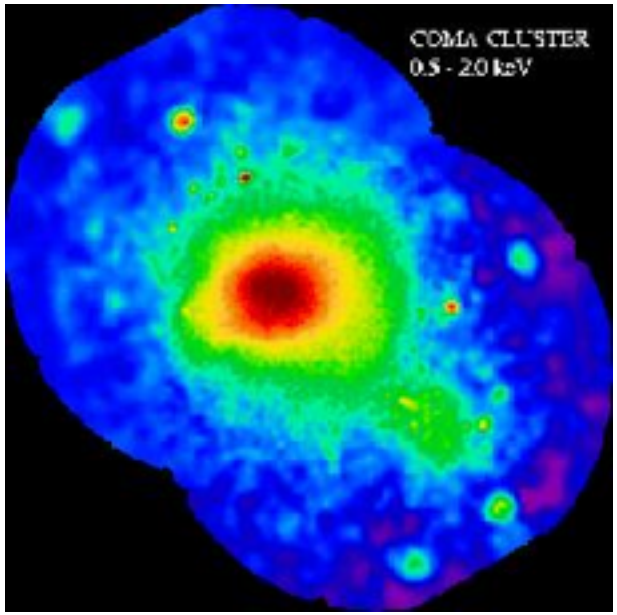

Absorption of Quasar Light

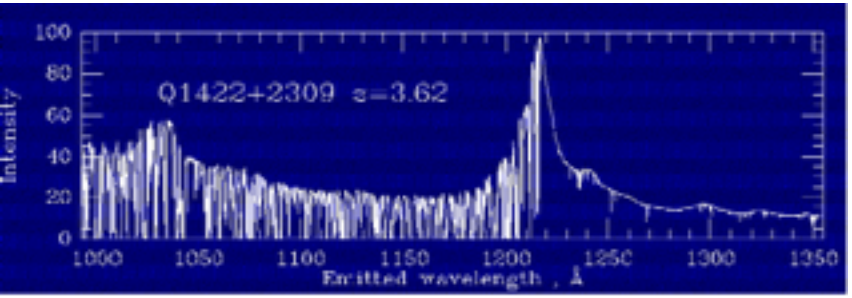

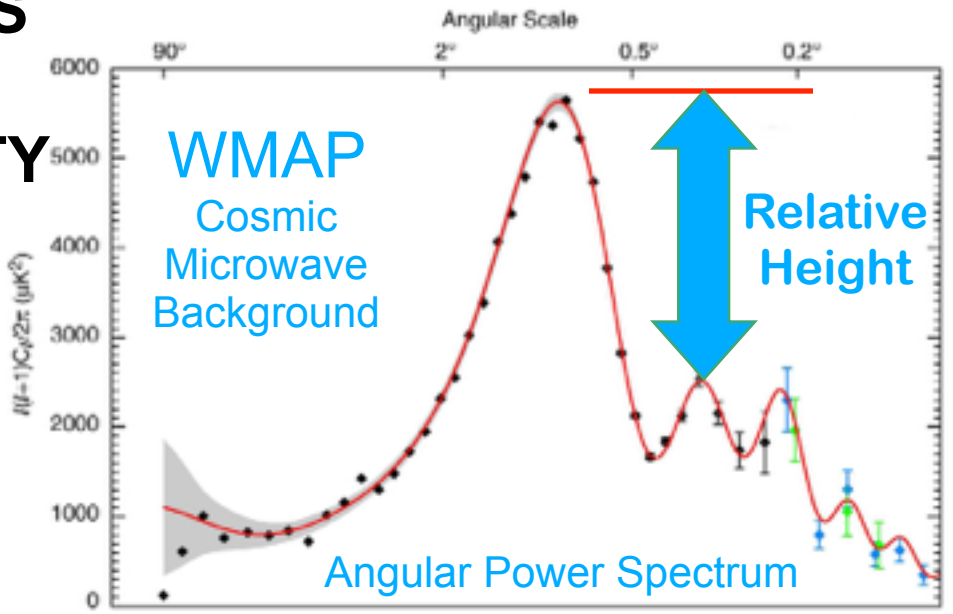

Deuterium Abundance
+ Big Bang Nucleosynthesis

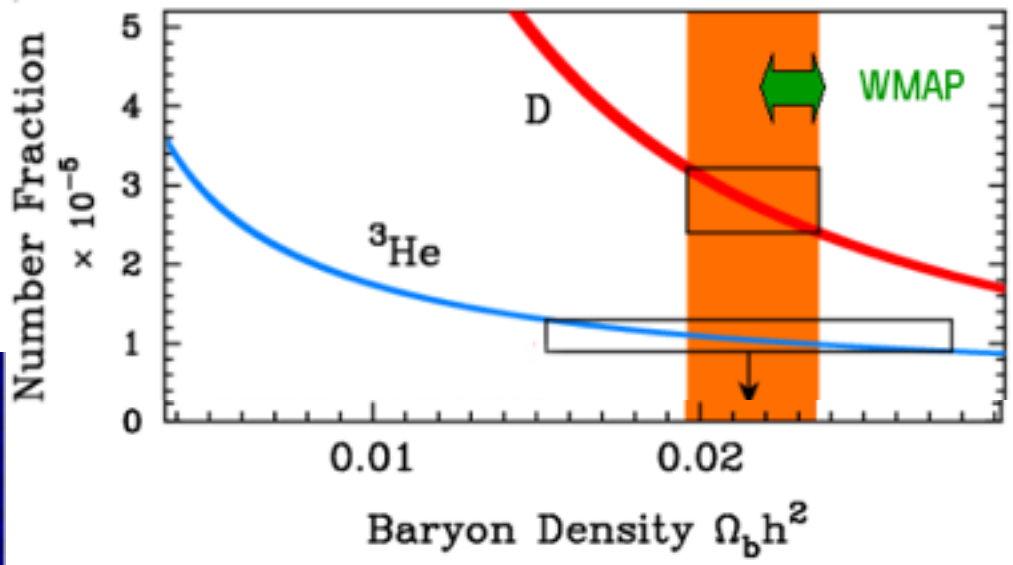

& WIGGLES IN GALAXY P(k)

BAO WIGGLES IN GALAXY P(k)

Sound waves that propagate in the opaque early universe imprint a characteristic scale in the clustering of matter, providing a “standard ruler” whose length can be computed using straightforward physics and parameters that are tightly constrained by CMB observations. Measuring the angle subtended by this scale determines a distance to that redshift and constrains the expansion rate.

The detection of the acoustic oscillation scale is one of the key accomplishments of the SDSS, and even this moderate signal-to-noise measurement substantially tightens constraints on cosmological parameters. Observing the evolution of the BAO standard ruler provides one of the best ways to measure whether the dark energy parameters changed in the past.

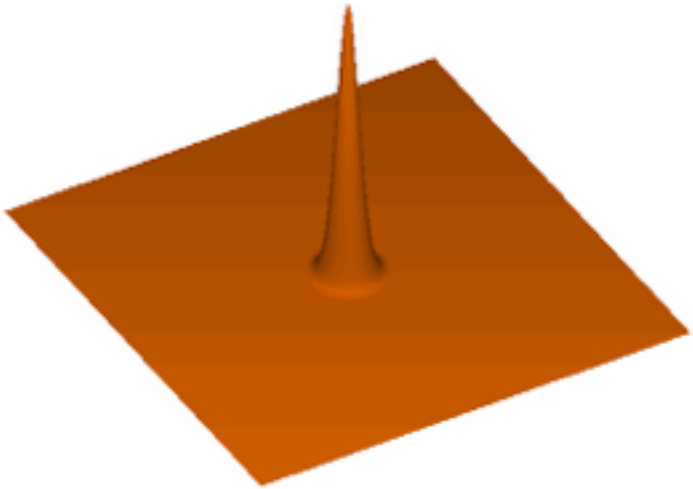

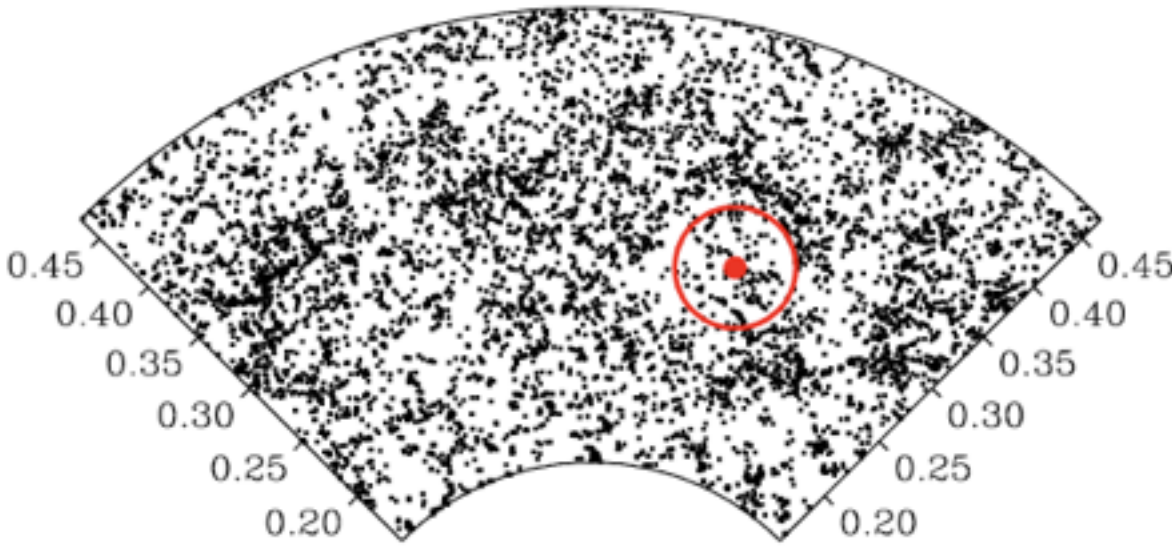

M. White lectures 08

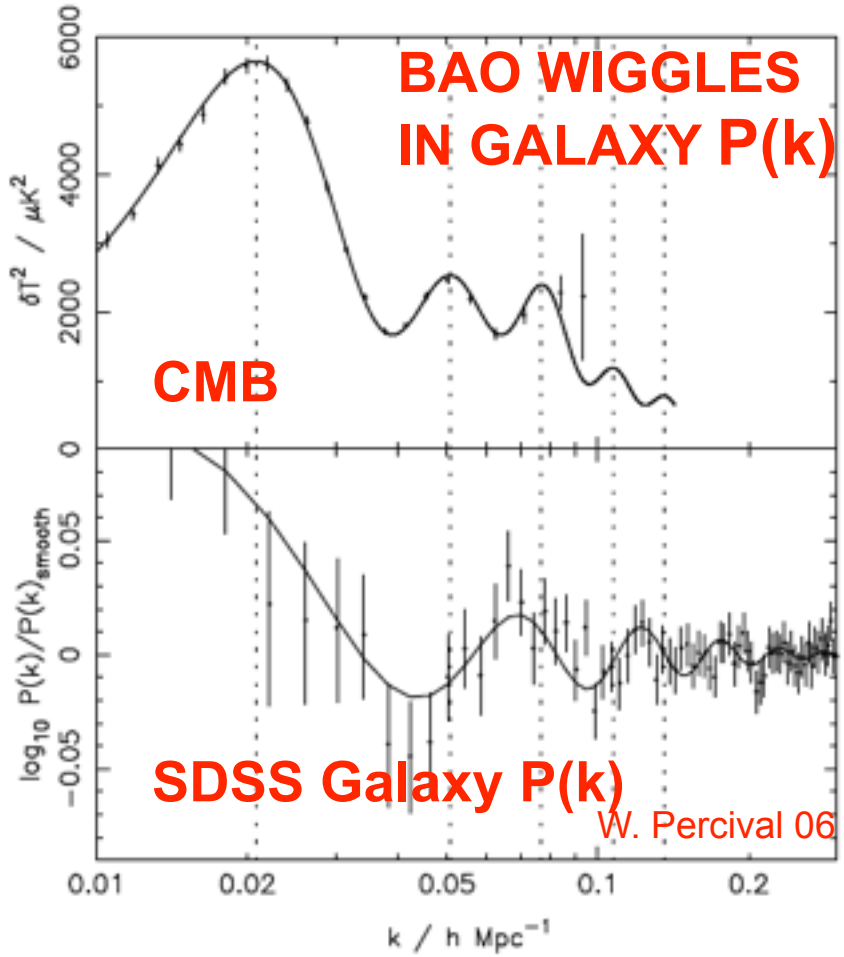

Fig. 3. Upper panel: The TT power spectrum recovered from the 3-year WMAP data (Hinshaw et al. 2006), projected into comoving space assuming a cosmological model with $\Omega_m = 0.25$ and $\Omega_\nu = 0.75$. For comparison, in the lower panel we plot the baryon oscillations calculated by dividing the SDSS power spectrum with a smooth cubic spline fit (Percival et al. 2007a). Vertical dotted lines show the positions of the peaks in the CMB power spectrum. As can be seen, there is still a long way to go before low redshift observations can rival the CMB in terms of the significance of the acoustic oscillation signal.

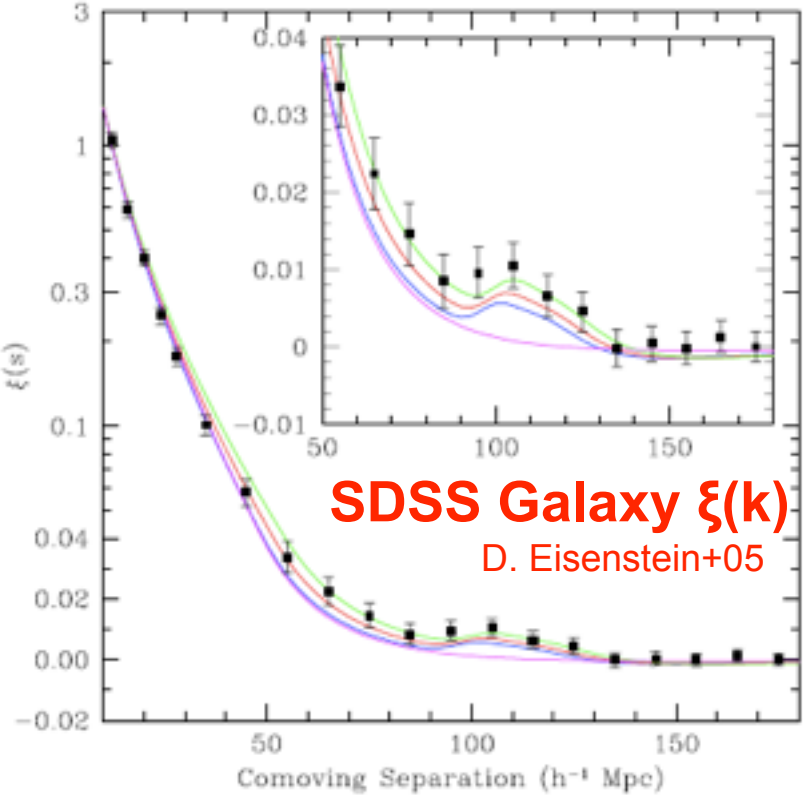

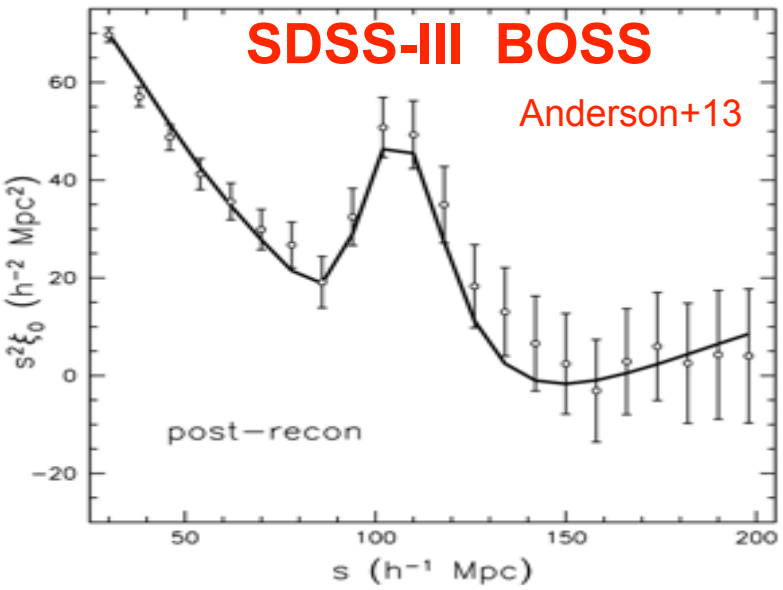

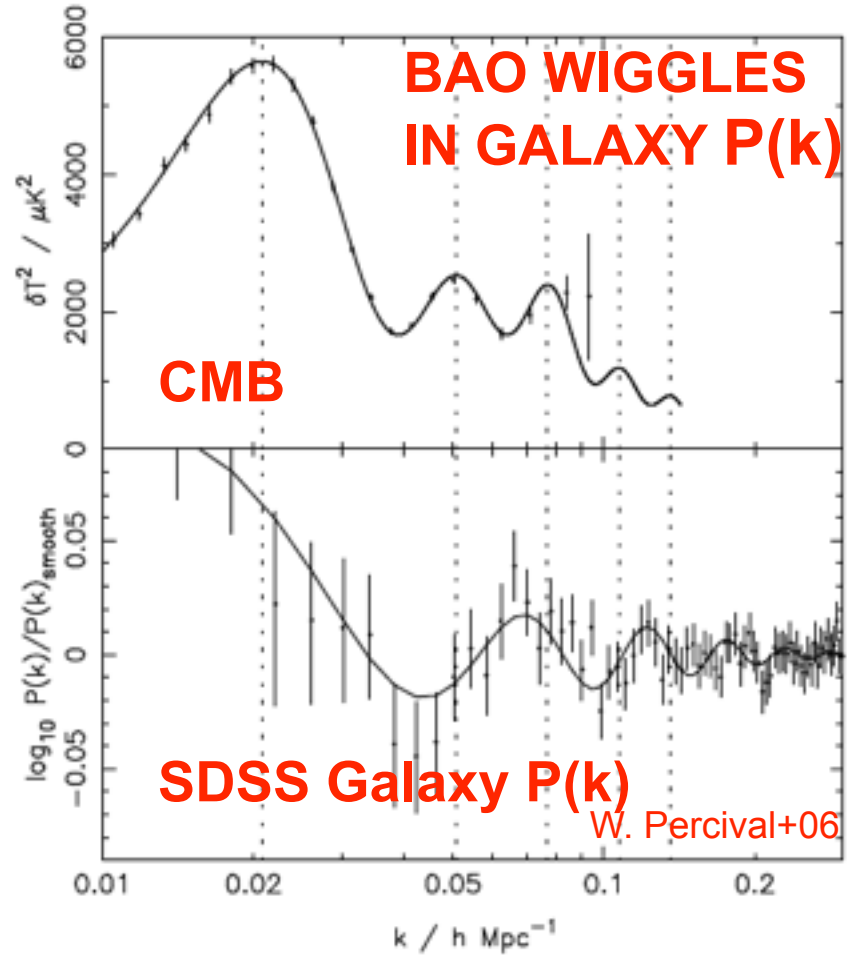
BAO WIGGLES
IN GALAXY P(k)
CMB
SDSS Galaxy P(k)
W. Percival+06
δT² / μK²
log₁₀ P(k)/P(k)smooth
k / h Mpc⁻¹

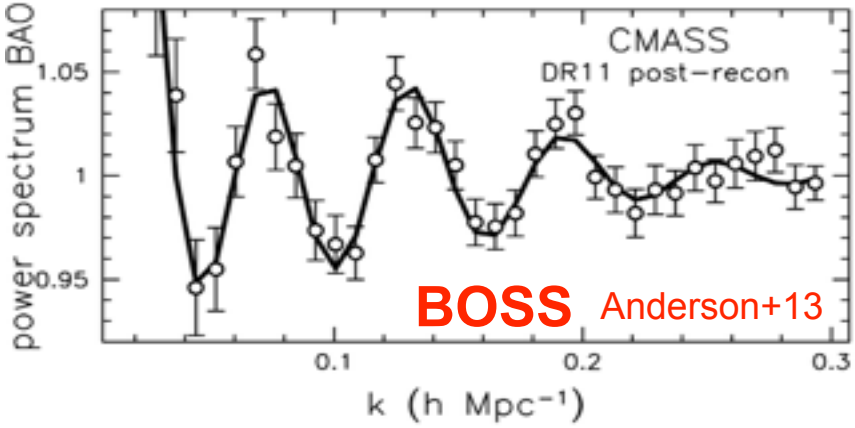
CMASS
DR11 post−recon
power spectrum BAO
BOSS Anderson+13
k (h Mpc⁻¹)

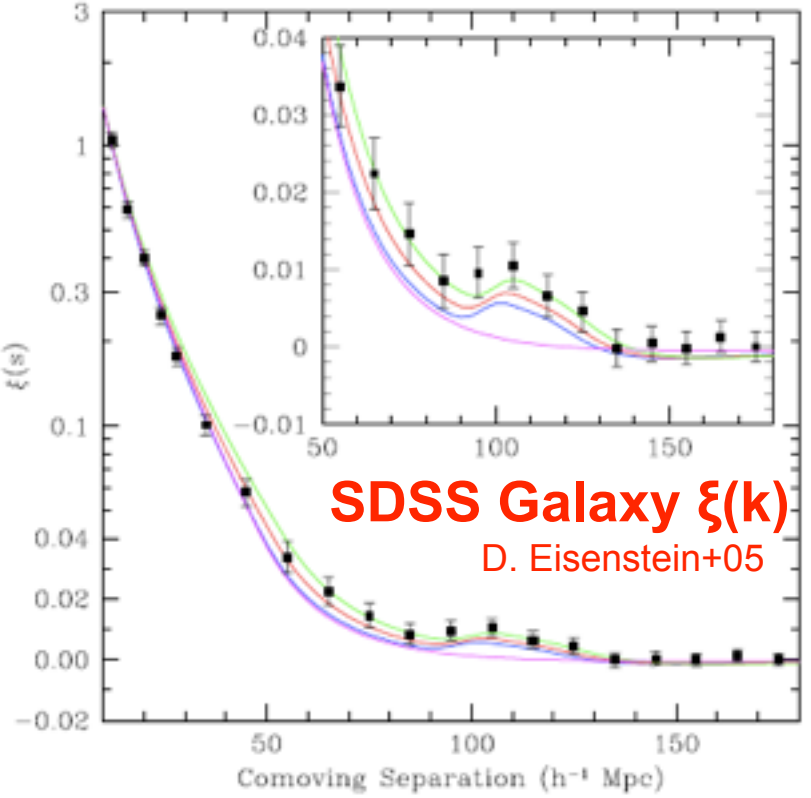
SDSS Galaxy ξ(k)
D. Eisenstein+05
ξ(s)
Comoving Separation (h⁻¹ Mpc)

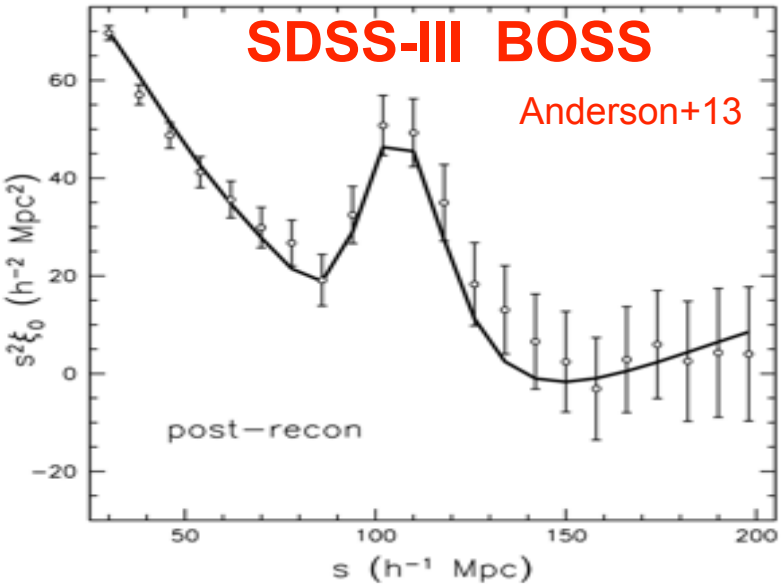
SDSS-III BOSS
Anderson+13
post−recon
s²ξ₀ (h⁻² Mpc²)
s (h⁻¹ Mpc)

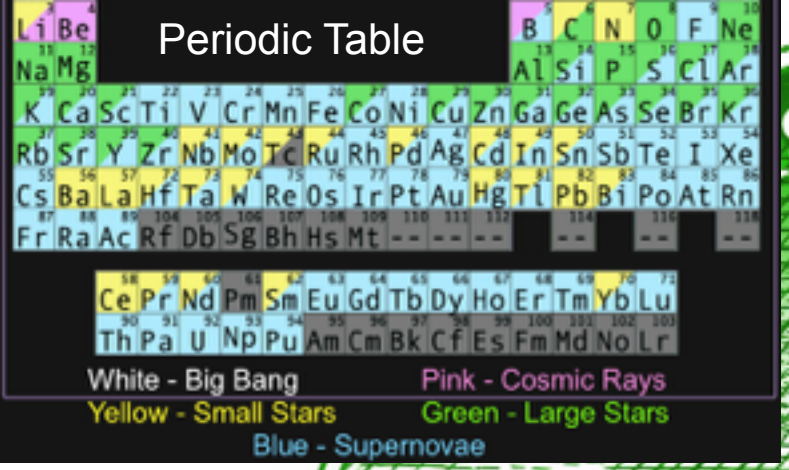

stardust

stars

COSMIC DENSITY PYRAMID

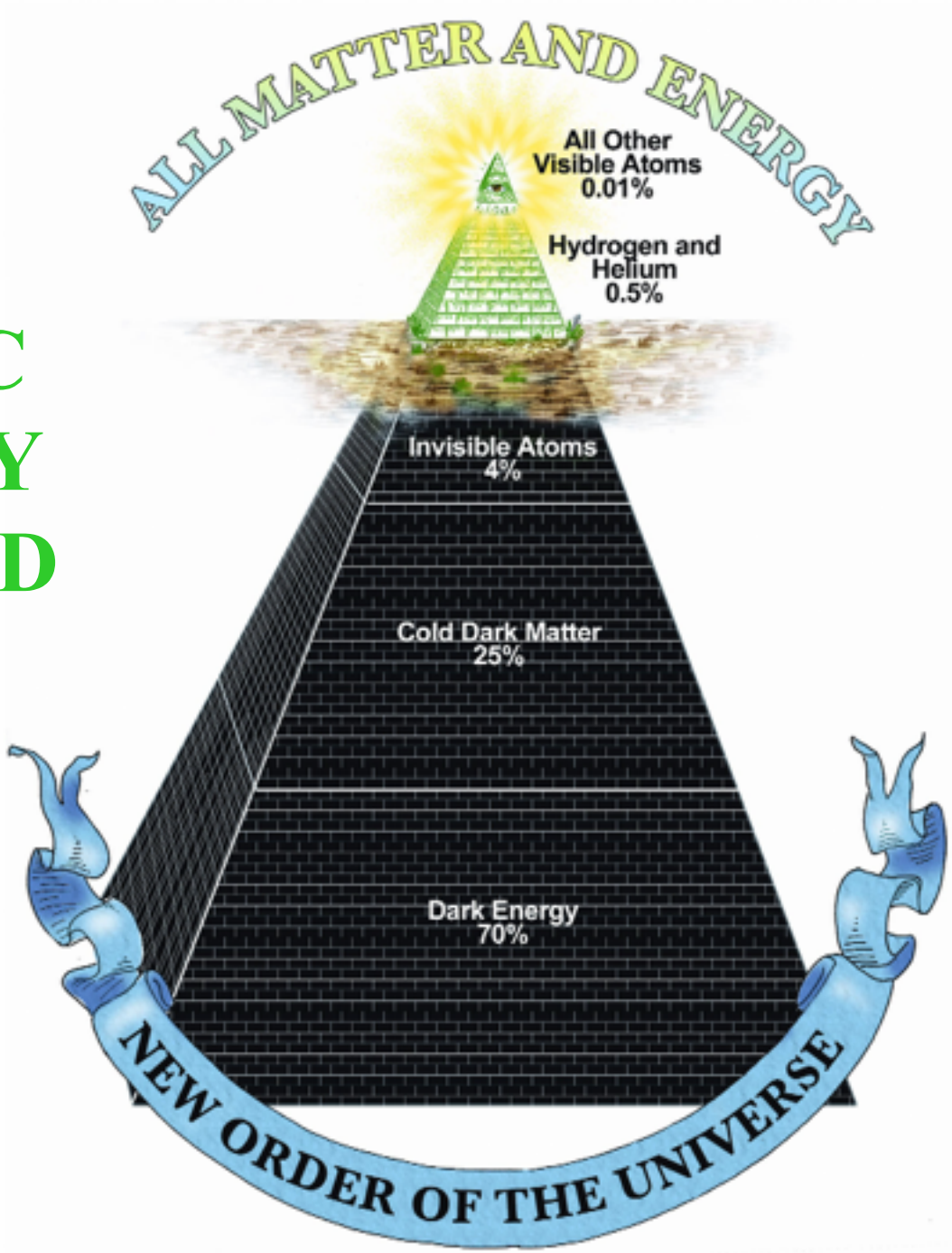

BBN Predicted vs. Measured Abundances of D, ^{3}He, ^{4}He, and ^{7}Li

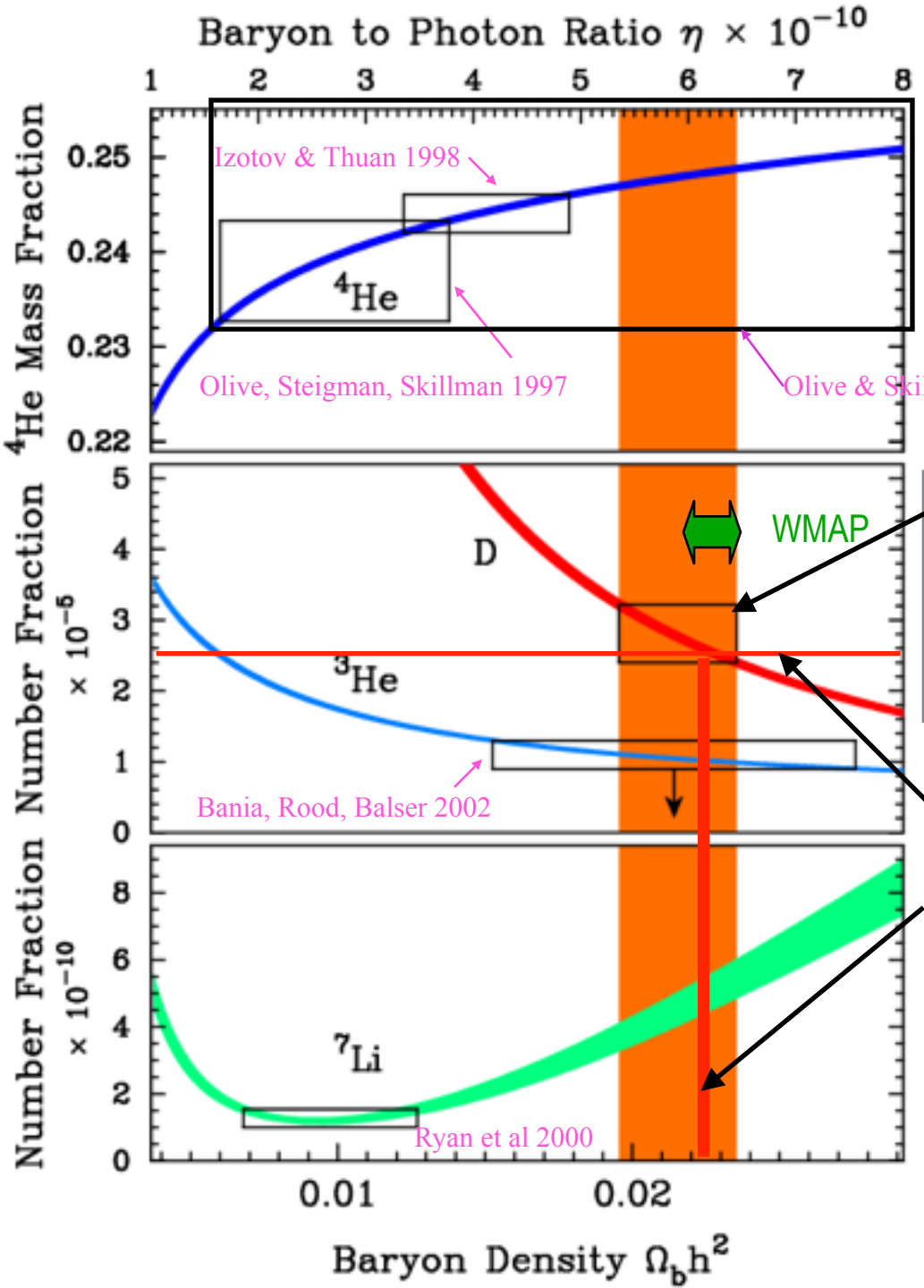

Izotov & Thuan 2004: $\Omega_b h^2 = 0.012 \pm 0.0025$

D/H is from Kirkman, Tytler, Suzuki, O'Meara, & Lubin 2004, giving $\Omega_b h^2 = 0.0214 \pm 0.0020$

D/H from Ryan Cooke+2014, which implies $\Omega_b h^2 = 0.0220 \pm 0.0005$

BBN predictions are from Burles, Nollett, & Turner 2001

^{7}Li IS NOW DISCORDANT unless stellar diffusion destroys ^{7}Li

Deuterium absorption at redshift 2.525659 towards Q1243+3047

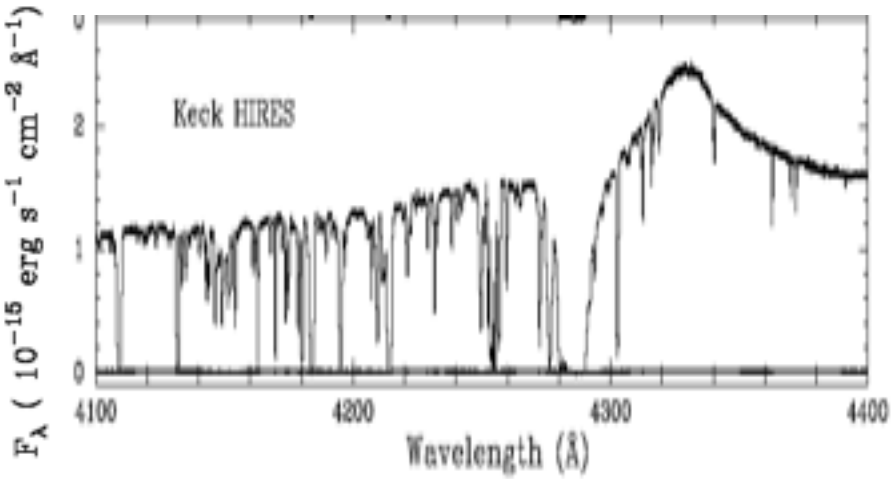

The Lyα absorption near 4285 Å is from the system in which we measure D/H.

The detection of Deuterium and the modeling of this system seem convincing. This is just a portion of the evidence that the Tytler group presented in this paper. They have similarly convincing evidence for several other Lyman alpha clouds in quasar spectra.

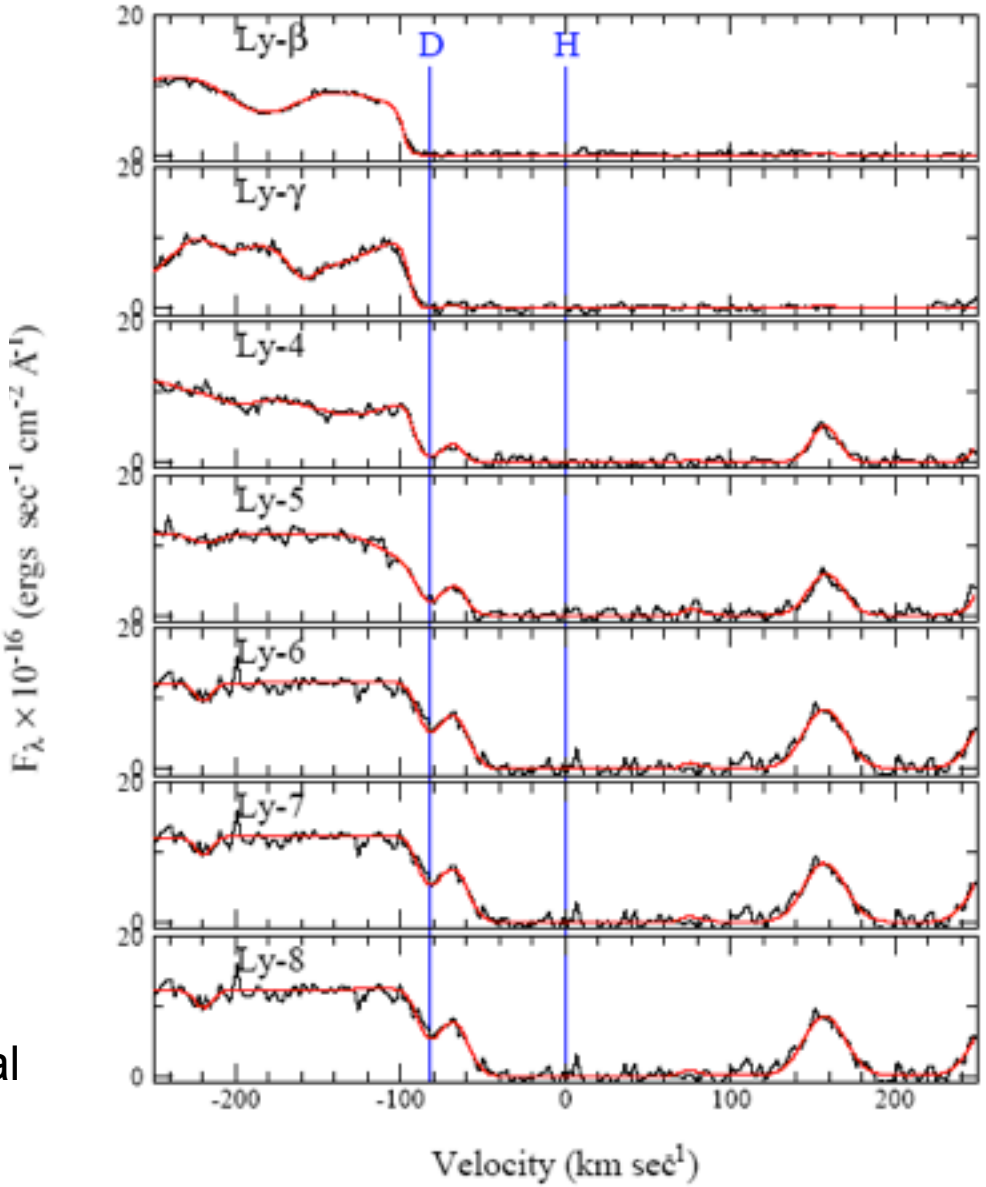

FIG. 7.— The HIRES spectrum of Ly-2 to 8, together with our model of the system, as given in Table 3.

Kirkman, Tytler, Suzuki, O'Meara, & Lubin 2004

The Astrophysical Journal, 781:31 (16pp), 2014 January 20

PRECISION MEASURES OF THE PRIMORDIAL ABUNDANCE OF DEUTERIUM

Ryan J. Cooke, Max Pettini, Regina A. Jorgenson, Michael T. Murphy, and Charles C. Steidel

ABSTRACT

We report the discovery of deuterium absorption in the very metal-poor ([Fe/H] = −2.88) damped Lyα system at z_{abs} = 3.06726 toward the QSO SDSS J1358+6522. On the basis of 13 resolved D i absorption lines and the damping wings of the H i Lyα transition, we have obtained a new, precise measure of the primordial abundance of deuterium. Furthermore, to bolster the present statistics of precision D/H measures, we have reanalyzed all of the known deuterium absorption-line systems that satisfy a set of strict criteria. We have adopted a blind analysis strategy (to remove human bias) and developed a software package that is specifically designed for precision D/H abundance measurements. For this reanalyzed sample of systems, we obtain a weighted mean of $(D/H)_p = (2.53 \pm 0.04) \times 10^{-5}$, corresponding to a universal baryon density $100\ \Omega_{b,0}\ h^2 = 2.202 \pm 0.046$ for the standard model of big bang nucleosynthesis (BBN). By combining our measure of $(D/H)_p$ with observations of the cosmic microwave background (CMB), we derive the effective number of light fermion species, $N_{eff} = 3.28 \pm 0.28$. We therefore rule out the existence of an additional (sterile) neutrino (i.e., $N_{eff} = 4.046$) at 99.3% confidence...

Montage of the full Lyman series absorption in the DLA at zabs = 3.067259 toward J1358+6522. The black histogram shows the data, fully adjusted to the best-fitting continuum and zero levels, while the red continuous line is the model fit. The minimum χ^2/dof for this fit is 6282.3/6401. Tick marks above the spectrum indicate the location of the velocity components (red ticks for H I, green ticks for D I).

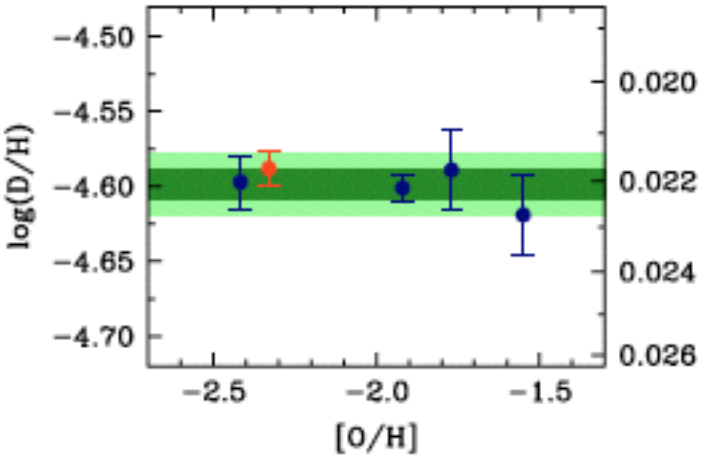

Values of D/H for the Precision Sample of DLA measurements analyzed in this paper. The orange point represents the new case reported here (J1358+6522).

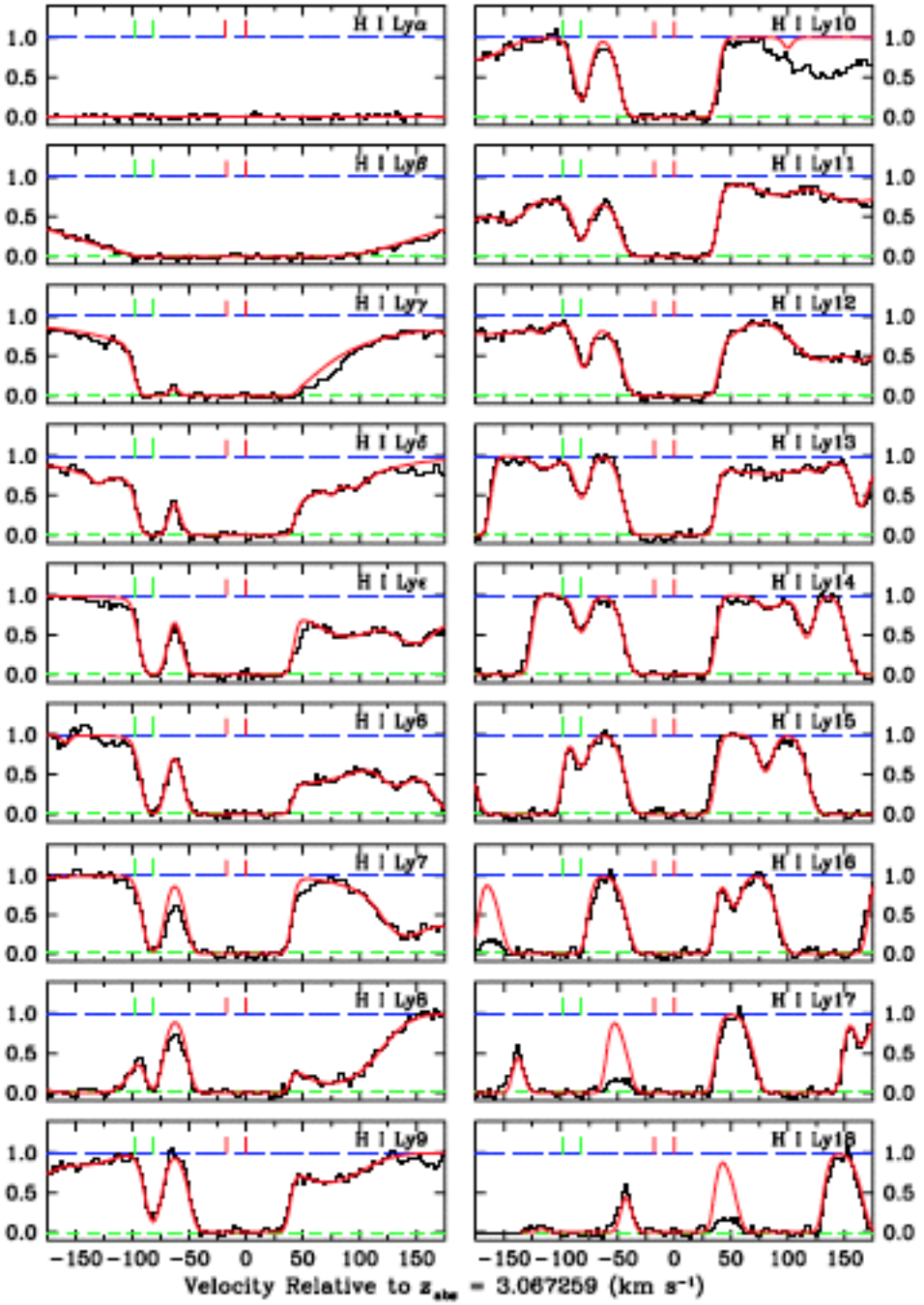

Determination of primordial He^4 abundance Y_p by linear regression

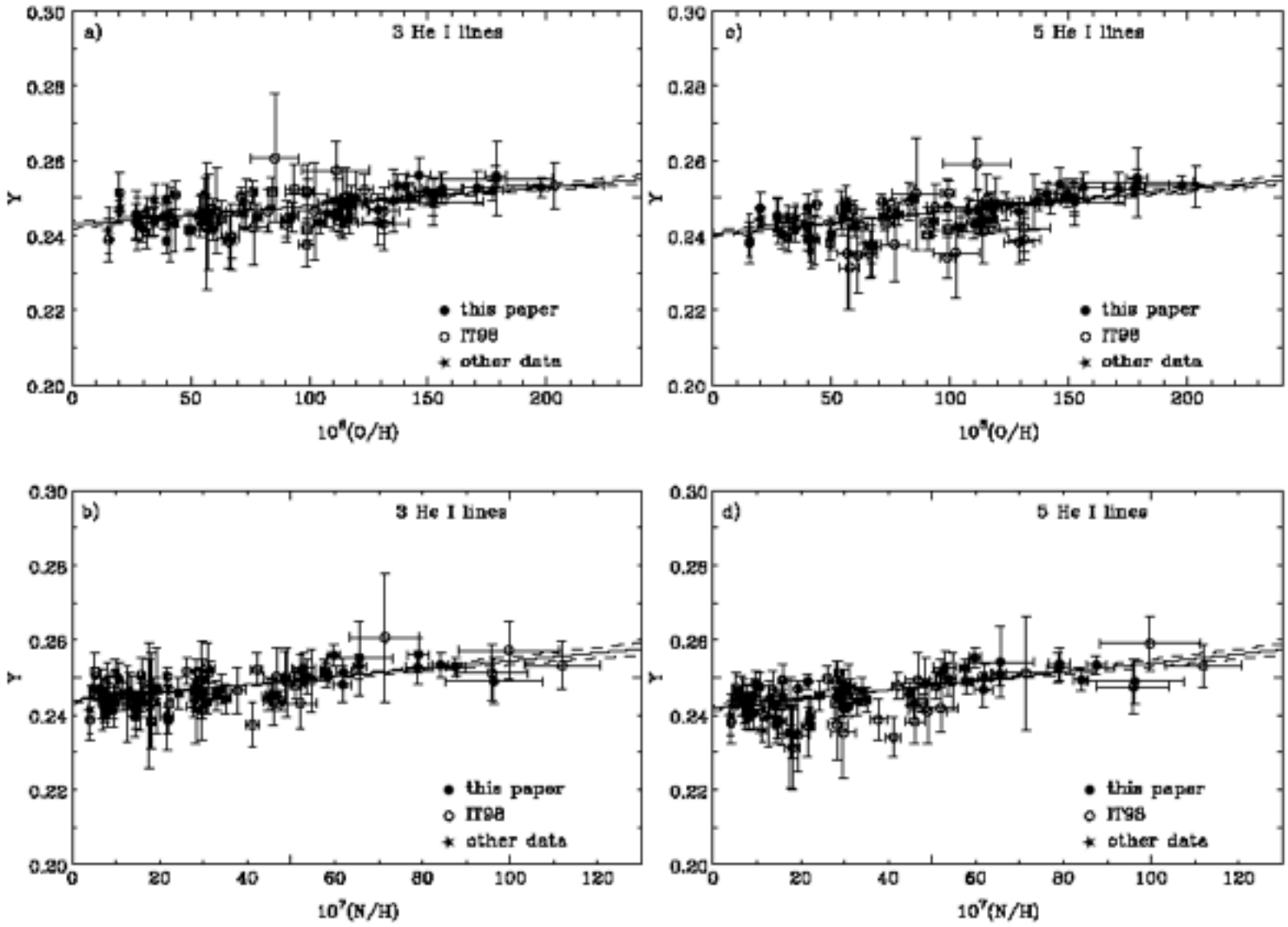

Y = M(^{4}He)/M(baryons), Primordial Y ≡ Yp = zero intercept

Note: BBN plus D/H ⇒ Yp = 0.247± 0.001

Izotov & Thuan 2004

The Li abundance disagreement with BBN may indicate new physics

Did Something Decay, Evaporate, or Annihilate during Big Bang Nucleosynthesis?

Karsten Jedamzik Phys.Rev. D70 (2004) 063524

Laboratoire de Physique Mathémathique et Théorique, C.N.R.S., Université de Montpellier II, 34095 Montpellier Cedex 5, France

Results of a detailed examination of the cascade nucleosynthesis resulting from the putative hadronic decay, evaporation, or annihilation of a primordial relic during the Big Bang nucleosynthesis (BBN) era are presented. It is found that injection of energetic nucleons around cosmic time 10^3sec may lead to an observationally favored reduction of the primordial ^{7}Li/H yield by a factor $2-3$. Moreover, such sources also generically predict the production of the ^{6}Li isotope with magnitude close to the as yet unexplained high ^{6}Li abundances in low-metallicity stars. The simplest of these models operate at fractional contribution to the baryon density $\Omega_b h^2 \gtrsim 0.025$, slightly larger than that inferred from standard BBN. Though further study is required, such sources, as for example due to the decay of the next-to-lightest supersymmetric particle into GeV gravitinos or the decay of an unstable gravitino in the TeV range of abundance $\Omega_G h^2 \sim 5 \times 10^{-4}$ show promise to explain both the ^{6}Li and ^{7}Li abundances in low metallicity stars.

See also “Supergravity with a Gravitino LSP” by Jonathan L. Feng, Shufang Su, Fumihiro Takayama Phys.Rev. D70 (2004) 075019

“Gravitino Dark Matter and the Cosmic Lithium Abundances” by Sean Bailly, Karsten Jedamzik, Gilbert Moultaka, arXiv:0812.0788

The Li abundance disagreement with BBN may be caused by stellar diffusion

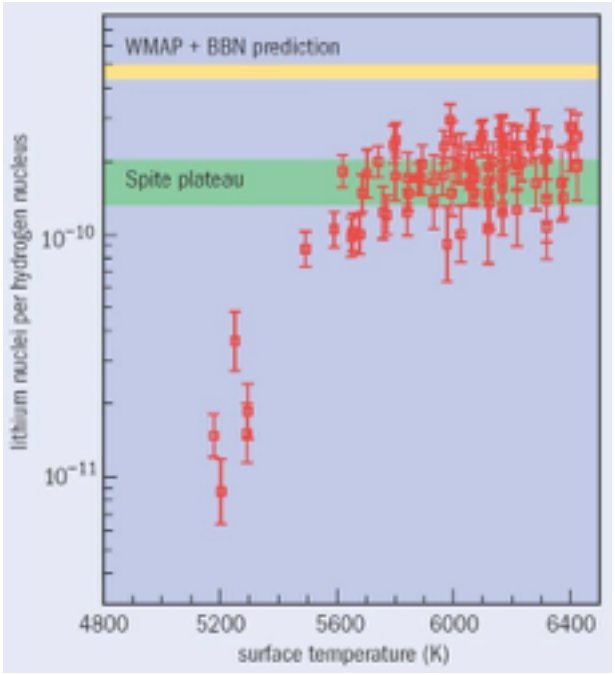

Lithium abundance in very old stars that formed from nearly primordial gas. The amount of ^{7}Li in these "Spite-plateau" stars (green) is much less than has been inferred by combining BBN with measurements of the cosmic microwave background made using WMAP (yellow band). Our understanding of stellar astrophysics may be at fault. Those Spite-plateau stars that have surface temperatures between 5700 and 6400 K have uniform abundances of ^{7}Li because the shallow convective envelopes of these warm stars do not penetrate to depths where the temperature exceeds that for ^{7}Li to be destroyed ($T_{destruct} = 2.5 \times 10^6$ K). The envelopes of cooler stars (data points towards the left of the graph) do extend to such depths, so their surfaces have lost ^{7}Li to nuclear reactions. **If the warm stars gradually circulate ^{7}Li from the convective envelope to depths where $T > T_{destruct}$, then their surfaces may also slowly lose their ^{7}Li.** From http://physicsworld.com/cws/article/print/30680

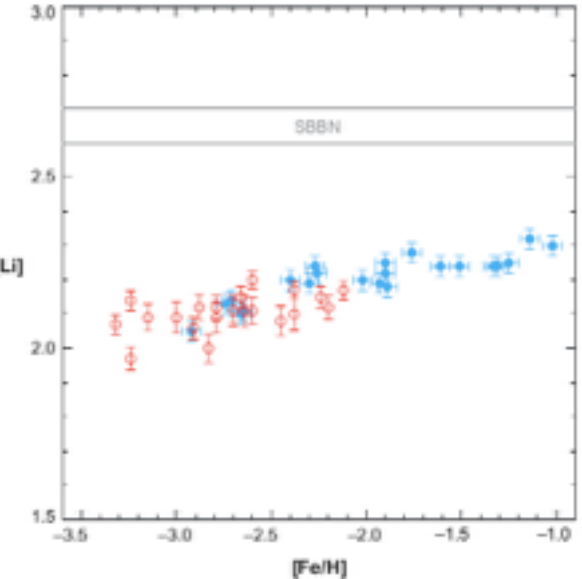

Lithium abundances, [Li] ≡ 12+ log(Li/H), versus metallicity (on a log scale relative to solar) from (red) S. Ryan et al. 2000, ApJ, 530, L57; (blue) M. Asplund et al.2006, ApJ, 644, 229. Figure from G. Steigman 2007, ARAA 57, 463.

Korn et al. 2006 find that both lithium and iron have settled out of the atmospheres of these old stars, and they infer for the unevolved abundances, [Fe/H] = –2.1 and [Li] = 2.54 ± 0.10, in excellent agreement with SBBN.

The most stringent constraint on a mixing model is that it must maintain the observed tight bunching of plateau stars that have the same average ^{7}Li abundance. In a series of papers that was published between 2002 and 2004, Olivier Richard and collaborators at the Université de Montréal in Canada proposed such a mixing model that has since gained observational support. It suggests that all nuclei heavier than hydrogen settle very slowly out of the convective envelope under the action of gravity. In particular, the model makes specific predictions for settling as a star evolves, which are revealed as variations of surface composition as a function of mass in stars that formed at the same time.

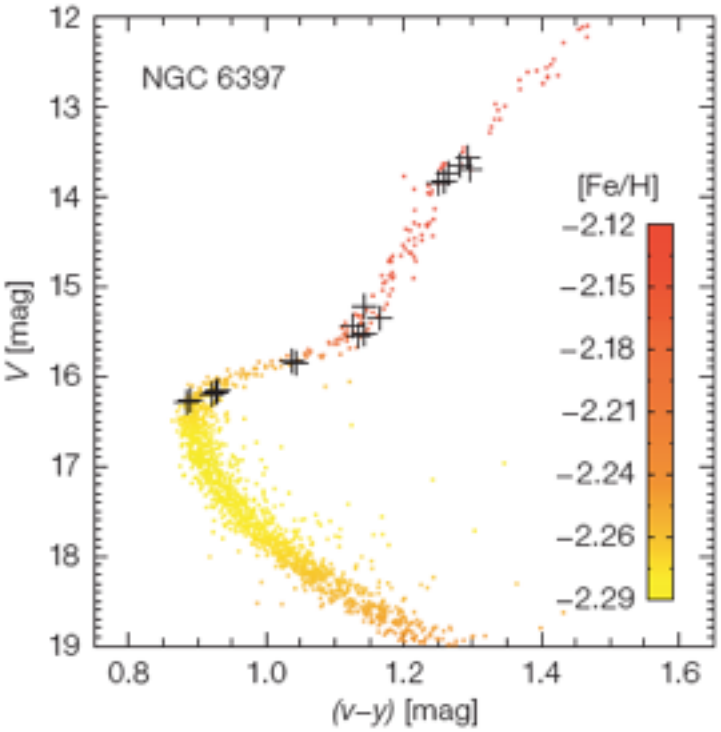

Korn et al. The Messenger 125 (Sept 2006); Korn et al. 2006, Nature 442, 657.

By spring 2006, Andreas Korn of Uppsala University in Sweden and colleagues had used the European Southern Observatory's Very Large Telescope (VLT) in Chile to study 18 chemically primitive stars in a distant globular cluster called NGC 6397 that were known to have the same age and initial composition. From this Korn et al. showed that the iron and lithium abundances in these stars both varied according to stellar mass as predicted by Richard's model. In fact, the model indicated that the observed stars started out with a ^{7}Li abundance that agrees with the WMAP data. Corroboration of these results is vital because **if the result stands up to scrutiny based on a wide range of data, then we have solved the lithium problem.**

Nature **442**, 657-659 (10 August 2006)

A probable stellar solution to the cosmological lithium discrepancy

A Korn et al.

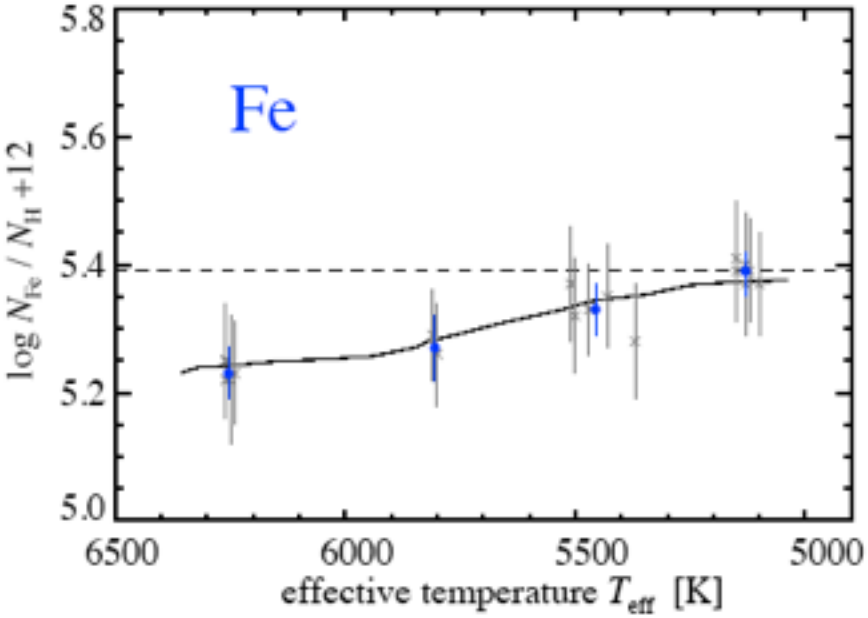

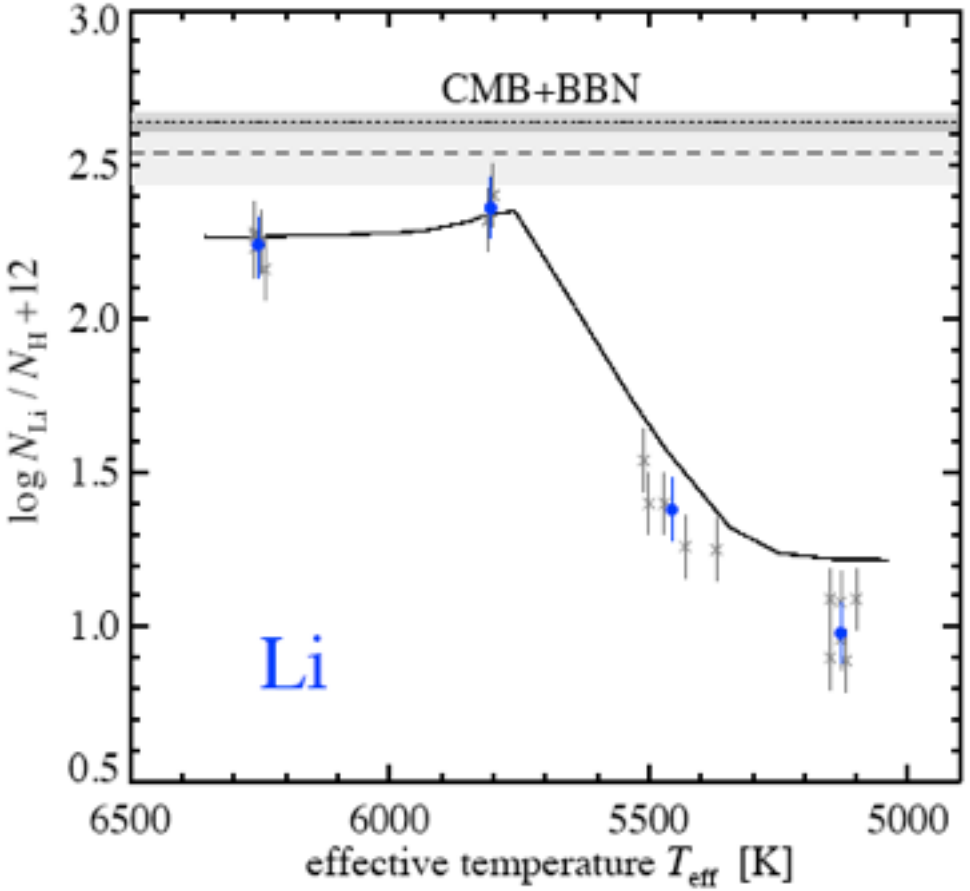

Figure 1: Trends of iron and lithium as a function of the effective temperatures of the observed stars compared to the model predictions. The grey crosses are the individual measurements, while the bullets are the group averages. The solid lines are the predictions of the diffusion model, with the original abundance given by the dashed line. In *b*, the grey-shaded area around the dotted line indicates the 1σ confidence interval of CMB + BBN[1]: $\log[\varepsilon(\mathrm{Li})] = \log(N_{\mathrm{Li}}/N_{\mathrm{H}}) + 12 = 2.64 \pm 0.03$. In *a*, iron is treated in non-equilibrium[20] (non-LTE), while in *b*, the equilibrium (LTE) lithium abundances are plotted, because the combined effect of 3D and non-LTE corrections was found to be very small[29]. For iron, the error bars are the line-to-line scatter of Fe I and Fe II (propagated into the mean for the group averages), whereas for the absolute lithium abundances 0.10 is adopted. The 1σ confidence interval around the inferred primordial lithium abundance ($\log[\varepsilon(\mathrm{Li})] = 2.54 \pm 0.10$) is indicated by the light-grey area.We attribute the modelling shortcomings with respect to lithium in the bRGB and RGB stars to the known need for extra mixing[30], which is not considered in the diffusion model.

Another way to determine the amount of ^{7}Li destroyed in stars is to observe the element's other, less stable, isotope: ^{6}Li. ^{6}Li is not made in detectable quantities by BBN but instead comes from spallation: collisions between nuclei in cosmic rays and in the interstellar gas. Since ^{6}Li is even more easily destroyed than ^{7}Li, detecting it allows us to place limits on the destruction of ^{7}Li.

In 2006 Martin Asplund and co-workers at the Mount Stromlo Observatory in Australia made extensive observations of ^{6}Li in plateau stars using the VLT. In each of the nine stars where they found ^{6}Li, roughly 5% of the lithium consisted of this isotope – which was larger than expected although at the limit of what was detectable with the equipment. This has huge implications not only for BBN but also for the history of cosmic rays in the galaxy and for stellar astrophysics. For example, the production of such large amounts of ^{6}Li must have required an enormous flux of cosmic rays early in the history of our galaxy, possibly more than could have been provided by known acceleration mechanisms. Moreover, if the plateau stars have truly destroyed enough ^{7}Li to bring the WMAP prediction of the mean baryon density into agreement with that obtained with the observed Spite plateau, the greater fragility of ^{6}Li implies that the stars initially contained ^{6}Li in quantities comparable to the observed ^{7}Li plateau.

All of these facts make the ^{6}Li observations an uncomfortable fit for BBN, stellar physics and models of cosmic-ray nucleosynthesis – particularly since the production of large amounts of ^{6}Li via cosmic rays has to be accompanied by a similar production of ^{7}Li. Although ^{6}Li can be produced in some exotic particle-physics scenarios, it is vital that we independently confirm Asplund's results. Indeed, the hunt for primordial lithium (of both isotopes) is currently ongoing at the VLT, as well as at the Keck Observatory and the Japanese Subaru Telescope, although such observations are right at the limit of what can be achieved.

Light elements in the Universe
Proceedings IAU Symposium No. 268, 2010
C. Charbonnel, M. Tosi, F. Primas & C. Chiappini, eds.

DOI: 00.0000/X000000000000000X

Observational signatures for depletion in the Spite plateau: solving the cosmological Li discrepancy?

Jorge Meléndez[1], Luca Casagrande[2], Iván Ramírez[2], Martin Asplund[2] and William J. Schuster[3]

[1]Centro de Astrofísica, Universidade do Porto, Rua das Estrelas, 4150-762 Porto, Portugal
email: jorge@astro.up.pt

[2]Max-Planck-Institut für Astrophysik, Karl-Schwarzschild-Str. 1, Postfach 1317, D-85741 Garching, Germany

[3]Observatorio Astronómico Nacional, UNAM, Apartado Postal 877, Ensenada, BC, CP 22800, Mexico

Abstract. We present Li abundances for 73 stars in the metallicity range -3.5 < [Fe/H] < -1.0 using improved IRFM temperatures (Casagrande et al. 2010) with precise *E(B-V)* values obtained mostly from interstellar NaI D lines, and high-quality equivalent widths ($\sigma_{EW} \sim 3\%$). At all metallicities we uncover a fine-structure in the Li abundances of Spite plateau stars, which we trace to Li depletion that depends on both metallicity and mass. Models including atomic diffusion and turbulent mixing seem to reproduce the observed Li depletion assuming a primordial Li abundance $A_{\rm Li} = 2.64$ dex (MARCS models) or 2.72 (Kurucz overshooting models), in good agreement with current predictions ($A_{\rm Li} = 2.72$) from standard BBN. We are currently expanding our sample to have a better coverage of different evolutionary stages at the high and low metallicity ends, in order to verify our findings.

Recent references on BBN and Lithium

M Asplund et al. 2006, "Lithium isotopic abundances in metalpoor halo stars" ApJ 644 229–259

A Korn et al. 2006 "A probable stellar solution to the cosmological lithium discrepancy" Nature 442, 657–659; 2007 "Atomic Diffusion and Mixing in Old Stars. I. Very Large Telescope FLAMES-UVES Observations of Stars in NGC 6397" ApJ 671, 402

C Charbonnel 2006, "Where all the lithium went" Nature 442, 636-637

K Nollett 2007, "Testing the elements of the Big Bang" physicsworld.com

R H Cyburt, B D Fields, K A Olive 2008, "An update on the big bang nucleosynthesis prediction for 7Li: the problem worsens" JCAP 11, 12 (also arXiv:0808.2818)

A J Korn 2008 "Atomic Diffusion in Old Stars --- Helium, Lithium and Heavy Elements" ASPC 384, 33

J Melendez et al. 2010 "Observational Signatures for Depletion in the Spite Plateau: Solving the Cosmological Li Discrepancy?" IAU Symposium 268, 211

M Prospelov and J Pradler 2010 "Big Bang Nucleosynthesis as a Probe of New Physics" Annual Reviews of Nuclear and Particle Physics (also on astro-ph)

B Fields 2011 "The Primordial Li Problem" Annual Reviews of Nuclear and Particle Science (also on astro-ph)

BBN is a Prototype for Hydrogen Recombination and DM Annihilation

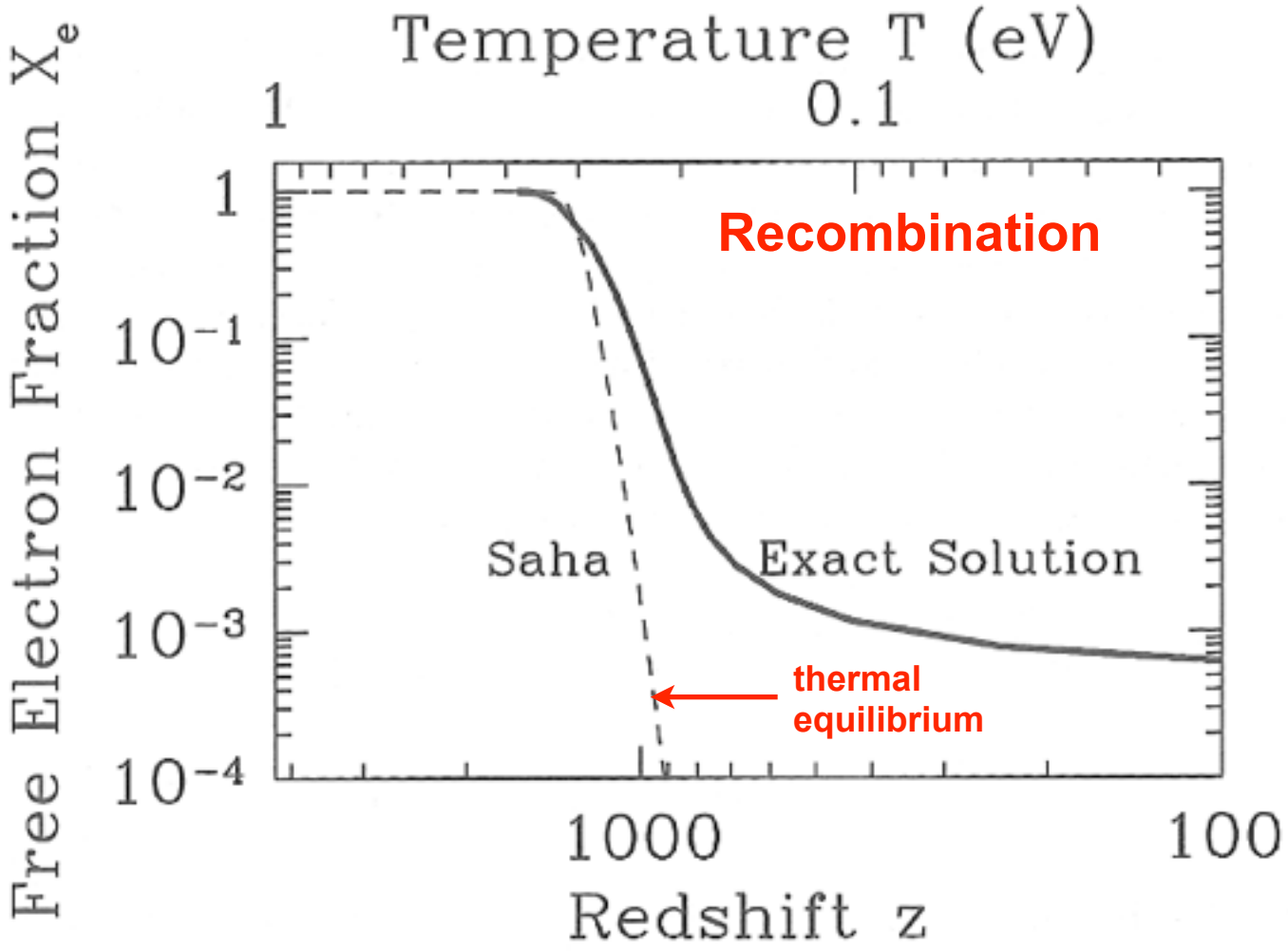

Figure 3.4. Free electron fraction as a function of redshift. Recombination takes place suddenly at $z \sim 1000$ corresponding to $T \sim 1/4$ eV. The Saha approximation, Eq. (3.37), holds in equilibrium and correctly identifies the redshift of recombination, but not the detailed evolution of X_e. Here $\Omega_b = 0.06, \Omega_m = 1, h = 0.5$.

Dodelson, *Modern Cosmology*, p. 72

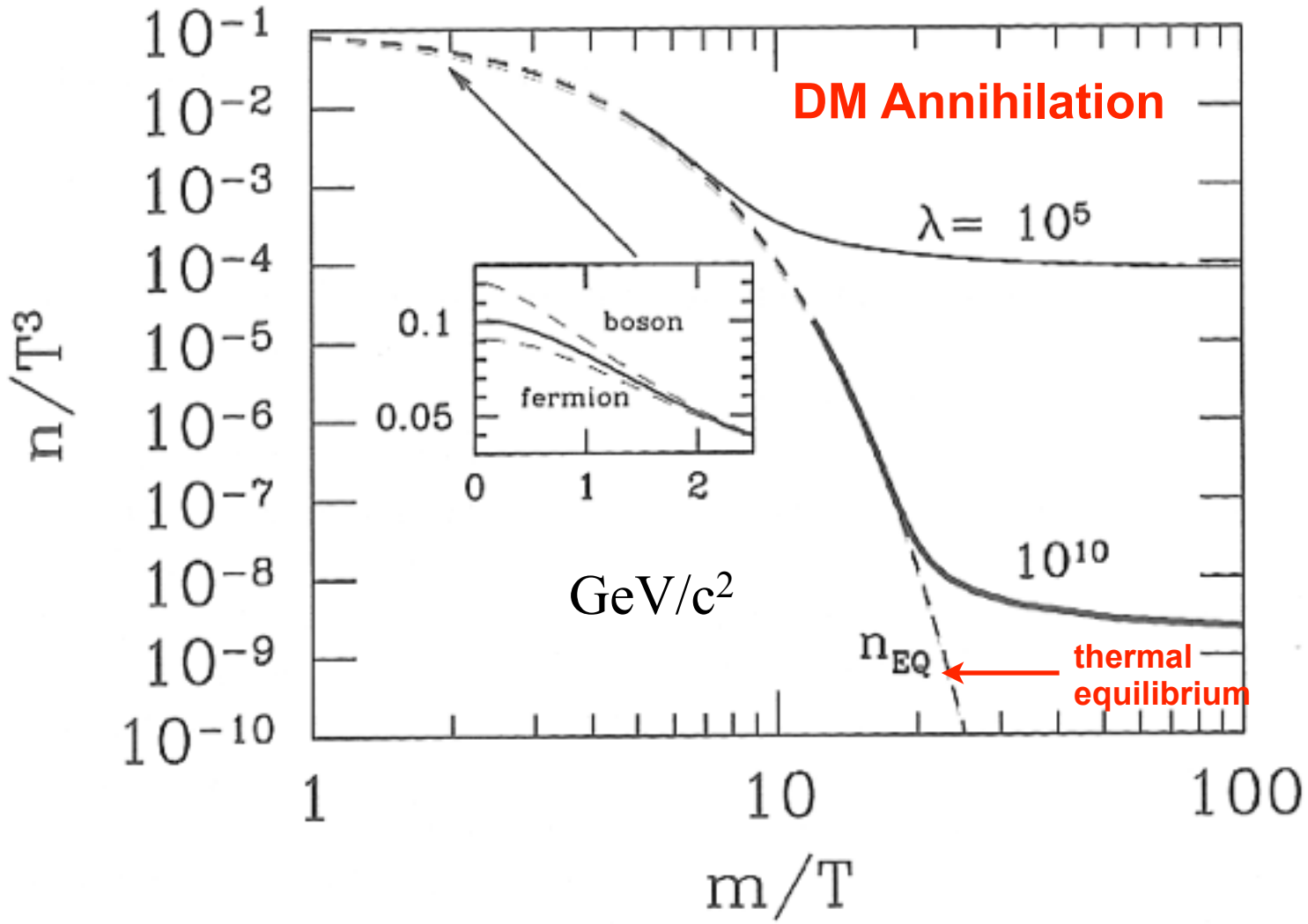

Figure 3.5. Abundance of heavy stable particle as the temperature drops beneath its mass. Dashed line is equilibrium abundance. Two different solid curves show heavy particle abundance for two different values of λ, the ratio of the annihilation rate to the Hubble rate. Inset shows that the difference between quantum statistics and Boltzmann statistics is important only at temperatures larger than the mass.

Dodelson, *Modern Cosmology*, p. 76

(Re)combination: $e^- + p \rightarrow H$

As long as e- + p ⇔ H remains in equilibrium, the condition

$$\left\{ \frac{n_3 n_4}{n_3^{(0)} n_4^{(0)}} - \frac{n_1 n_2}{n_1^{(0)} n_2^{(0)}} \right\} = 0$$

with 1 = e^-, 2 = p, 3 = H, ensures that

$$\frac{n_e n_p}{n_H} = \frac{n_e^{(0)} n_p^{(0)}}{n_H^{(0)}}.$$

Neutrality ensures $n_p = n_e$. Defining the free electron fraction

$$X_e \equiv \frac{n_e}{n_e + n_H} = \frac{n_p}{n_p + n_H},$$

the equation above becomes

$$\frac{X_e^2}{1 - X_e} = \frac{1}{n_e + n_H} \left[\left(\frac{m_e T}{2\pi} \right)^{3/2} e^{-[m_e + m_p - m_H]/T} \right]$$

, which

$\varepsilon = 13.6$ eV

is known as the *Saha equation*. When T ~ ε, the rhs ~ 10^{15}, so X_e is very close to 1 and very little recombination has yet occurred. As T drops, the free electron fraction also drops, and as it approaches 0 equilibrium cannot be maintained. To follow the freezeout of the electron fraction, it is necessary to use the Boltzmann equation

$$a^{-3} \frac{d\left(n_e a^3\right)}{dt} = n_e^{(0)} n_p^{(0)} \langle \sigma v \rangle \left\{ \frac{n_H}{n_H^{(0)}} - \frac{n_e^2}{n_e^{(0)} n_p^{(0)}} \right\}$$

$$= n_b \langle \sigma v \rangle \left\{ (1 - X_e) \left(\frac{m_e T}{2\pi} \right)^{3/2} e^{-\epsilon_0/T} - X_e^2 n_b \right\}$$

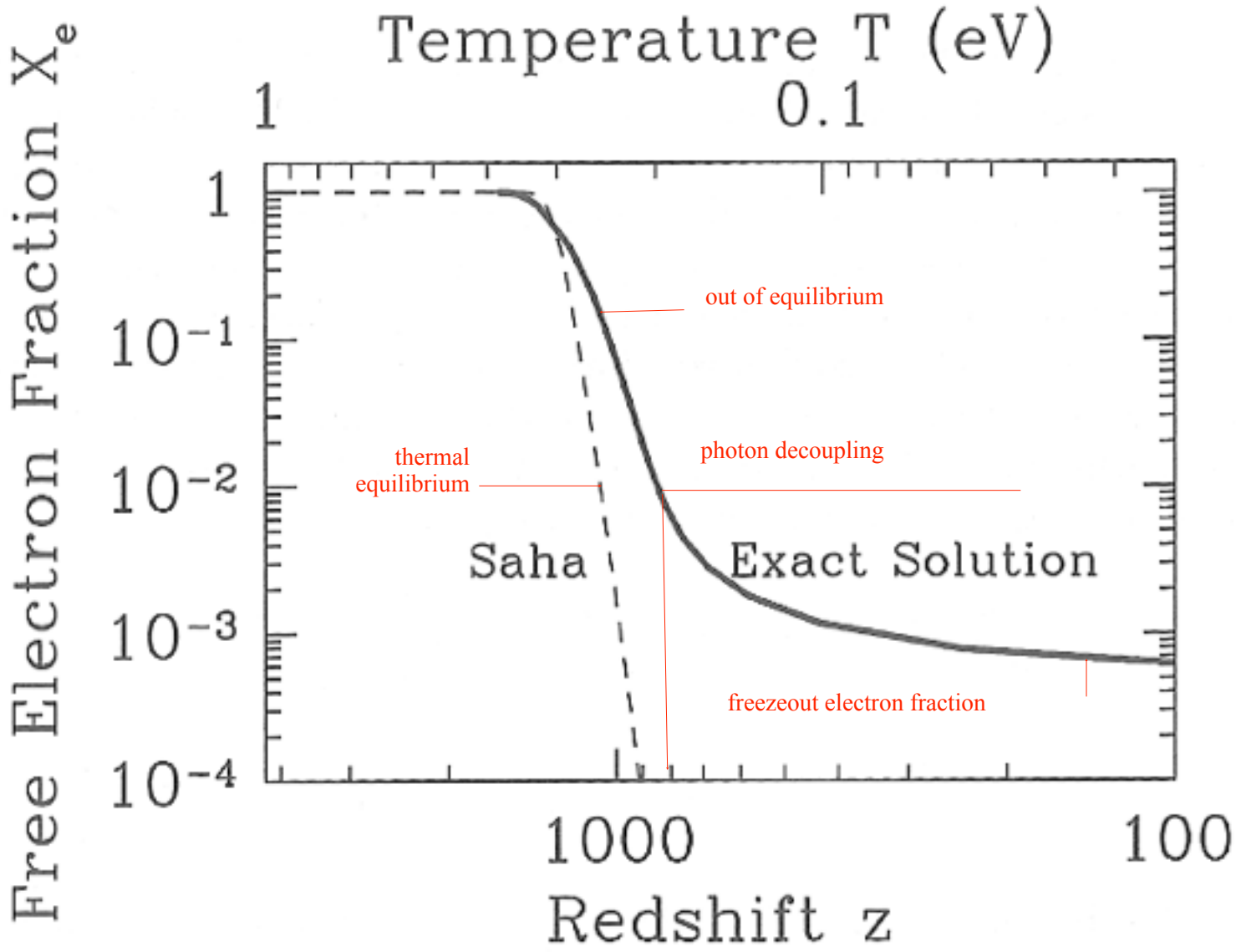

Figure 3.4. Free electron fraction as a function of redshift. Recombination takes place suddenly at $z \sim 1000$ corresponding to $T \sim 1/4$ eV. The Saha approximation, Eq. (3.37), holds in equilibrium and correctly identifies the redshift of recombination, but not the detailed evolution of X_e. Here $\Omega_b = 0.06, \Omega_m = 1, h = 0.5$.

Dodelson, *Modern Cosmology*, p. 72

Dark Matter Annihilation

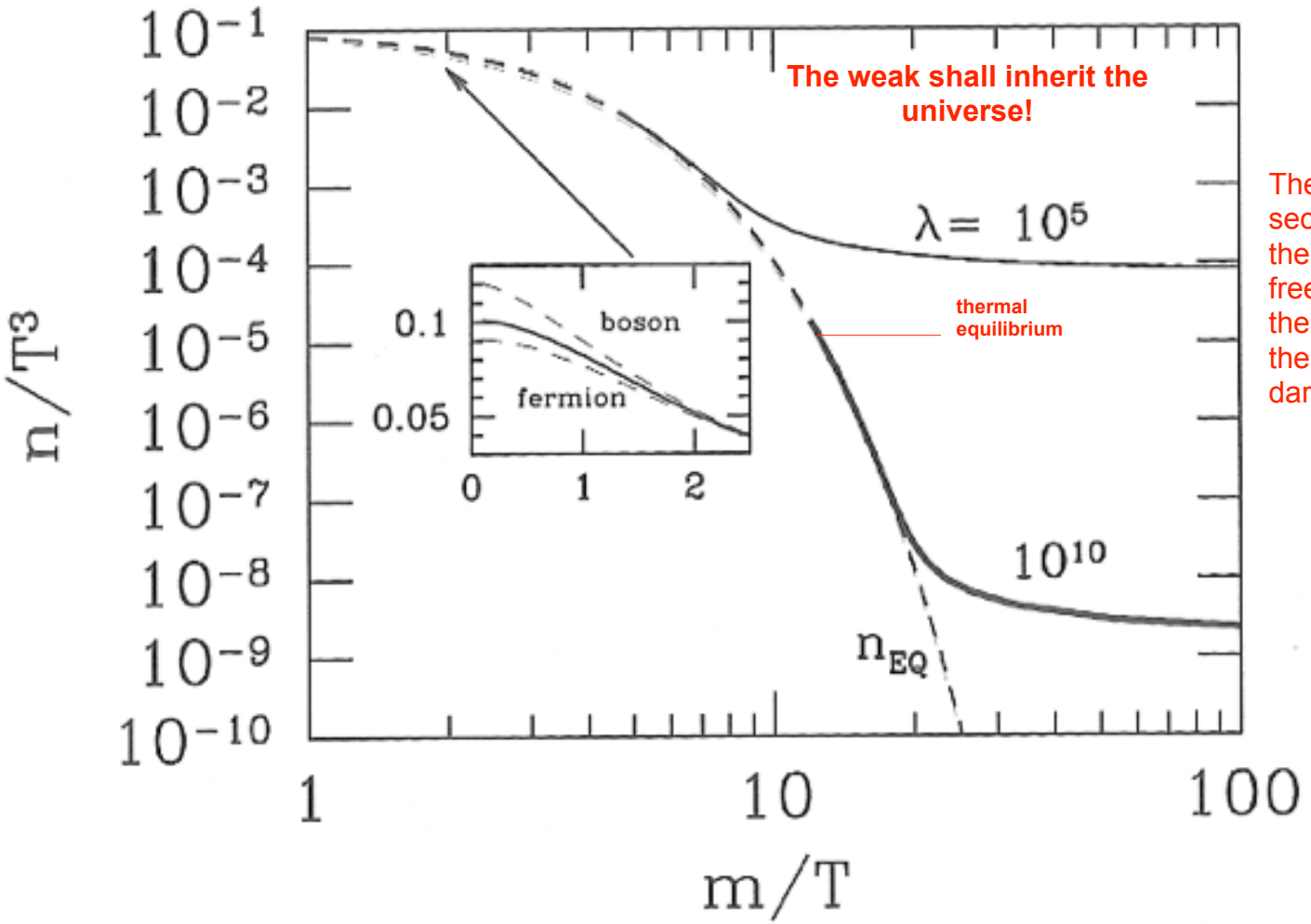

The weaker the cross section, the earlier freezeout occurs, and the larger the resulting dark matter density.

Figure 3.5. Abundance of heavy stable particle as the temperature drops beneath its mass. Dashed line is equilibrium abundance. Two different solid curves show heavy particle abundance for two different values of λ, the ratio of the annihilation rate to the Hubble rate. Inset shows that the difference between quantum statistics and Boltzmann statistics is important only at temperatures larger than the mass.

Dodelson, *Modern Cosmology*, p. 76

Dark Matter Annihilation

The abundance today of dark matter particles X of the WIMP variety is determined by their survival of annihilation in the early universe. Supersymmetric ("susy") neutralinos can annihilate with each other (and sometimes with other particles: "co-annihilation").

Dark matter annihilation follows the same pattern as the previous discussions: initially the abundance of dark matter particles X is given by the equilibrium Boltzmann exponential $\exp(-m_X/T)$, but as they start to disappear they have trouble finding each other and eventually their number density freezes out. The freezeout process can be followed using the Boltzmann equation, as discussed in Kolb and Turner, Dodelson, Mukhanov, and other textbooks. For a detailed discussion of Susy WIMPs, see the review article by Jungman, Kamionkowski, and Griest (1996). The result is that the abundance today of WIMPs X is given in most cases by (Dodelson's Eqs. 3.59-60)

$$\Omega_X = \left[\frac{4\pi^3 G g_*(m)}{45}\right]^{1/2} \frac{x_f T_0^3}{30\langle\sigma v\rangle\rho_{cr}} = 0.3h^{-2}\left(\frac{x_f}{10}\right)\left(\frac{g_*(m)}{100}\right)^{1/2}\frac{10^{-39}\mathrm{cm}^2}{\langle\sigma v\rangle}.$$

Here $x_f \approx 10$ is the ratio of m_X to the freezeout temperature T_f, and $g_*(m_X) \approx 100$ is the density of states factor in the expression for the energy density of the universe when the temperature equals m_X

$$\rho = \frac{\pi^2}{30}T^4\left[\sum_{i=\mathrm{bosons}} g_i + \frac{7}{8}\sum_{i=\mathrm{fermions}} g_i\right] \equiv g_*\frac{\pi^2}{30}T^4.$$

The sum is over relativistic species *i* (see the graph of $g(T)$ on the next slide). Note that more X's survive, the weaker the cross section σ. For Susy WIMPs the natural values are $\sigma \sim 10^{-39}$ cm^2, so $\Omega_X \approx 1$ naturally.

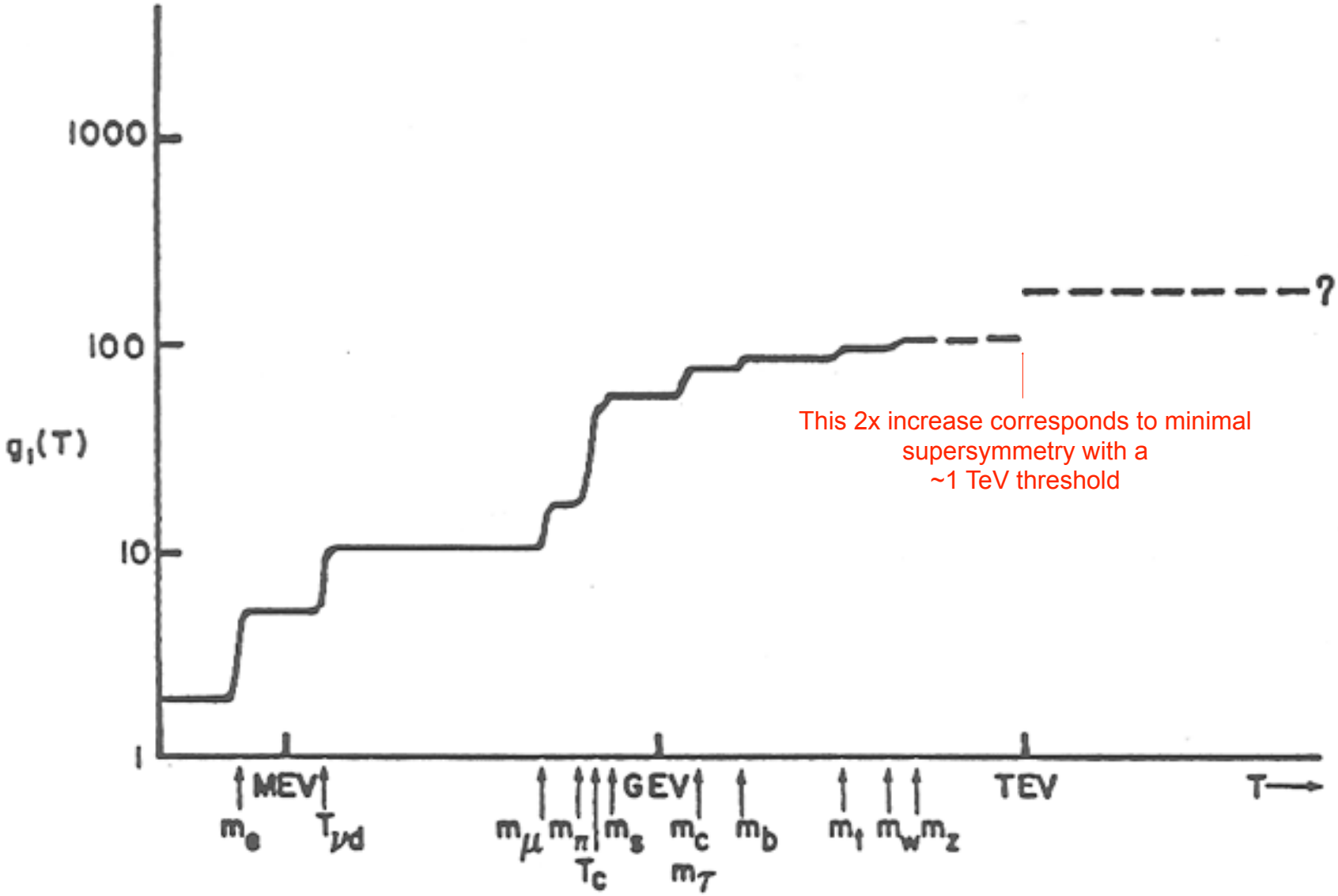

Fig. 1 The effective number of degrees of freedom of thermally interacting relativistic particles as a function of temperature.

Supersymmetry is the basis of most attempts, such as superstring theory, to go beyond the current "Standard Model" of particle physics. Heinz Pagels and Joel Primack pointed out in a 1982 paper that the lightest supersymmetric partner particle is stable because of R-parity, and is thus a good candidate for the dark matter particles – weakly interacting massive particles (**WIMP**s).

Michael Dine and others pointed out that the **axion**, a particle needed to save the strong interactions from violating CP symmetry, could also be the dark matter particle. Searches for both are underway.

Supersymmetric WIMPs

When the British physicist Paul Dirac first combined Special Relativity with quantum mechanics, he found that this predicted that for every ordinary particle like the electron, there must be another particle with the opposite electric charge – the anti-electron (positron). Similarly, corresponding to the proton there must be an anti-proton. Supersymmetry appears to be required to combine General Relativity (our modern theory of space, time, and gravity) with the other forces of nature (the electromagnetic, weak, and strong interactions). The consequence is another doubling of the number of particles, since supersymmetry predicts that for every particle that we now know, including the antiparticles, there must be another, thus far undiscovered particle with the same electric charge but with *spin* differing by half a unit.

Spin	**Matter** (fermions)	**Forces** (bosons)
2		graviton
1		photon, $W^{\pm}, Z^0$ gluons
1/2	quarks u,d,... leptons $e, \nu_e, \ldots$	
0		Higgs bosons axion

Supersymmetric WIMPs

When the British physicist Paul Dirac first combined Special Relativity with quantum mechanics, he found that this predicted that for every ordinary particle like the electron, there must be another particle with the opposite electric charge – the anti-electron (positron). Similarly, corresponding to the proton there must be an anti-proton. Supersymmetry appears to be required to combine General Relativity (our modern theory of space, time, and gravity) with the other forces of nature (the electromagnetic, weak, and strong interactions). The consequence is another doubling of the number of particles, since supersymmetry predicts that for every particle that we now know, including the antiparticles, there must be another, thus far undiscovered particle with the same electric charge but with *spin* differing by half a unit.

after doubling

Spin	**Matter** (fermions)	**Forces** (bosons)	**Hypothetical Superpartners**	**Spin**
2		graviton	gravitino	3/2
1		photon, $W^{\pm}, Z^0$ gluons	photino, winos, zino, gluinos	1/2
1/2	quarks u,d,... leptons $e, \nu_e, \ldots$		squarks $\tilde{u}, \tilde{d}, \ldots$ sleptons $\tilde{e}, \tilde{\nu}_e, \ldots$	0
0		Higgs bosons axion	Higgsinos axinos	1/2

Note: Supersymmetric cold dark matter candidate particles are underlined.

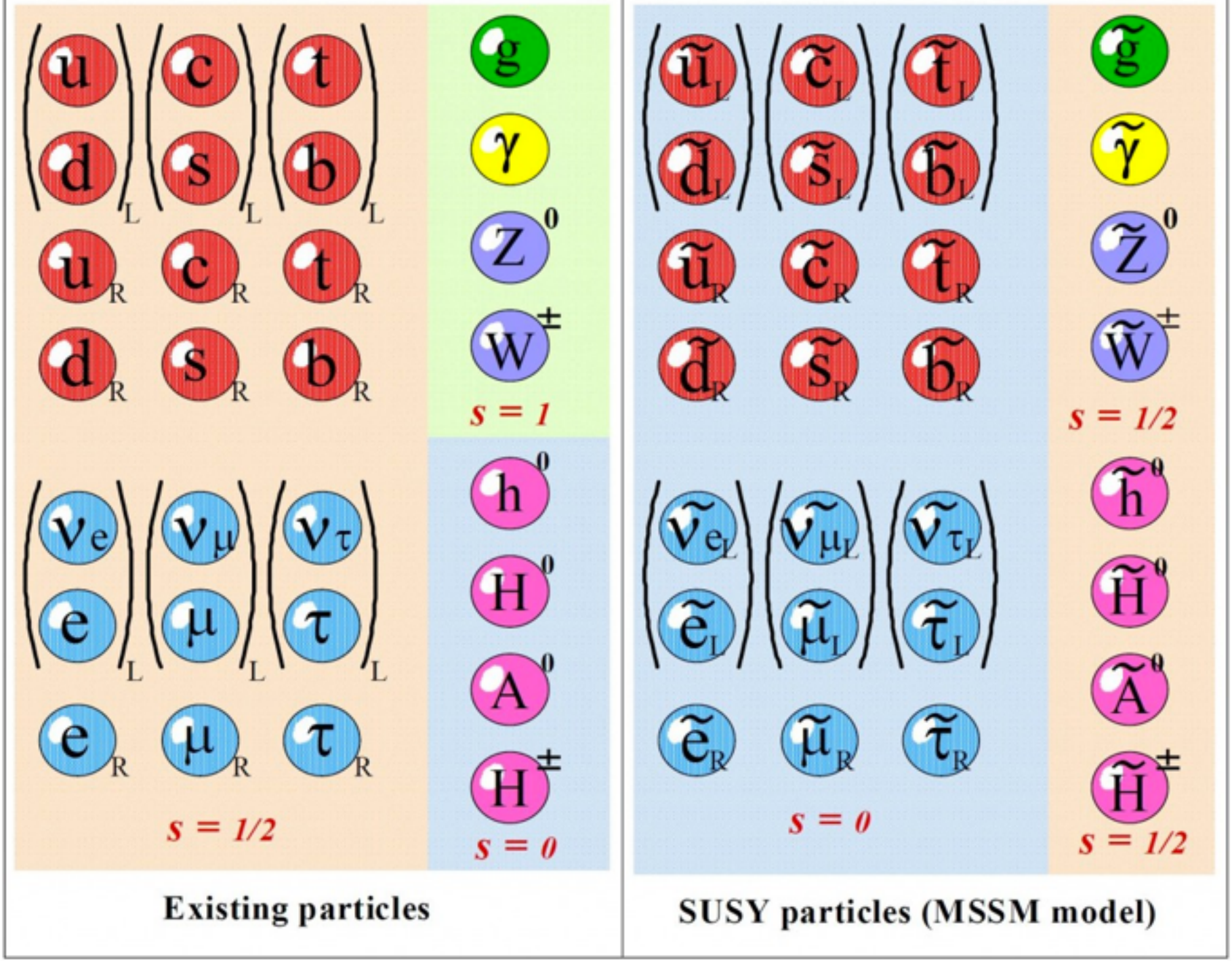
u c t
d s b
L L L
u c t
R R R
d s b
R R R
g
γ
Z 0
W ±
s = 1
h 0
H 0
A 0
H ±
s = 0
νe νμ ντ
e μ τ
L L L
e μ τ
R R R
s = 1/2
ũL c̃L t̃L
d̃L s̃L b̃L
ũR c̃R t̃R
d̃R s̃R b̃R
g̃
γ̃
Z̃ 0
W̃ ±
s = 1/2
ν̃eL ν̃μL ν̃τL
ẽL μ̃L τ̃L
ẽR μ̃R τ̃R
s = 0
h̃ 0
H̃ 0
Ã 0
H̃ ±
s = 1/2
Existing particles
SUSY particles (MSSM model)

Supersymmetric WIMPs, continued

Spin is a fundamental property of elementary particles. Matter particles like electrons and quarks (protons and neutrons are each made up of three quarks) have spin ½, while force particles like photons, W,Z, and gluons have spin 1. The supersymmetric partners of electrons and quarks are called selectrons and squarks, and they have spin 0. The supersymmetric partners of the force particles are called the photino, Winos, Zino, and gluinos, and they have spin ½, so they might be matter particles. The lightest of these particles might be the photino. Whichever is lightest should be stable, so it is a natural candidate to be the dark matter WIMP. Supersymmetry does not predict its mass, but it must be more than 50 times as massive as the proton since it has not yet been produced at accelerators. But it will be produced soon at the LHC, if it exists and its mass is not above ~1 TeV!

ATLAS SUSY Searches* - 95% CL Lower Limits (CMS results are similar)

Status: SUSY 2013

ATLAS Preliminary

$\int \mathcal{L}\,dt$ = (4.6 - 22.9) fb^{-1} $\sqrt{s}$ = 7, 8 TeV

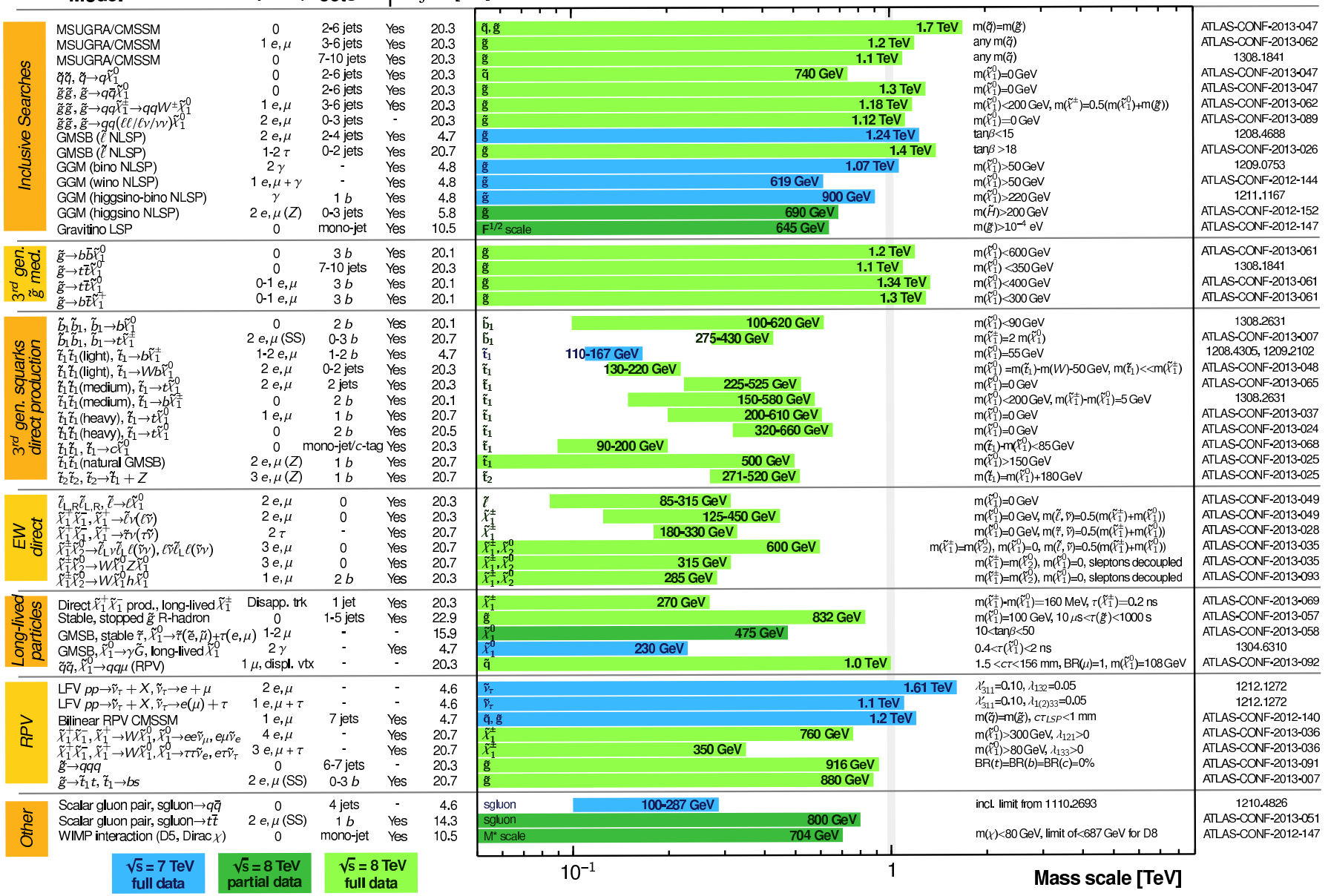

*Only a selection of the available mass limits on new states or phenomena is shown. All limits quoted are observed minus 1σ theoretical signal cross section uncertainty.

(From PDG Supersymmetry Experiment - Sept 2013)

SUPERSYMMETRY

The only experimental evidence for supersymmetry is that running of coupling constants in the Standard Model (dashed lines in figure) does not lead to Grand Unification of the weak, electromagnetic, and strong interactions, while with supersymmetry the three couplings all do come together at a scale just above 10^{16} GeV. The figure assumes the Minimal Supersymmetric Standard Model (MSSM) with sparticle masses between 250 GeV and 1 TeV.

Other arguments for SUSY include: helps unification of gravity since it controls the vacuum energy and moderates loop divergences (fermion and boson loop divergences cancel), solves the hierarchy problem, and naturally leads to DM with $\Omega \sim 1$.

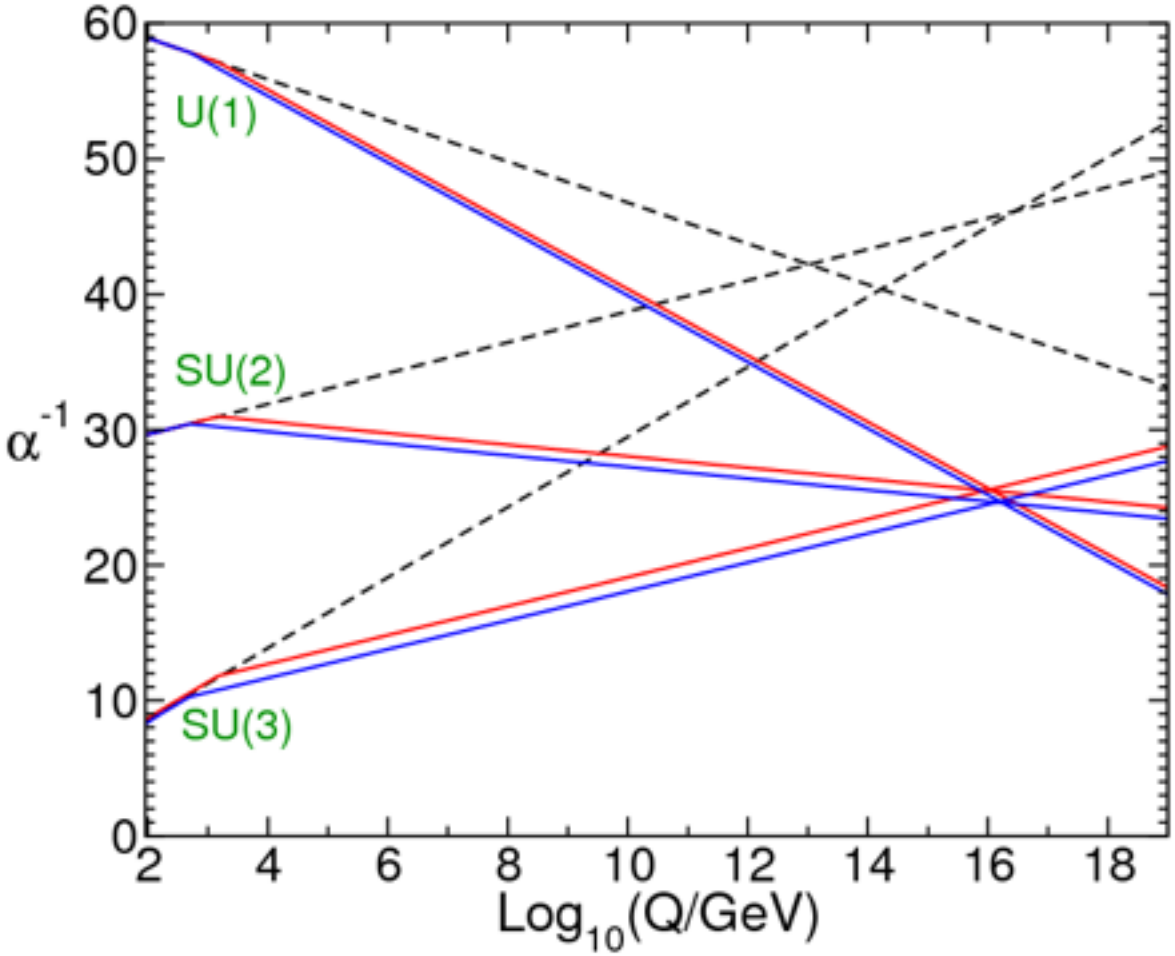

figs from S. P. Martin, A Supersymmetry Primer, arXiv:hep-ph/9709356v5

Experiments are Underway for Detection of WIMPs

Direct detection - general principles

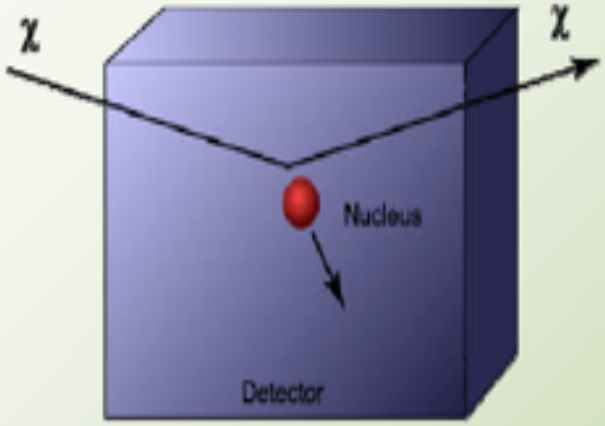

- WIMP + nucleus → WIMP + nucleus
- Measure the nuclear recoil energy
- Suppress backgrounds enough to be sensitive to a signal, or...

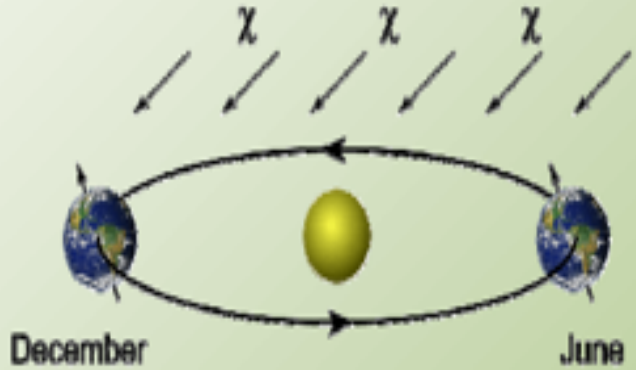

- Search for an annual modulation due to the Earth's motion around the Sun

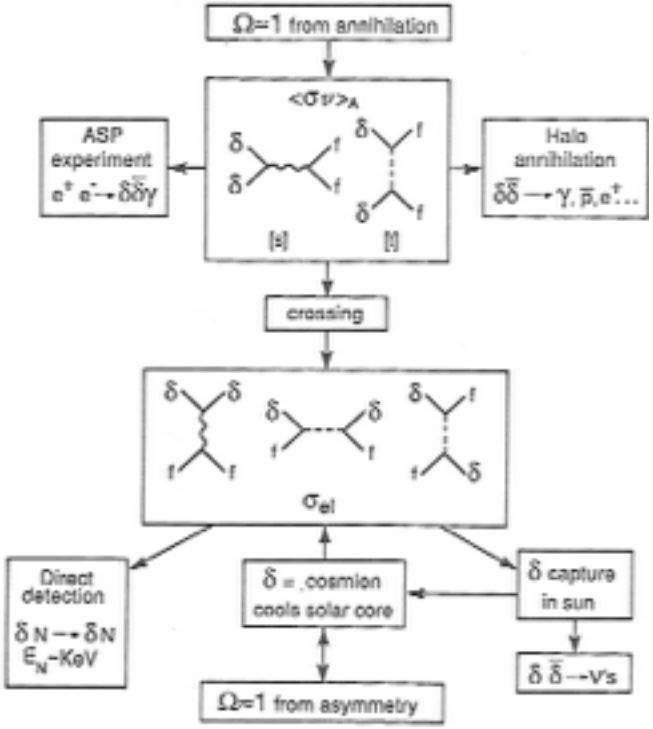

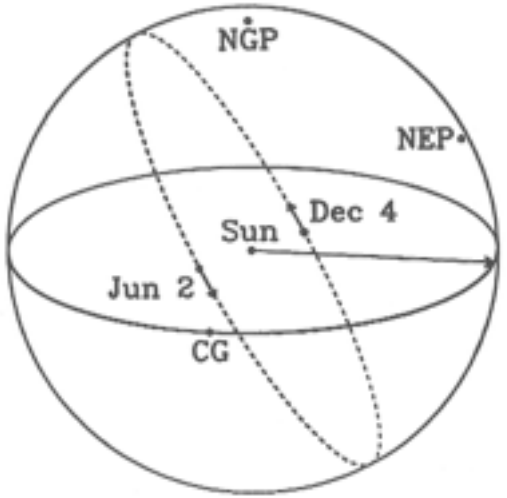

Primack, Seckel, & Sadoulet (1987)

and also AXIONs

The diagram at right shows the layout of the axion search experiment now underway at the Lawrence Livermore National Laboratory. Axions would be detected as extra photons in the Microwave Cavity.

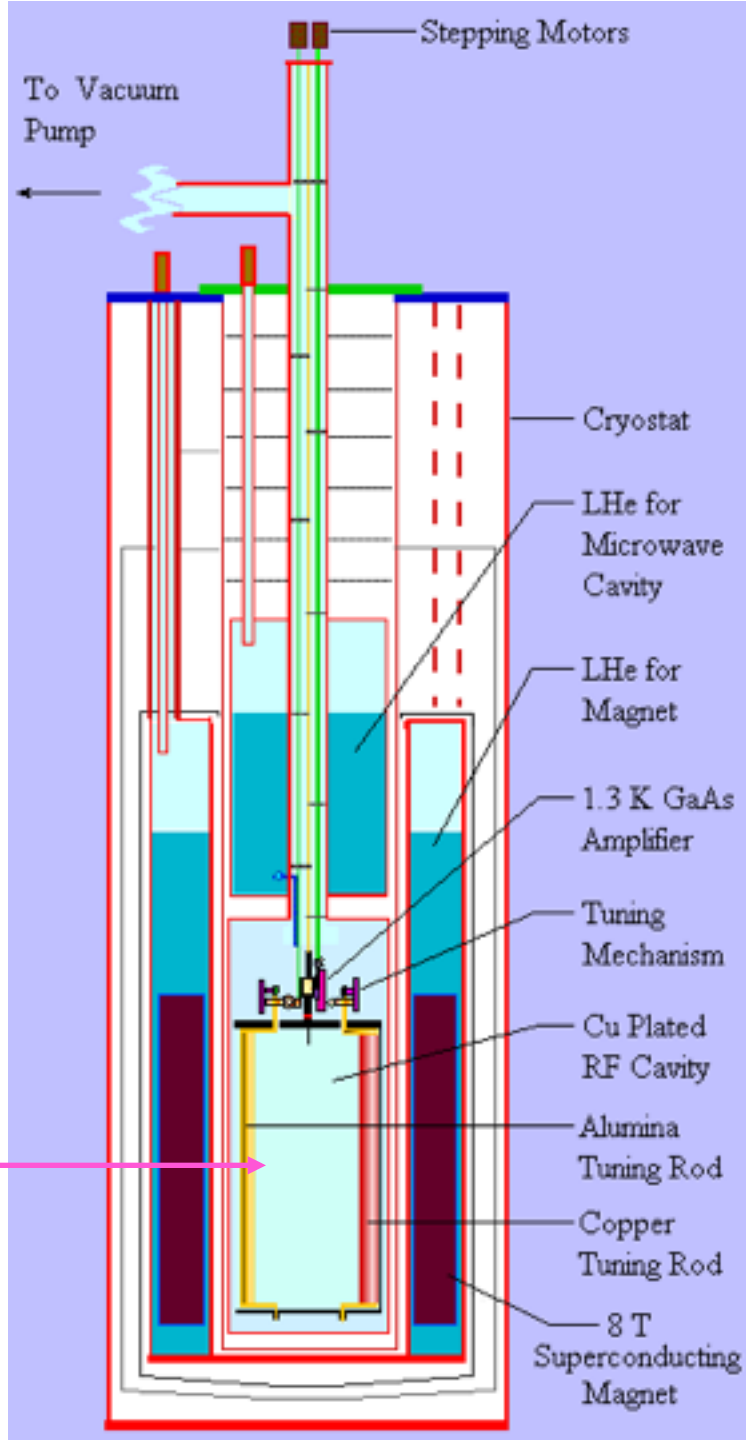

Types of Dark Matter

Ω_i represents the fraction of the critical density $\rho_c = 10.54\ h^2$ keV/cm^3 needed to close the Universe, where h is the Hubble constant H_0 divided by 100 km/s/*Mpc*.

Dark Matter Type	Fraction of Critical Density	Comment
Baryonic	$\Omega_b \sim 0.04$	about 10 times the visible matter
Hot	$\Omega_\nu \sim 0.001$–0.1	light neutrinos
Cold	$\Omega_c \sim 0.3$	most of the dark matter in galaxy halos

Dark Matter and Associated Cosmological Models

Ω_m represents the fraction of the critical density in all types of matter.
Ω_Λ is the fraction contributed by some form of "dark energy."

Acronym	Cosmological Model	Flourished
HDM	hot dark matter with $\Omega_m = 1$	1978–1984
SCDM	standard cold dark matter with $\Omega_m = 1$	1982–1992
CHDM	cold + hot dark matter with $\Omega_c \sim 0.7$ and $\Omega_\nu = 0.2$–0.3	1994–1998
ΛCDM	cold dark matter $\Omega_c \sim 1/3$ and $\Omega_\Lambda \sim 2/3$	1996–today

Joel Primack, *Beam Line*, Fall 2001

WHAT IS THE DARK MATTER?

Prospects for DIRECT and INDIRECT detection of WIMPs are improving.

With many ongoing and upcoming experiments

- Production at Large Hadron Collider
- Better CMB data from PLANCK
- Direct Detection
  - Spin Independent - CDMS-II, XENON100, LUX
  - Spin Dependent - COUPP, PICASSO
- Indirect detection via
  - Fermi and larger ACTs
  - PAMELA and AMS

-- there could well be a big discovery in the next few years!

Four roads to dark matter: *catch it, infer it, make it, weigh it*

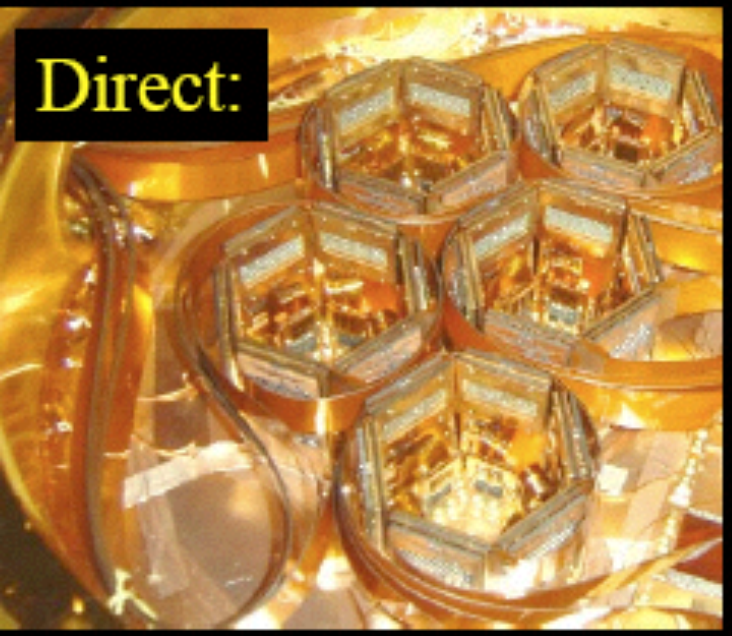

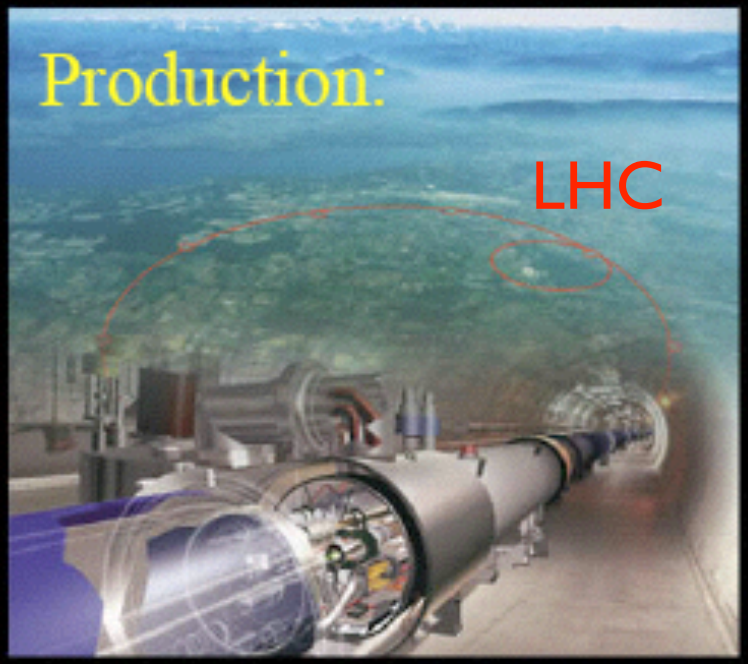

With all these upcoming experiments, the next few years will be very exciting!

Fermi (GLAST) launched June 11, 2008

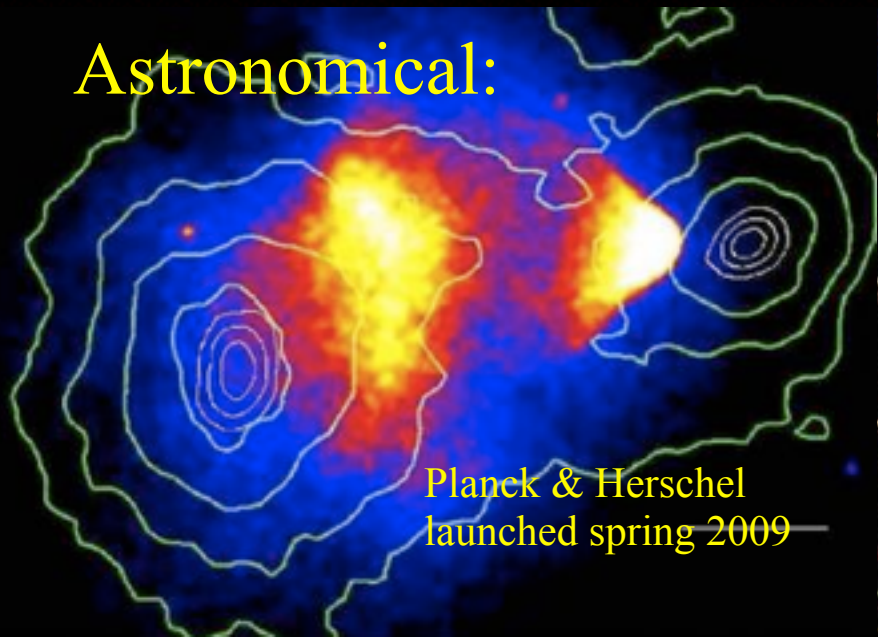

Planck & Herschel launched spring 2009

Supersymmetric WIMP (δ) annihilation is related by crossing to WIMP Direct Detection by Elastic Scattering

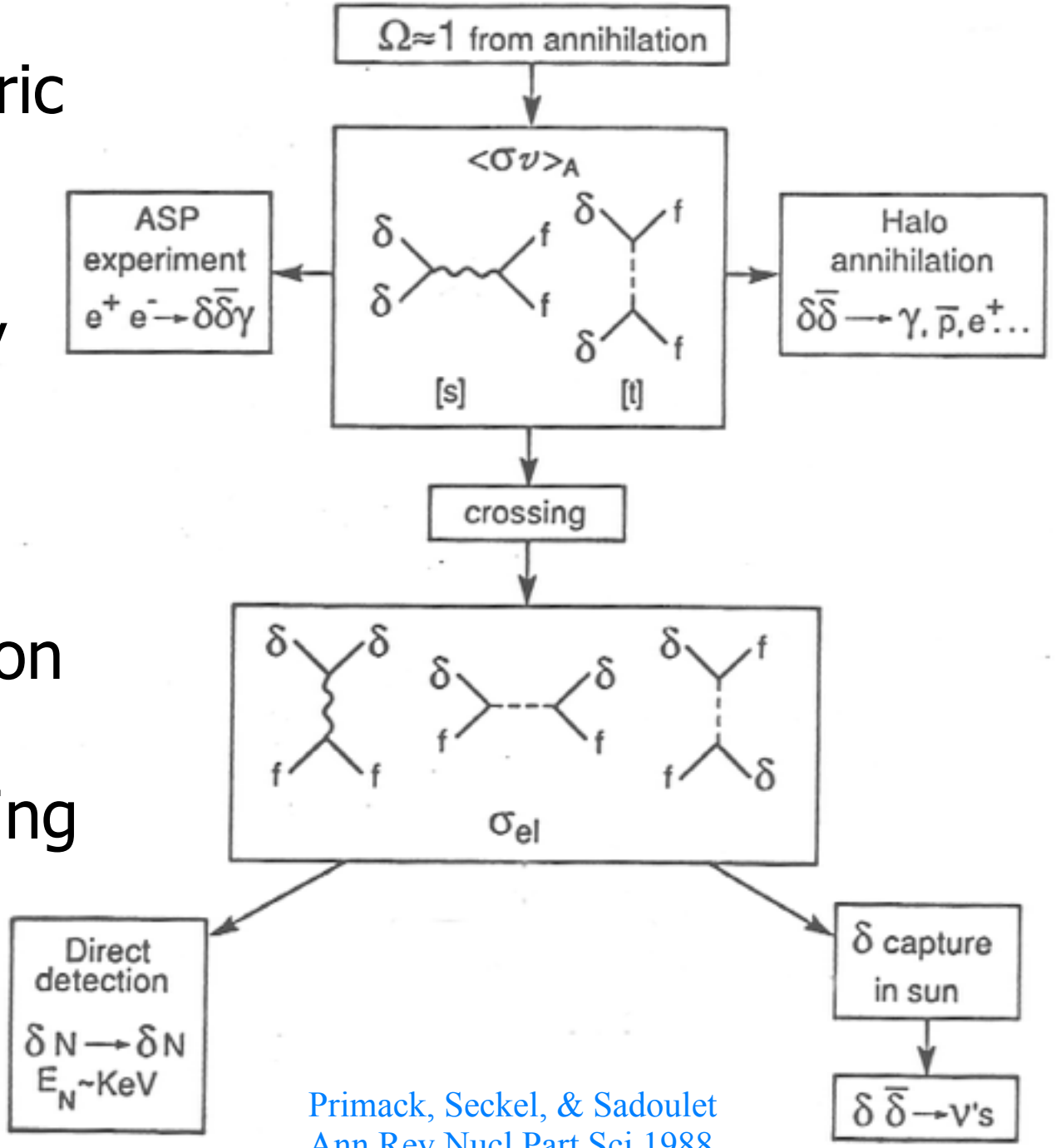

Primack, Seckel, & Sadoulet
Ann Rev Nucl Part Sci 1988

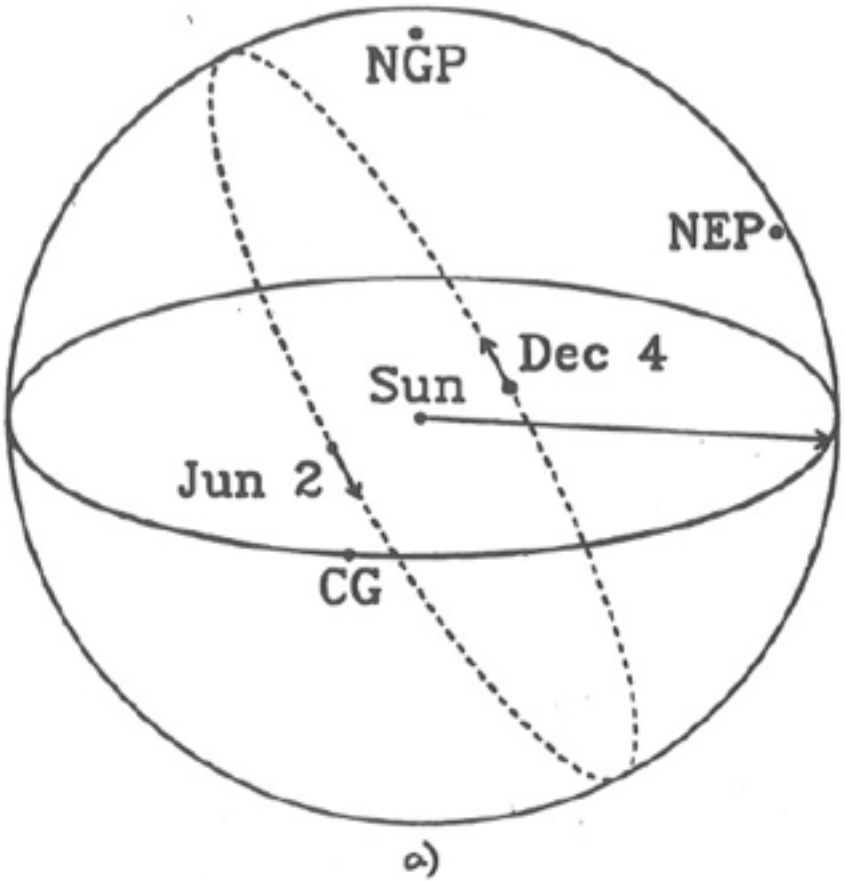

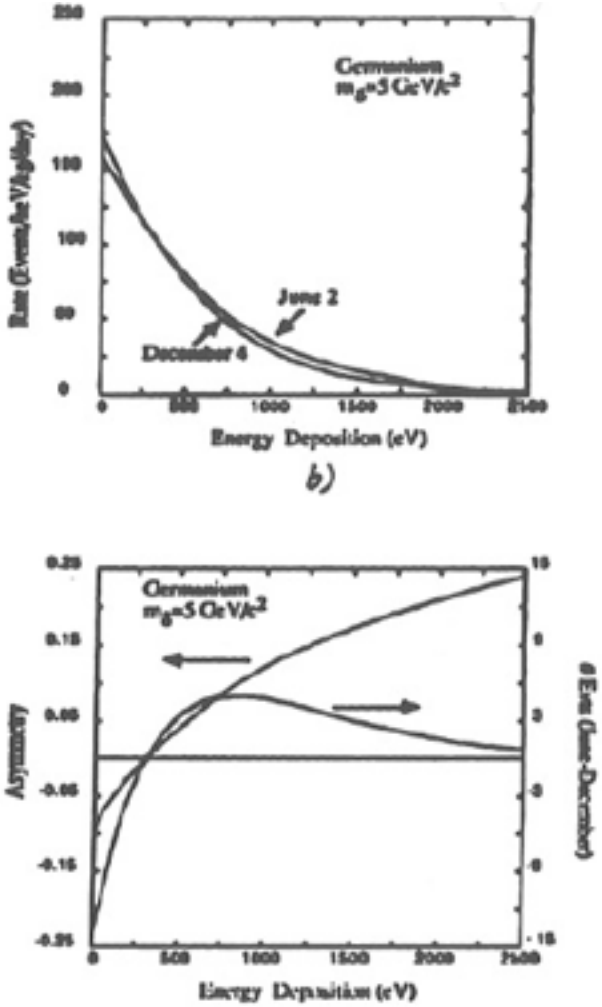

Figure 3. Annual effect in WIMP detection by elastic scattering. (a) Why expected: The solid line (darker in the front) shows the plane of the galactic disk and the Sun's orbit; the dashed circle is the orbit of the Earth (ecliptic plane). NGP and NEP are the north galactic and ecliptic poles. CG shows the direction toward the galactic center, and the long and short arrows show the Sun's and the Earth's velocities. The sum of the Sun's and Earth's velocities reaches its maximum on June 2 (248 km s^{-1}) and minimum on December 4 (219 km s^{-1}). (These velocities with respect to the galactic center are obtained neglecting the small eccentricity of the Earth's orbit, and assuming that the Sun's peculiar velocity is 16.5 km s^{-1} in the galactic direction $l = 53°$, $b = 25°$ with respect to the local standard of rest (cf. 116). Event rates in WIMP detectors actually depend on the Earth's velocity with respect to the DM halo, whose rotational velocity is uncertain.) (b) Rate for June 2 and December 4 vs. deposited energy. (c) June – December difference (right axis) and asymmetry (left axis) vs. deposited energy. Note that although the asymmetry increases with the energy deposition, the rate and therefore also the June – December rate difference both decrease at high energy deposition.

Primack, Seckel, & Sadoulet, Ann Rev Nucl Part Sci 1988

DAMA Evidence for WIMP detection

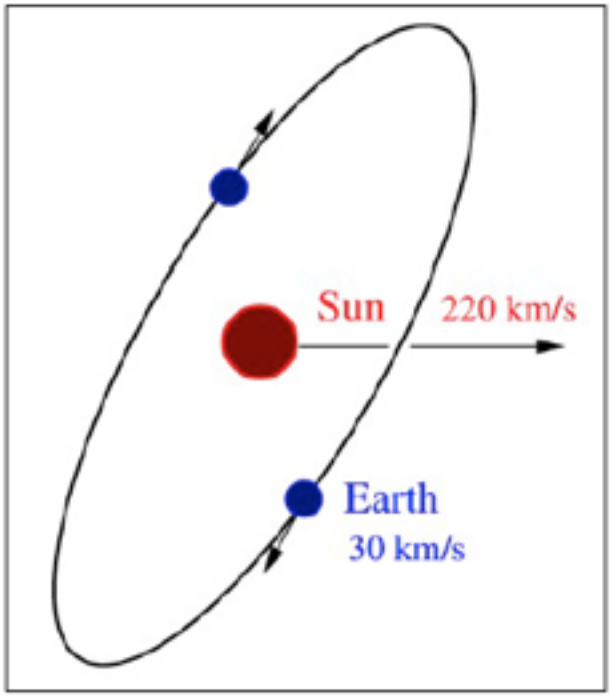

Annual modulation of WIMP signal a "smoking gun" signature

DAMA experiment in Gran Sasso (NaI scintillation detector) observes an annual modulation at a 6.3σ statistical CL, based on 110 ton-days of data [Riv. N. Cim. 26 (2003) 1–73]

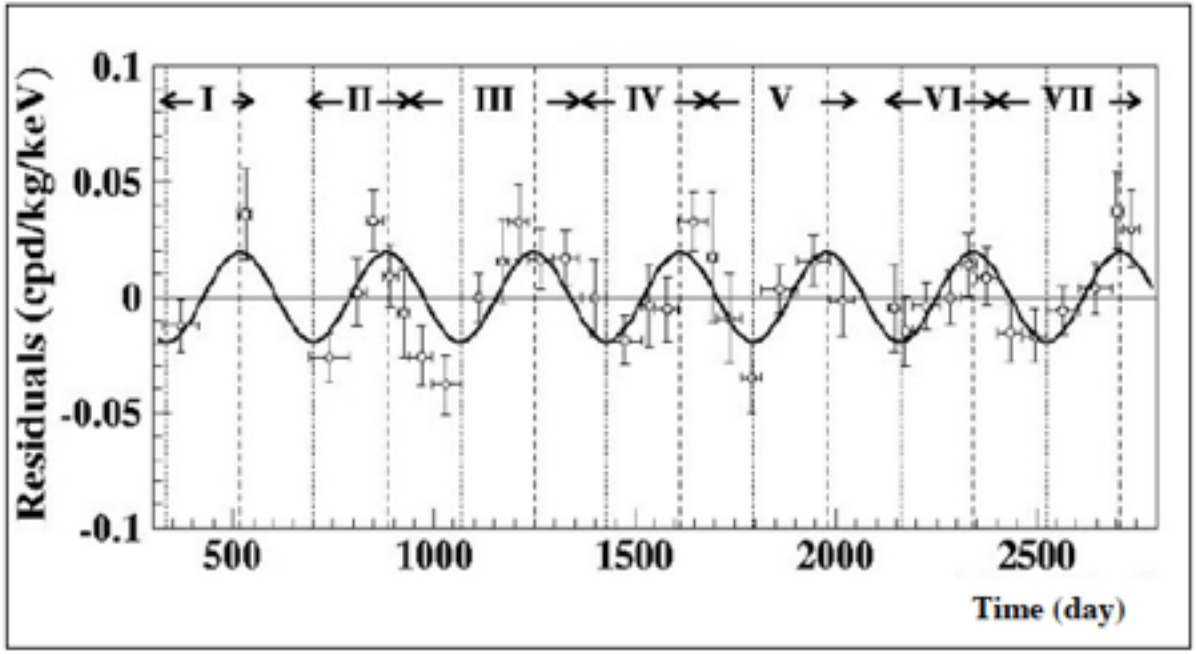

- Detector stability ?
- Background stability ?

DAMA / LIBRA

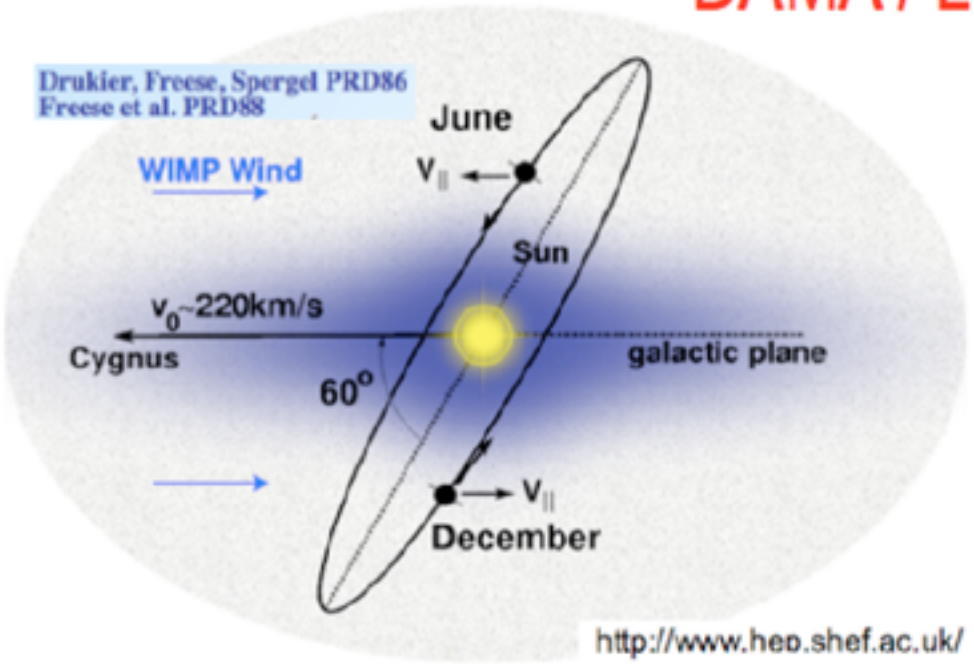

- Annual Modulation
  - Significance is 8.9σ
  - 1-2% effect in bin count rate
  - Appears in lowest energy bins
  - Can another experiment observe this effect?

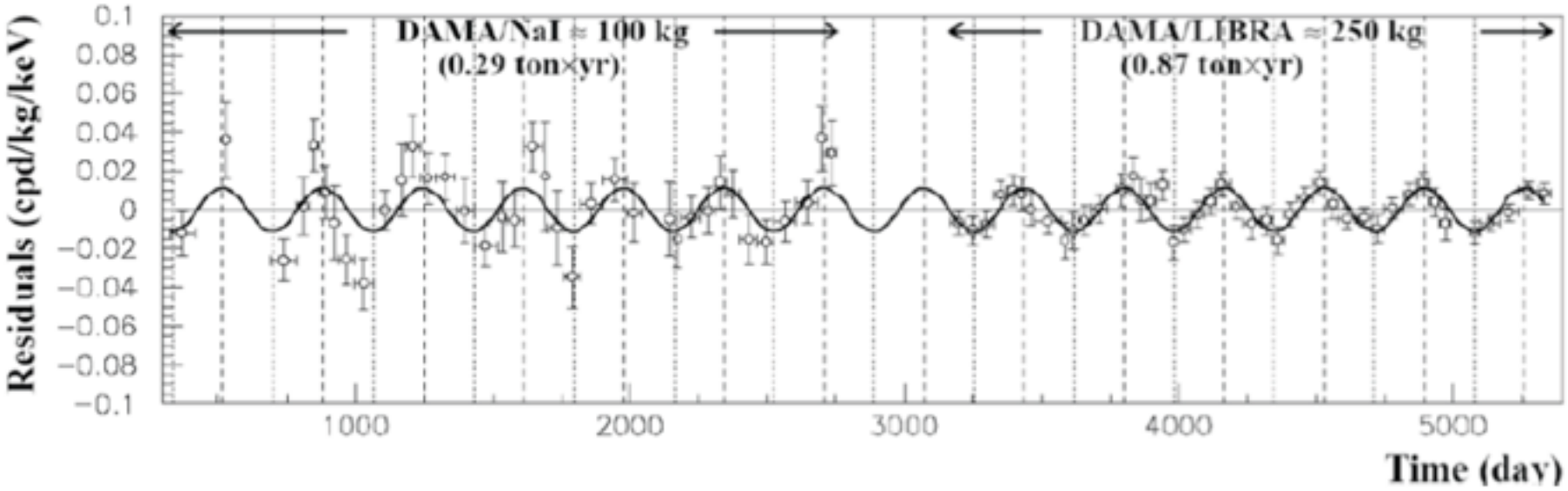

DAMA Interpretation vs. Other Limits

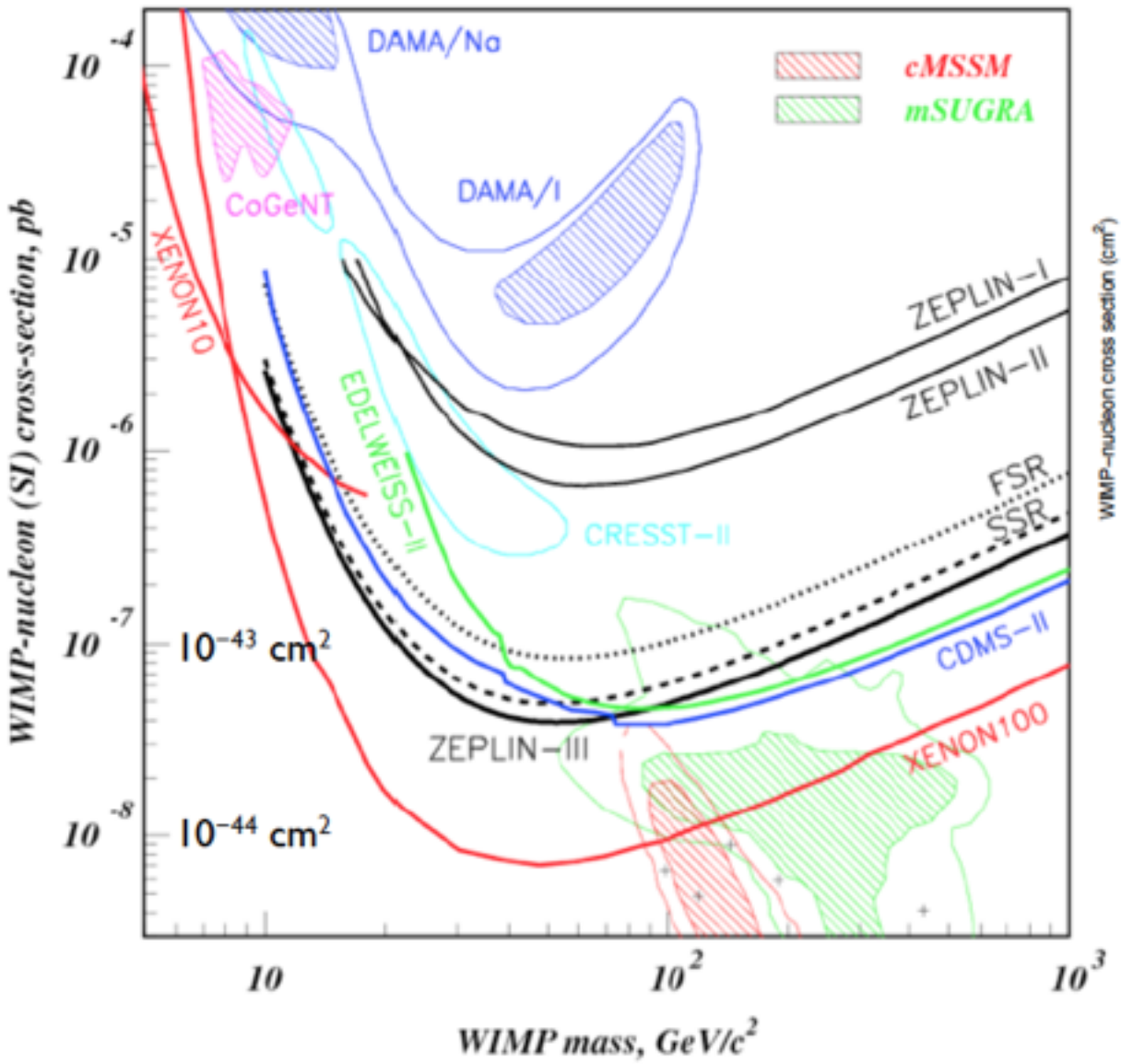

LUX Preliminary Upper Limits

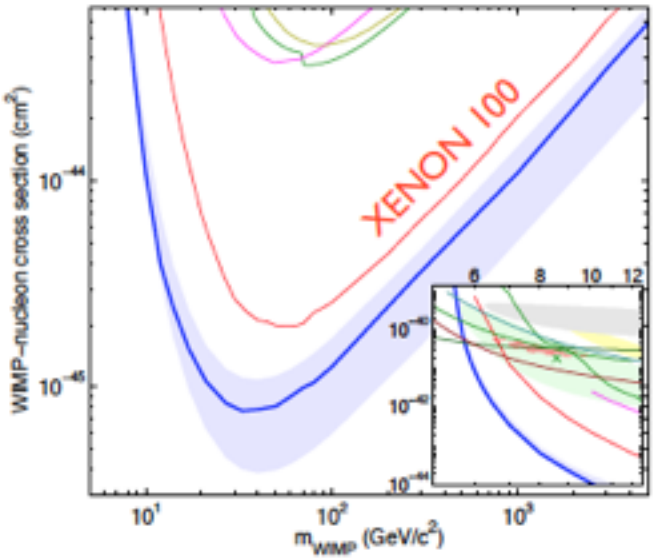

barn = 10^{-28} m^2 = 10^{-24} cm^2
picobarn = 10^{-12} barn
= 10^{-36} cm^2

Low Mass WIMPs - Fully Excluded by LUX

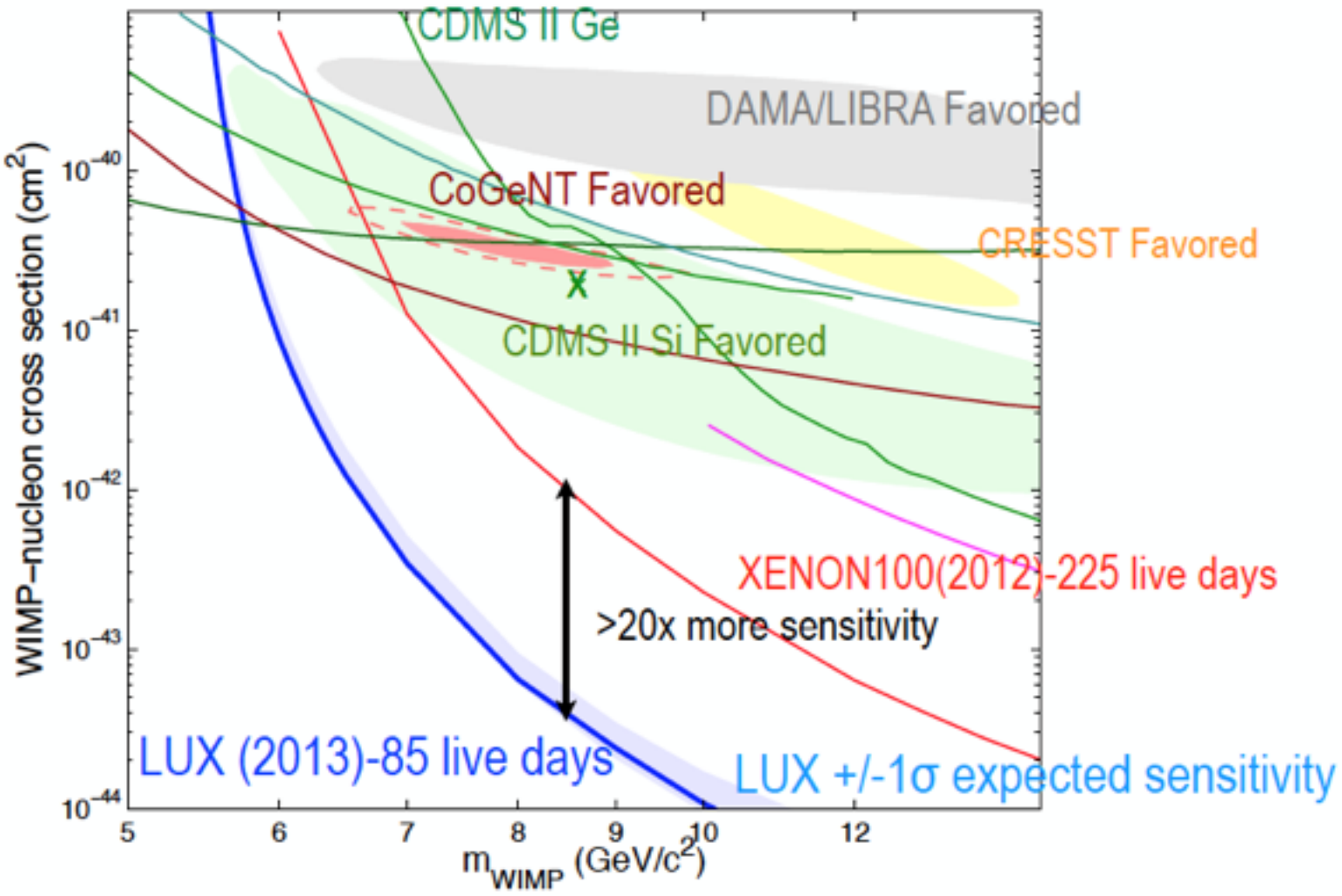

Direct Detection Methods

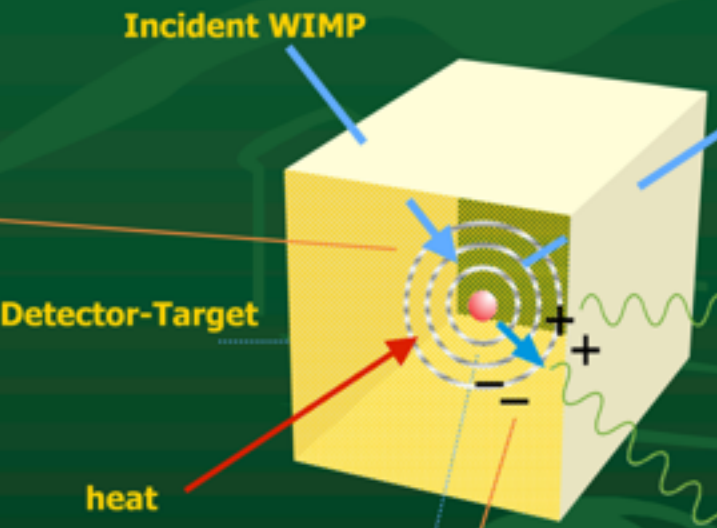

HEAT

Bolometers:
- MiDBD
- ROSEBUD-I
- CRESST-I
- CUORICINO

Metastable p.det:
- SSD Micrograins
- SDD Droplets

LIGHT

Xe-scintillators:
- DAMA-Xe
- ZEPLIN-I

NaI scintillators:
- NAIAD
- ANAIS
- DAMA, LIBRA
- ELEGANTS

HEAT+CHARGE
- CDMS
- EDELWEISS

CHARGE

Ge-experiments:
- H/M
- IGEX
- GENIUS-TF

Tracking Chambers:
- DRIFT

HEAT+LIGHT
- ROSEBUD-II
- CRESST-II

LIGHT+CHARGE
- ZEPLIN-II
- X-MASS
- XENON100
- LUX
- XENON 1000
- PANDA X

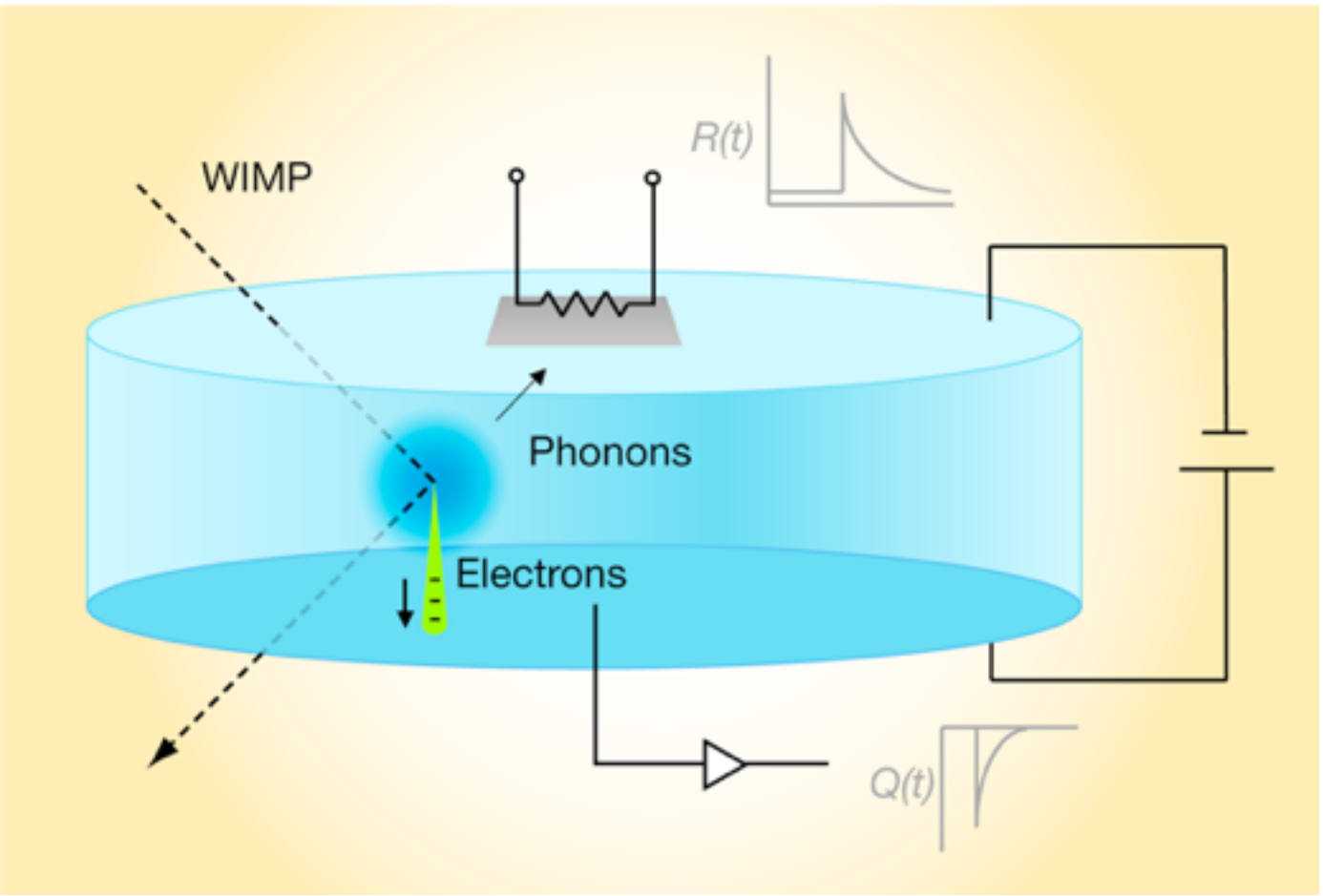

CDMS - Cryogenic DM Search

Berkeley-Stanford-led experiment has been at the forefront

Figure from: Perspective by Karl van Bibber http://physics.aps.org/viewpoint-for/10.1103/PhysRevLett.102.011301 on Z. Ahmed et al. CDMS Collaboration, "Search for Weakly Interacting Massive Particles with the First Five-Tower Data from the Cryogenic Dark Matter Search at the Soudan Underground Laboratory," Phys. Rev. Lett. 102, 011301 (2009) – Published January 05, 2009

Schematic of an individual detector within CDMS. A WIMP scattering from a germanium nucleus produces a low-energy nuclear recoil, resulting in both ionization and athermal phonons. Charge carriers drift out to one face of the detector under the influence of a small electric field, and are detected with a sensitive amplifer [signal shown as Q(t)]. Phonons reaching the other face break Cooper pairs in a thin superconducting aluminum layer; the resulting quasiparticles heat a transition-edge sensor (TES) bonded to the aluminum layer, causing a measurable momentary change in its resistance R(t). In reality, the readout elements on both sides are highly segmented, and the relative timing of the ionization and phonon signals recorded, to provide good event localization.

CDMS-II shielded underground detector array

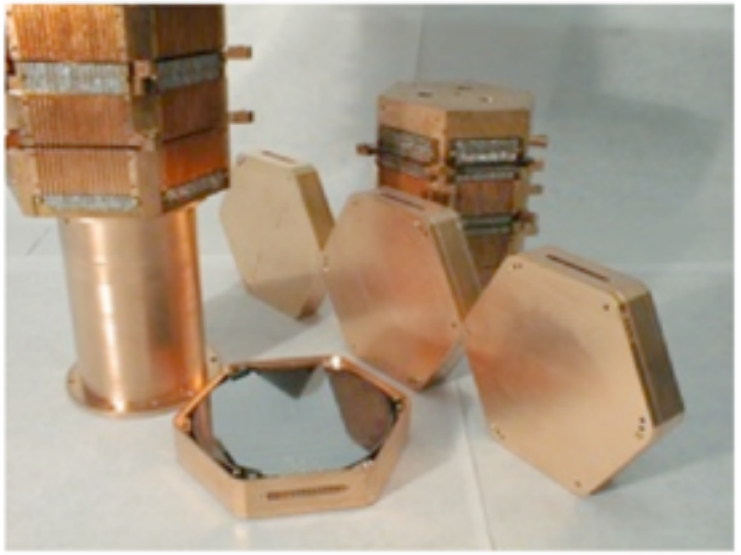

2000 mwe

Cu ft. @ 50 mK

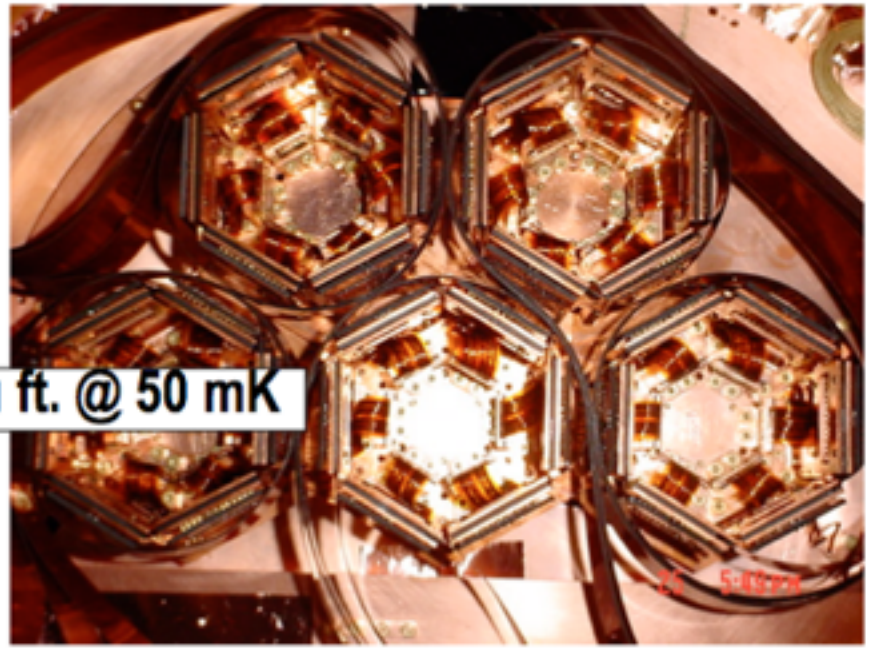

Slide from Sunil Golwal

From CDMS II to SuperCDMS and GEODM

CDMS II

Ø7.5cm x 1cm ZIP — 16 detectors = 4 kg
0.25 kg/detector — 2 yr, 1700 kg-d

SuperCDMS Soudan (G1)

Ø7.5cm x 2.5cm iZIP — 15 detectors = 10 kg*
0.64 kg/detector — 2 yr, 4000 kg-d
*iZIP has 2x larger fiducial efficiency than CDMS II ZIP

SuperCDMS SNOLAB (G2)

Ø10cm x 3.3cm iZIP — 72 detectors = 110 kg
1.5 kg/detector — 3 yr = 100,000 kg-d

GEODM (G3)

Ø15cm x 5cm iZIP — 300 detectors = 1.5 T
5.1 kg/detector — 3 yr, 1.5 M kg-d

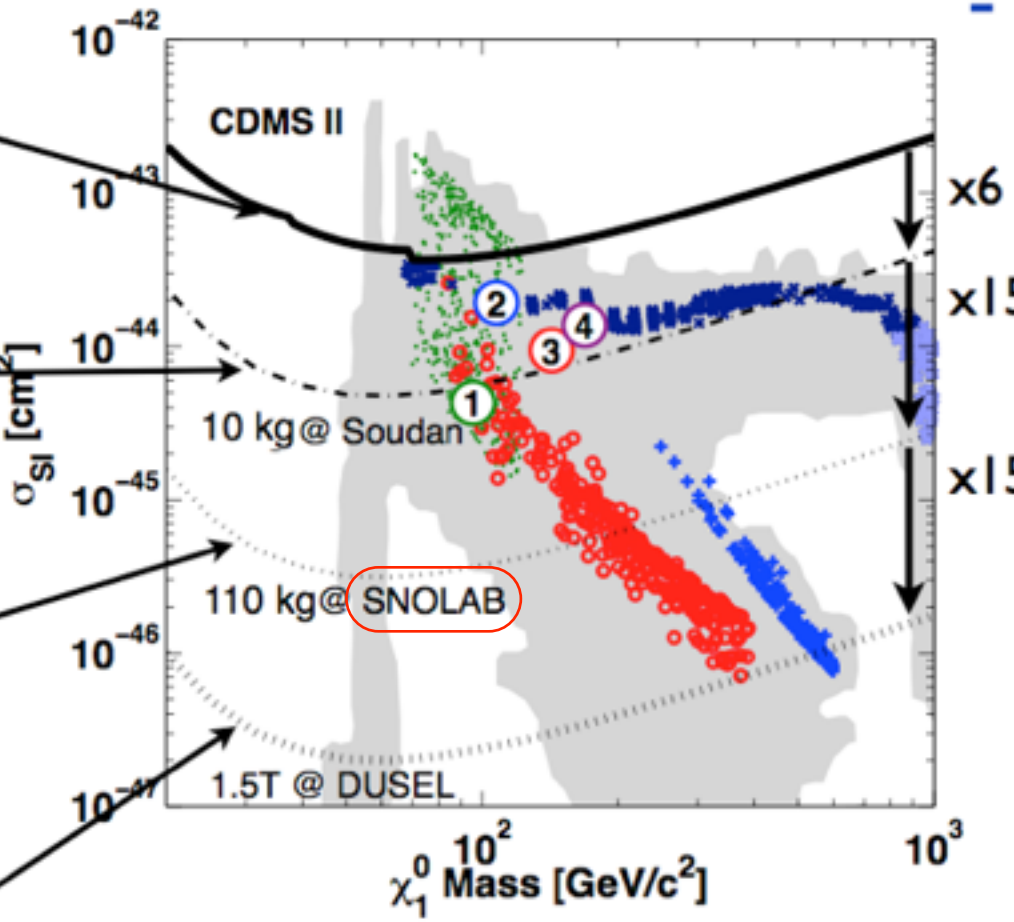

Staged three-prong program to explore MSSM or study a signal:

- decreased backgrounds
- improved background rejection
- increase in mass/detector and decrease in cost/detector

< 1 event misid'd bgnd at each stage

SuperCDMS Future

Slide reformatted from Sunil Golwala

- SuperCDMS Soudan (G1)
  - 15 iZIP detectors being commissioned, science running to begin soon
  - 2 yrs, ~4000 kg-d raw exposure expected
  - sensitivity will be set by residual radiogenic neutron background:
    - 5×10^{-45} cm^2 (0 events) to 8×10^{-45} cm^2 (expected bgnd)
- SuperCDMS SNOLAB (G2)
  - 2 SuperCDMS Soudan detectors with ^{210}Pb sources will establish rejection needed for SuperCDMS SNOLAB (~10^{-5})
  - R&D toward 10 cm x 3.3 cm detectors funded, actively pushing development of:
    - crystal quality demonstration from vendors with ionization-only tests
    - phonon sensor design
    - cryogenic electronics and hardware and 300K electronics
    - shielding/cryostat design incl. possible neutron veot
  - Will propose to 2012 NSF and DOE solicitations, hope for construction start FY14
- GEODM
  - Planning to continue in parallel "G3 long-term R&D" on 15-cm diameter crystals, multiplexed and alternate forms of phonon and ionization readout, shielding and cosmogenic neutron studies.


SNOLAB
Mining for knowledge
Creuser pour trouver... l'excellence


X5


AUG
SNO


USE AIR SH


USE AIR SHOWER


SEARCH FOR DARK MATTER WITH


GUINNESS

DM Direct Search Progress Over Time (2012)

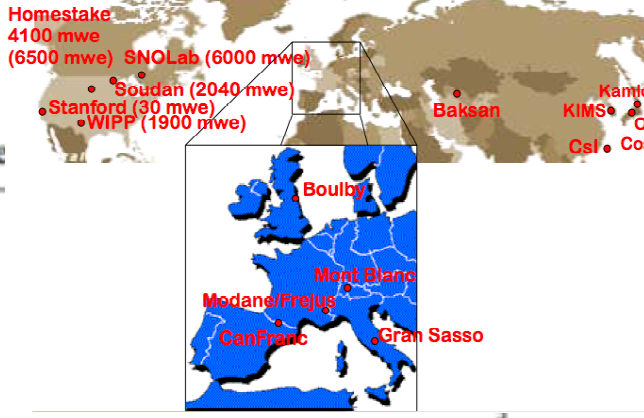

liquid noble detectors

- WIMP-nucleus elastic scattering produces ionization electrons and photons.
- Photons (primary scintillation) are detected by PMTs
- Electrons are drifted (by E field) to gas region, where they are accelerated and collide with gas atoms, producing secondary scintillation
- Shape of primary and ratio of primary to secondary signal depend on ionizing particle (WIMP looks different from ex. beta decay electron)

http://warp.lngs.infn.it/

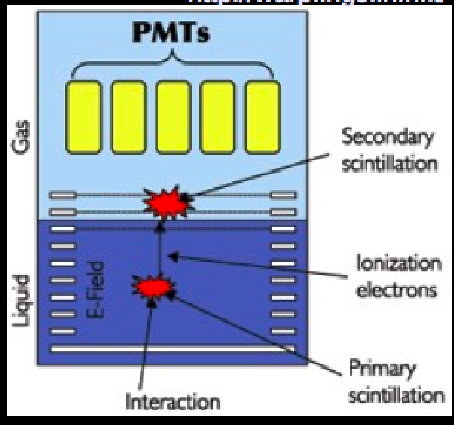

Noble Liquid Comparison (DM Detectors)

	Scintillation Light	Intrinsic Backgrounds	WIMP (100 GeV) Sensitivity vs Ge >10 keVr
Ne (A=20) $60/kg 100% even-even nucleus	85 nm Requires wavelength Shifter	Low BP (20K) - all impurities frozen out No radioactive isotopes	Scalar Coupling: Eth>50 keVr, 0.02x Axial Coupling: 0 (no odd isotope)
Ar (A=40) $2/kg (isotope separation >$1000/kg) ~100% even-even	125 nm Requires wavelength shifter	Nat Ar contains ~39Ar 1 Bq/kg == ~150 evts/keVee/kg/day at low energies. Requires isotope separation, low 39Ar source, or very good discrimination (~10^6 to match CDMS II)	Scalar Coupling: Eth>50 keVr, 0.10x Axial Coupling: 0 (no odd isotope)
Xe (A=131) $1000/kg 50% odd isotope	175 nm UV quartz PMT window	136Xe double beta decay is only long lived isotope - below pp solar neutrino signal. Relevant for DM search below ~10^{-47} cm^2. 85Kr can be removed by charcoal or distillation separation.	Scalar Coupling: Eth>5 keVr, 1.30x Axial Coupling: ~5x (model dep) Xe is 50% odd n isotope 129Xe, 131Xe

Future of Direct Detection

- Experiments under construction, to release results in 2009-2010
  - Target masses 10-300 kg
  - Expect 10-100x better reach than existing limits.
- Next Round, for results in 2011-2013
  - Target masses 1-3 tonne, 10^3 x better reach
  - Project cost $5-15M
- "Ultimate" Detectors, for results ~2014+
  - Target masses 3-50 tonne, 10^4 x better reach
  - Project cost $20-50M
- Labs with 1-20 tonne dm experiments on roadmap
  - Gran Sasso, Italy
  - Frejus, France
  - Canfranc, Spain
  - Kamioka, Japan
  - SNOLab, Canada
  - Sanford Lab/DUSEL (Homestake), US

LUX Dark Matter Experiment

- Brown [Gaitskell], Case [Shutt], LBNL [Lesko] , LLNL [Bernstein], Maryland [Hall], Rochester [Wolfs], Texas A&M [White], UC Davis [Svoboda/Tripathi], U South Dakota [Mei] , Yale [McKinsey]
  - XENON10,ZEPLIN II (US),CDMS; ν Detectors (Kamland/SuperK/SNO/Borexino); HEP/γ-ray astro
  - Also ZEPLIN III Groups in next phase
  - Co-spokespersons: Gaitskell (Brown) / Shutt (Case)
- 300 kg Dual Phase liquid Xe TPC with 100 kg fiducial
  - Using conservative assumptions: >99.4% ER background rejection for 50% NR acceptance, E>5 keVr (ER rejection is energy dependent)
    (Case+Columbia/Brown Prototypes + XENON10 + ZEPLIN II)
  - 3D-imaging TPC eliminates surface activity, defines fiducial
- Backgrounds:
  - Internal: strong self-shielding of PMT activity
    - Can achieve BG $\gamma+\beta < 8\times10^{-4}$ /keVee/kg/day, dominated by PMTs (Hamamatsu R8778).
    - Neutrons (α,n) & fission subdominant
  - External: large water shield with muon veto.
    - Very effective for cavern γ+n, and HE n from muons
    - Very low gamma backgrounds with readily achievable $<10^{-11}$ g/g purity.
- DM reach: 7×10^{-46} cm^2 in 10 months

In DUSEL

(Deep Underground Science and Engineering Laboratory)
Homestake Mine
Lead, South Dakota, USA
April 2012 - operation Sept 2012

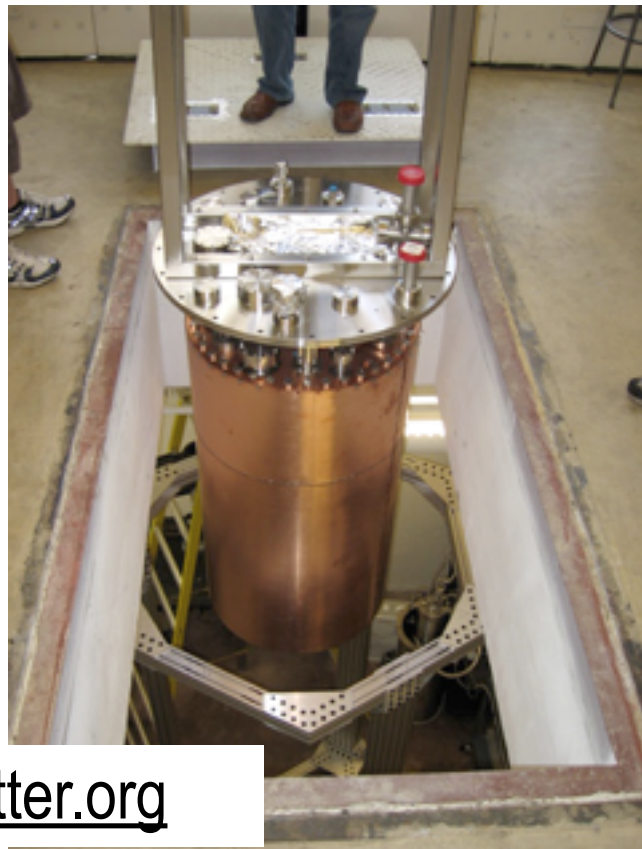

www.luxdarkmatter.org

LUX in the Davis Laboratory at the Homestake Mine in South Dakota (4850L)

- Construction/excavation design completed
  - New 300' access/safety tunnel being excavated
  - Shared with Majorana facility
- Two story, dedicated LUX 55' x 30' x 32' facility being built now

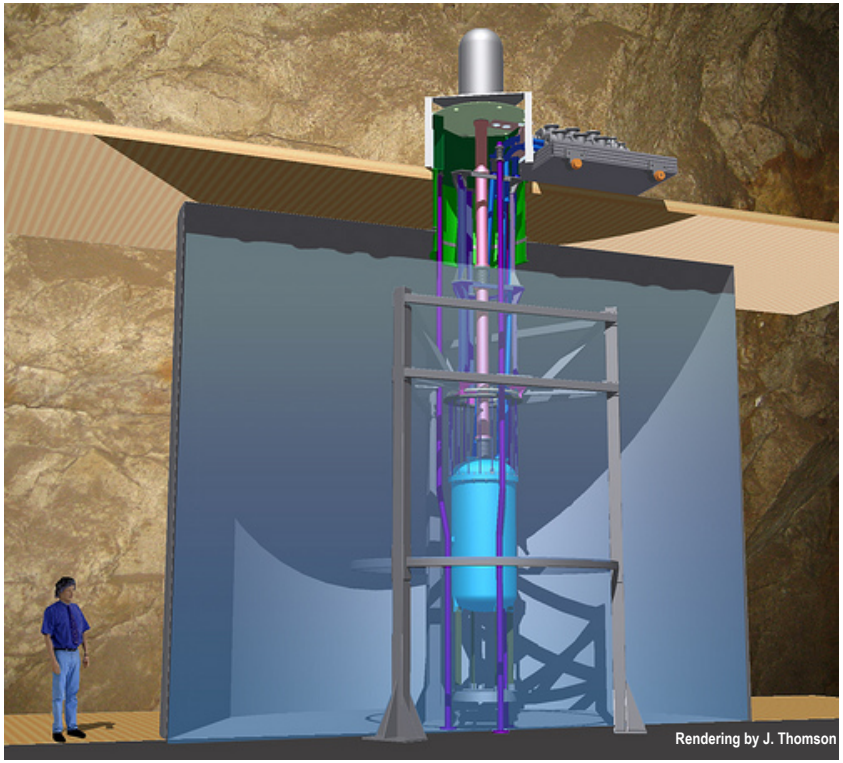

- Beneficial occupancy:
  ~~November/ December 2010~~
  April 2012

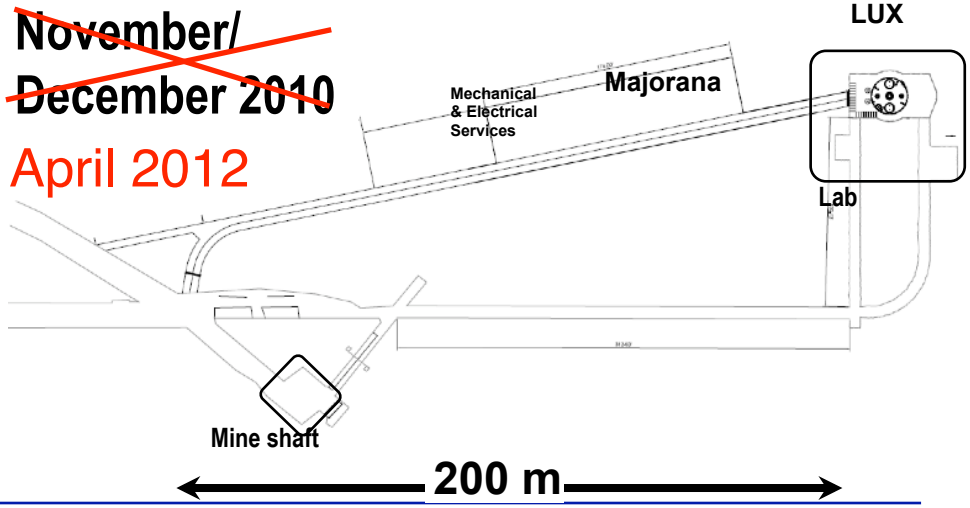

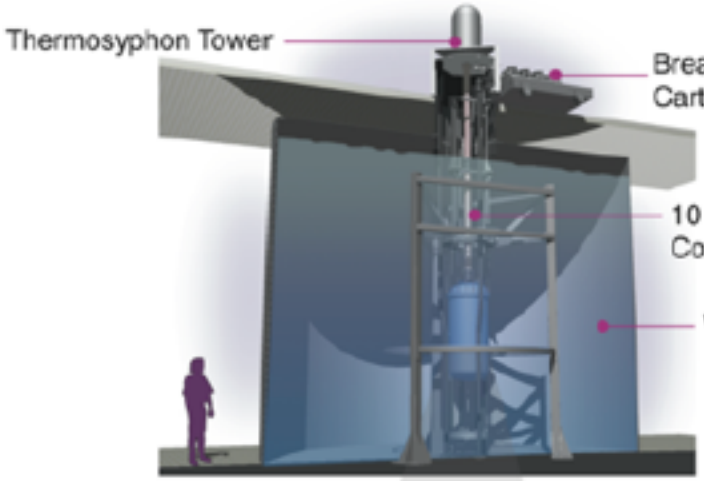
Thermosyphon Tower
Breakout Instrumentation Cart
10 m Instrumentation Conduits
Water Shield

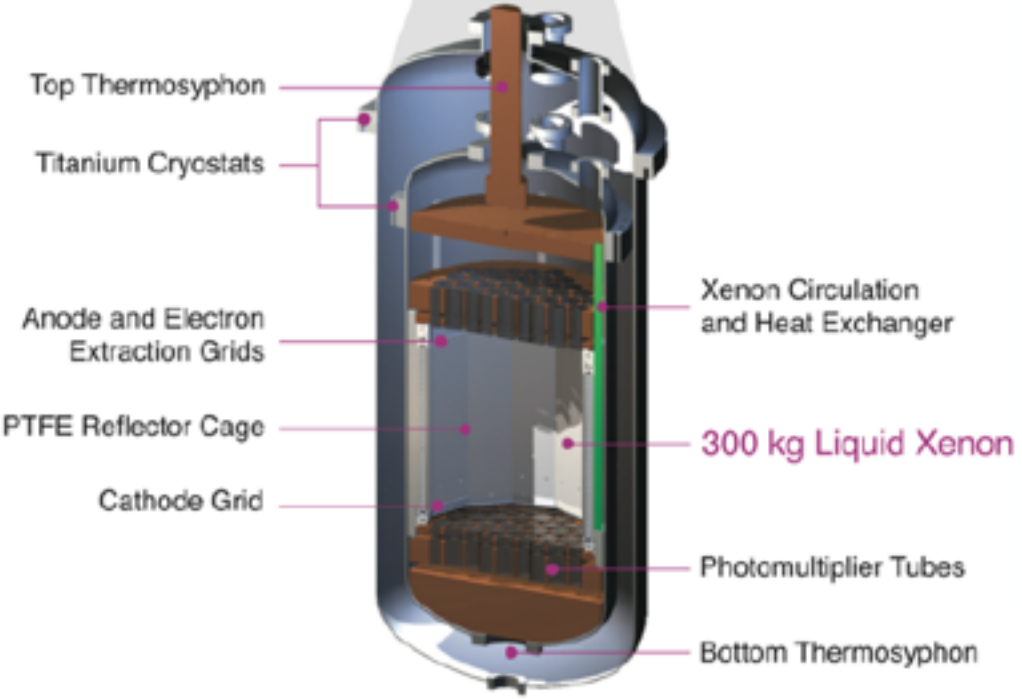
Top Thermosyphon
Titanium Cryostats
Anode and Electron Extraction Grids
PTFE Reflector Cage
Cathode Grid
Xenon Circulation and Heat Exchanger
300 kg Liquid Xenon
Photomultiplier Tubes
Bottom Thermosyphon

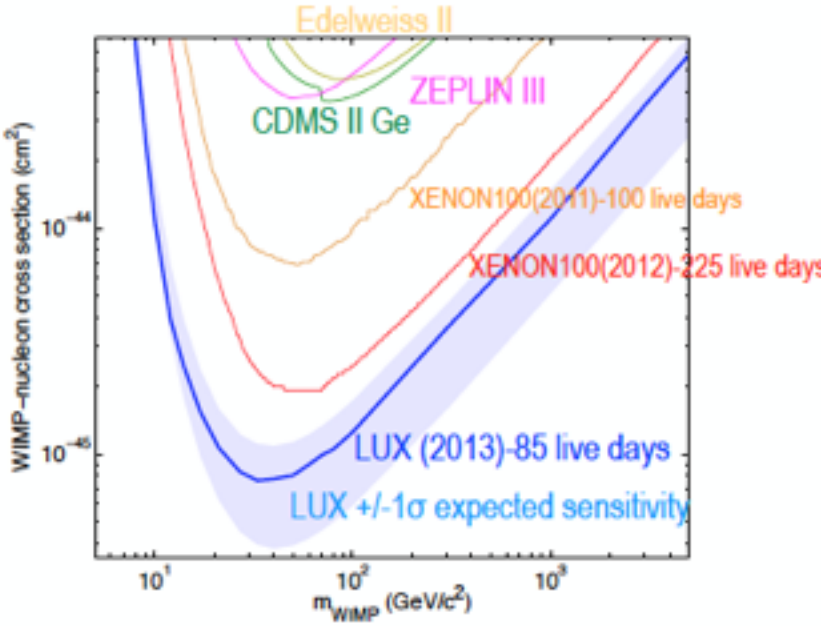
Edelweiss II
ZEPLIN III
CDMS II Ge
XENON100(2011)-100 live days
XENON100(2012)-225 live days
LUX (2013)-85 live days
LUX +/-1σ expected sensitivity
WIMP–nucleon cross section (cm²)
10⁻⁴⁴
10⁻⁴⁵
10¹
10²
10³
m_WIMP (GeV/c²)

The LUX Dark Matter Detector

- What is LUX?
  - a particle detector
  - a monolithic wallless fiducial region within 370 kg Xe TPC
  - viewed by 122 Photomultiplier Tubes
  - able to reconstruct (x,y,z) for each event
  - exceptional self-shielding from outer xenon layer
  - discrimination between electronic and nuclear recoils (99.6%)
- How would LUX see dark matter?
  - it detects scintillation photons and ionized electrons created by particle interactions
  - if dark matter interacted with a xenon atom, energy transferred to that atom would be visible to LUX
  - $\alpha_1 \sim O(0.10)$ and $\alpha_2 \sim O(10)$ are the amplification factors for each quanta
  - n_γ and n_e are the fundamental measured quantities

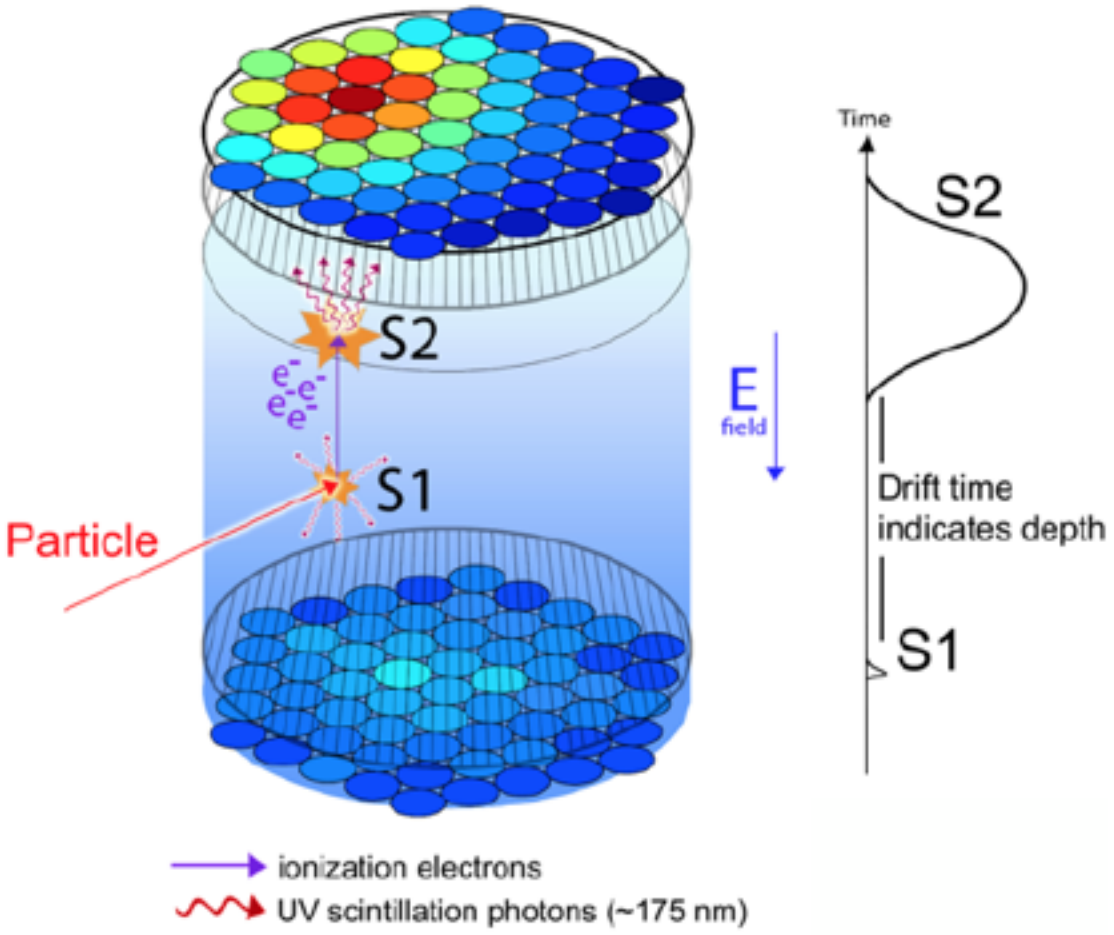

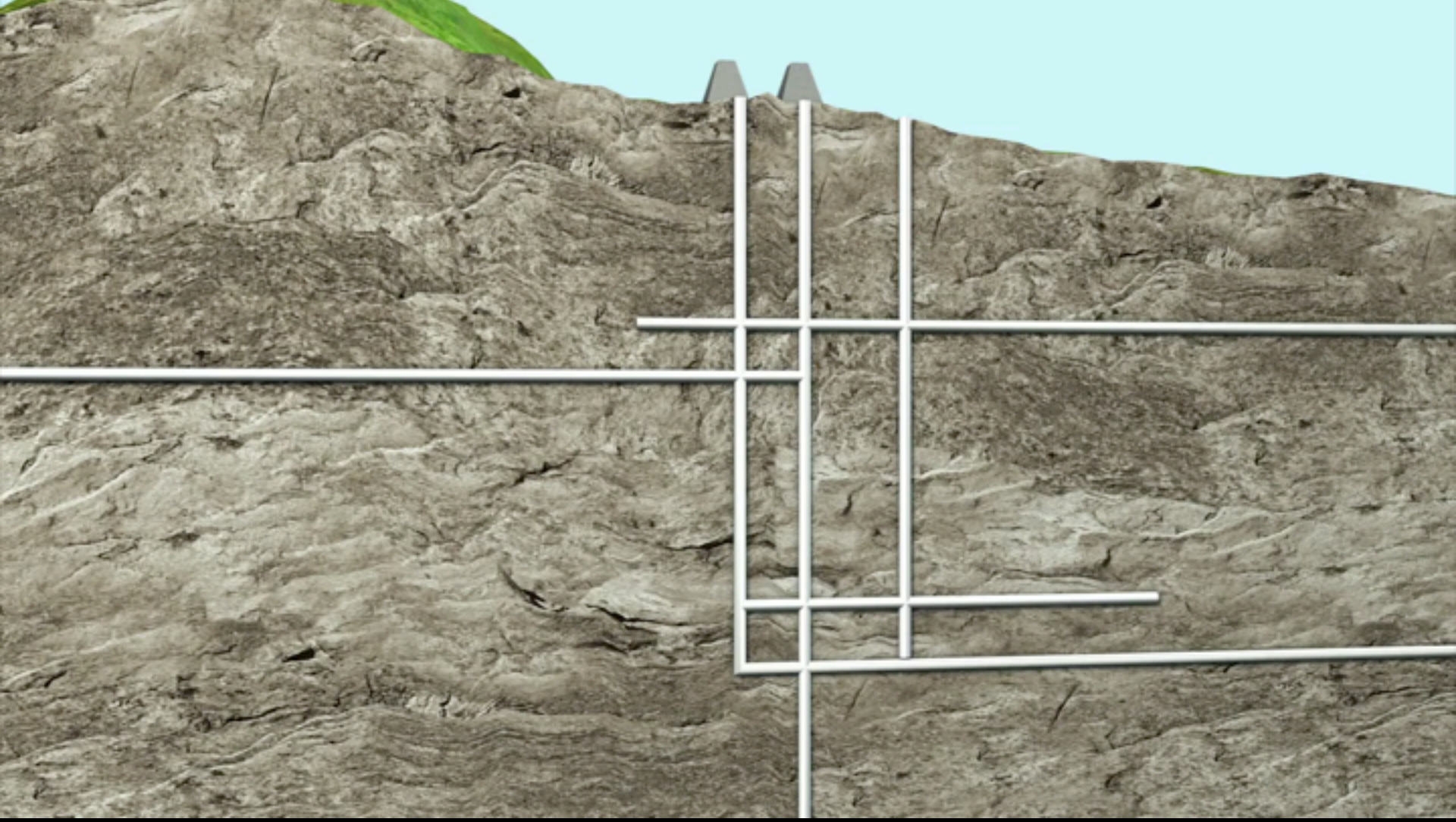

Projected LUX 300 day WIMP Search Run

- We intend to run LUX for a new run of 300 days in 2014/15
  - Extending sensitivity by another factor 5
  - Even though LUX sees no WIMP-like events in the current run, it is still quite possible to discover a signal when extending the reach
  - LUX does not exclude LUX
- WIMPs remain our favored quarry
- LZ 20x increase in target mass
  - If approved plans to be deployed in Davis Lab in 2016+

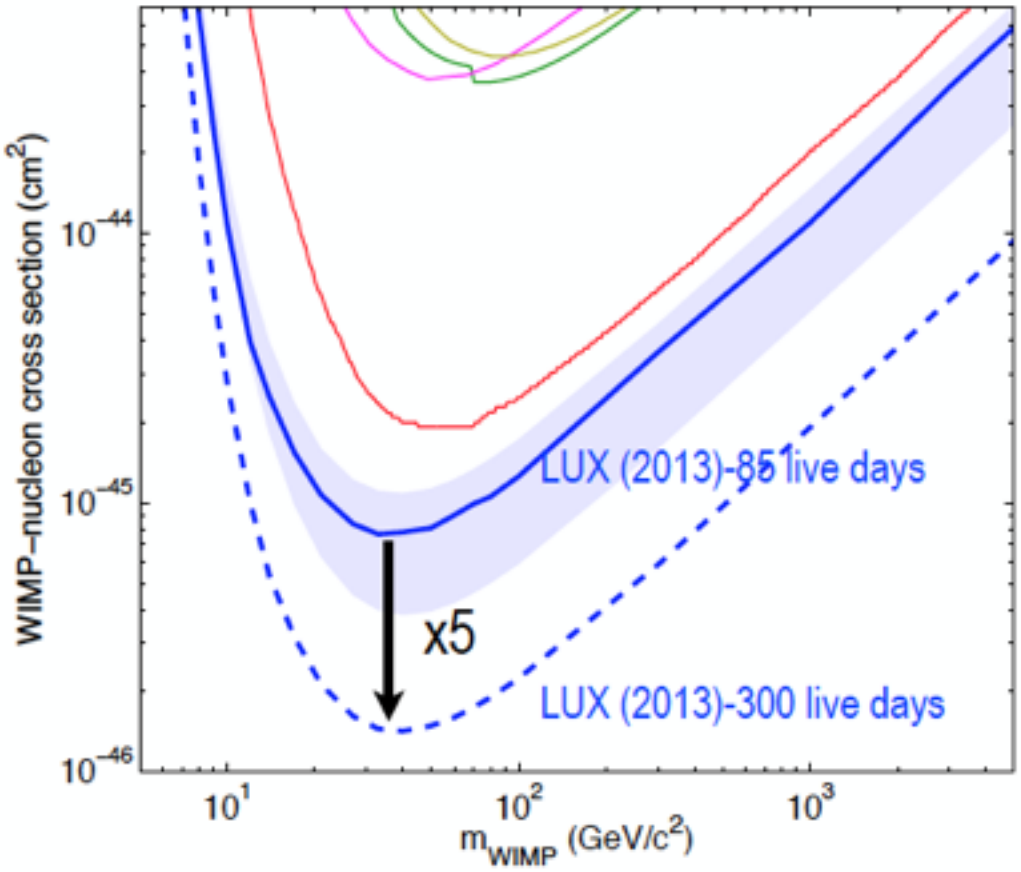

past
(2005 - 2007)

current
(2007-2012)

future
(2012-2017)

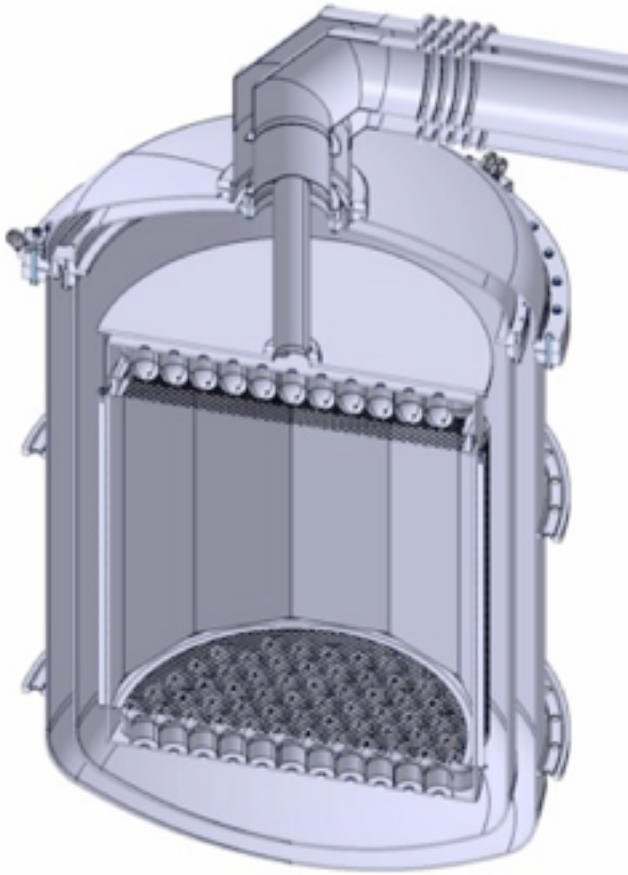

XENON10

Achieved (2007) $\sigma_{SI}=8.8 \times 10^{-44}$ cm^2

Phys. Rev. Lett. **100**, 021303 (2008)

Phys. Rev. Lett. **101**, 091301 (2008

XENON100

Achieved (2011) $\sigma_{SI}=7.0 \times 10^{-45}$ cm^2

Projected (2012) $\sigma_{SI} \sim 2 \times 10^{-45}$ cm^2

XENON1T

Projected (2017) $\sigma_{SI} \sim 10^{-47}$ cm^2

XENON100 is a collaboration including Columbia and Rice universities, University of Zurich, University of Coimbra, Gran Sasso National Laboratory, and UCLA.

XENON1T: OVERVIEW

- Detector: 1m drift TPC with 2.2 ton LXe target
- Shield: ~10 m x 10 m Water Cherenkov Muon Veto
- Background: 0.01 mdru (100 lower than XENON100
- Location: approved by INFN for LNGS Hall B
- Capital Cost: ~11 M$ (50% US and 50% non-US)
- Status: Construction start in Fall 2012
- Science Run: projected to start in 2015
- Sensitivity: 2 x 10^{-47} cm^2 at 50 GeV with 2.2 ton-years

COLUMBIA RICE UCLA PURDUE ZURICH COIMBRA

LNGS INFN MPIK BOLOGNA SJTU

MUENSTER SUBATECH NIKHEF WEIZMANN

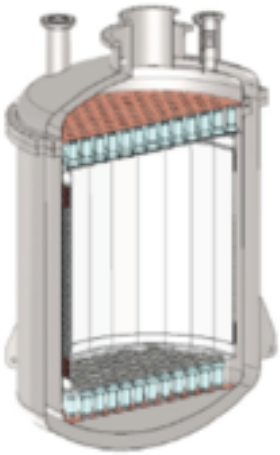

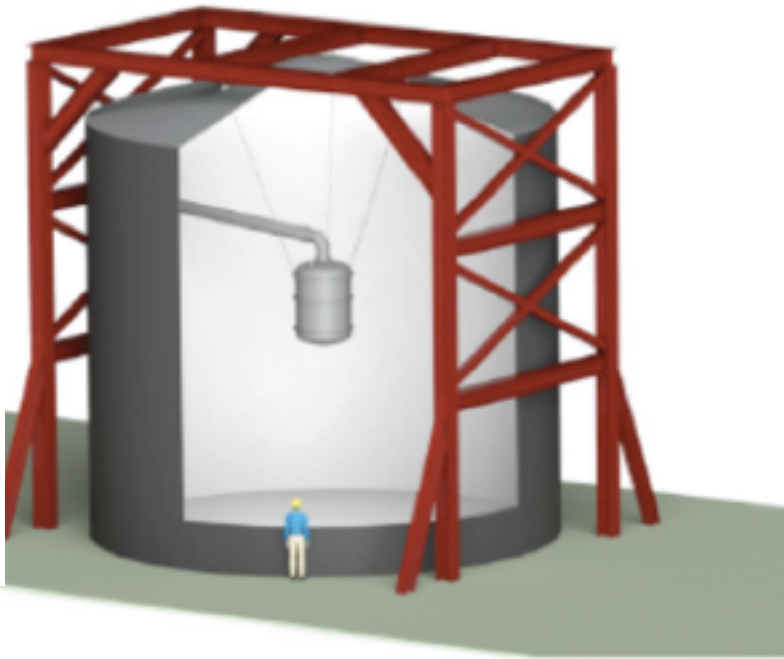

LNGS Underground Laboratory – Hall B

LNGS Underground Laboratory – Hall B

Dark Matter and Terascale Physics

V. Barger

The Gold Standard: mSUGRA

- SUSY stabilizes radiative corrections to the Higgs mass and realizes GUT unification of electroweak and strong couplings
- Weird quantum numbers of particles explained by 16 representation of SO(10)

- mSUGRA: SUSY broken by gravity
  - predictive--small number of parameters: $m_0, m_{1/2}, A_0, \tan\beta, sign(\mu)$

- Find well defined regions of parameter space consistent with the relic density from WMAP

$$0.099 < \Omega_{DM} h^2 < 0.123 \ (2\sigma)$$

- DM is associated with EWSB
  - weak scale cross section naturally gives $\Omega_{\rm CDM}$

mSUGRA parameter space

- Representative regions in mSUGRA parameter space (red points fully account for $\Omega_{\rm CDM}$)

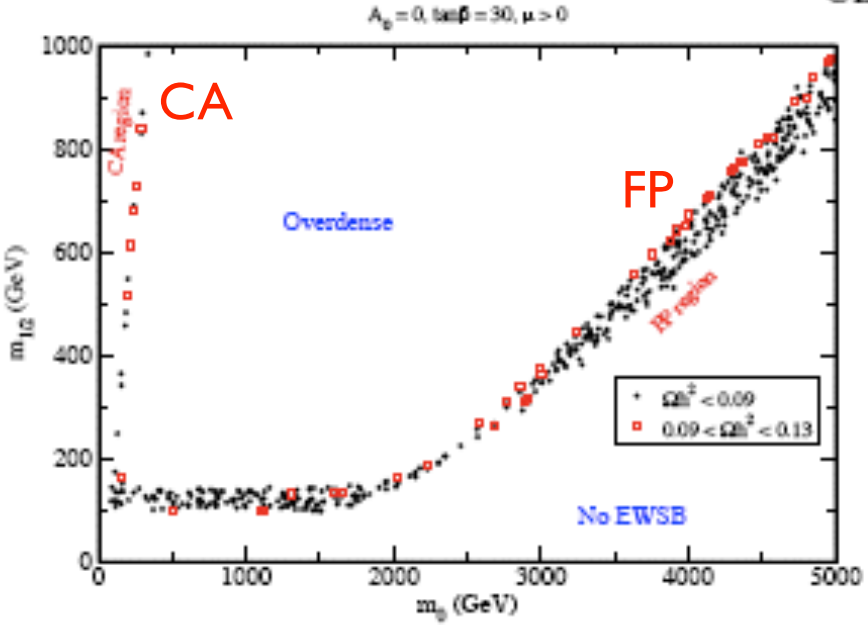

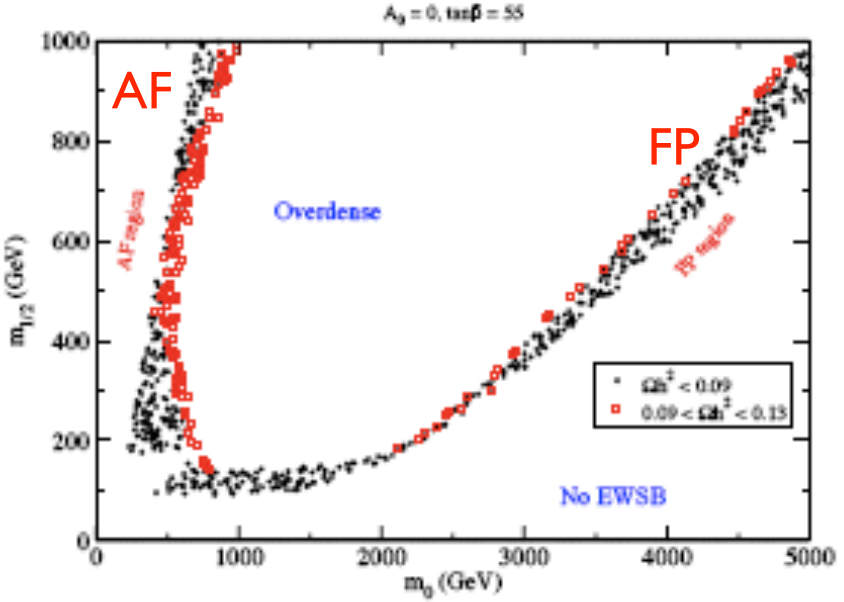

- Focus Point (FP) region: high mass scalar fermions
  - Preferred by $b - \tau$ unification
  - Solves SUSY FCNC and CP-violating problems
- A-funnel (AF) region: annihilation through CP-odd Higgs (A)
- $\tilde{\tau} - \chi_1^0$ coannihilation (CA) region
- Bulk region (BR) at low $m_0, m_{1/2}$ nearly excluded

Scattering rates in mSUGRA

- Different solutions to DM relic density populate different regions of σ_{SD} vs. σ_{SI} Spin Dependent vs. Spin Indenepdent

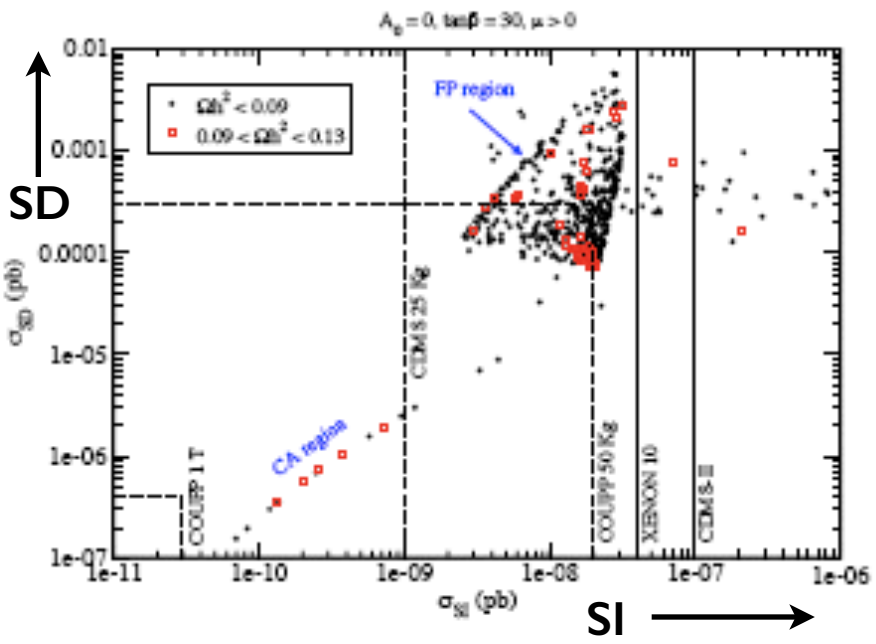

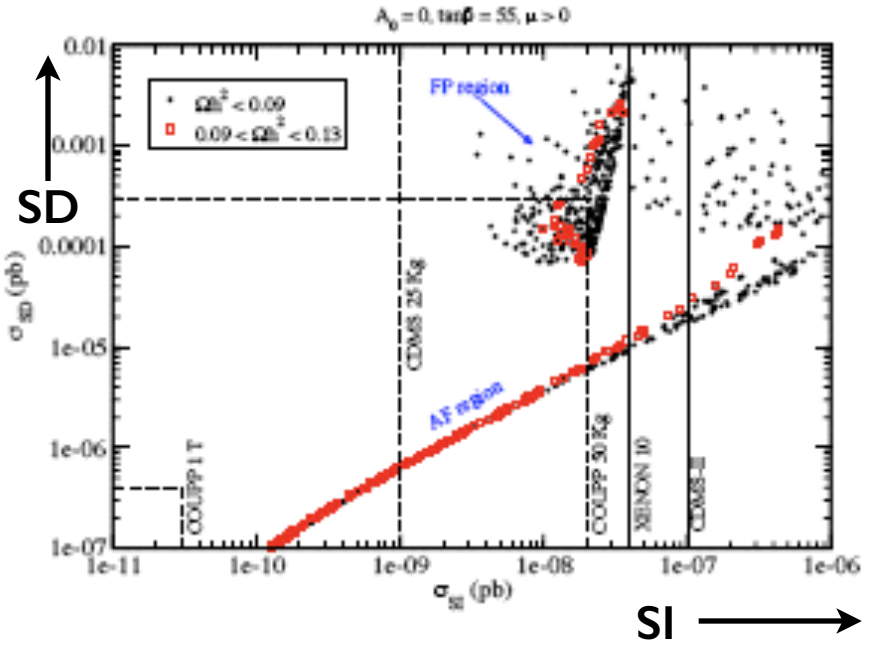

- FP region can be verified or disproved by both SD and SI measurements
- Detection in FP region would be of major significance for colliders (high mass scalars)

Scattering rates in mSUGRA

- Different solutions to DM relic density populate different regions of σ_{SD} vs. σ_{SI} Spin Dependent vs. Spin Indenepdent

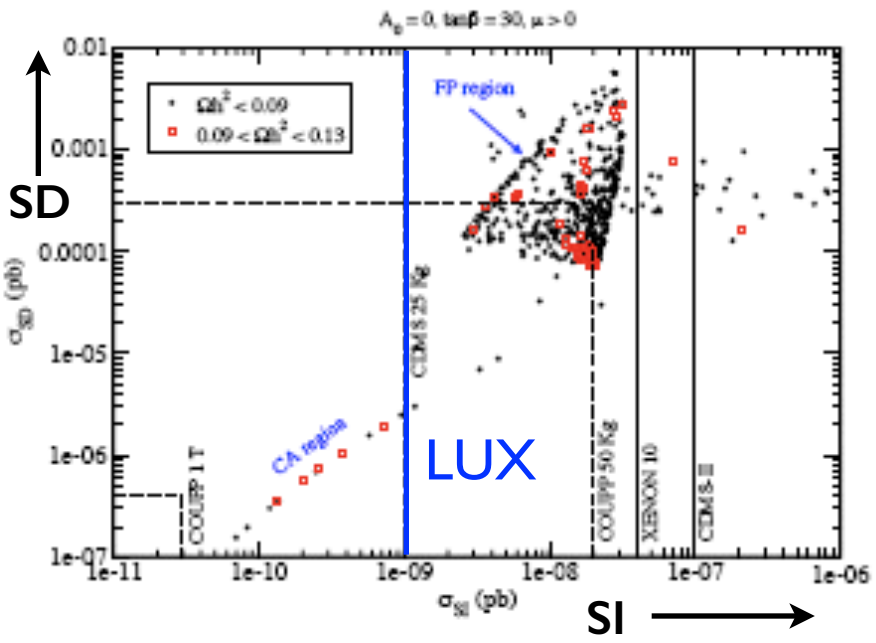

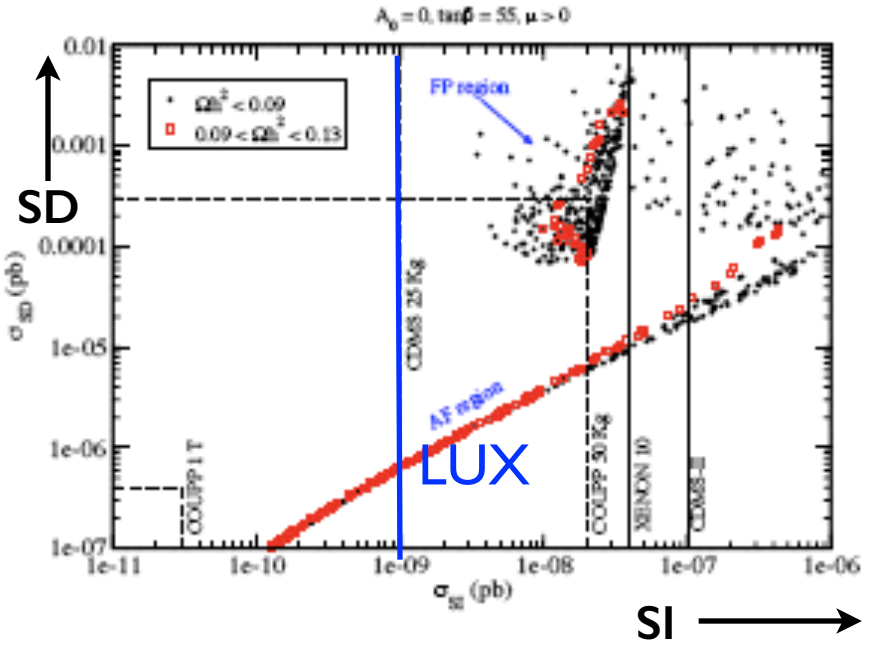

- FP region can be verified or disproved by both SD and SI measurements
- Detection in FP region would be of major significance for colliders (high mass scalars)

By ~2015 Direct Detection could probe most of the CMSSM (constrained minimal supersymmetric standard model) and mSUGRA (minimal supergravity) WIMP parameter space! If LUX and other large noble gas detectors succeed, they will leapfrog over CDMS and have great discovery potential during 2012-15.

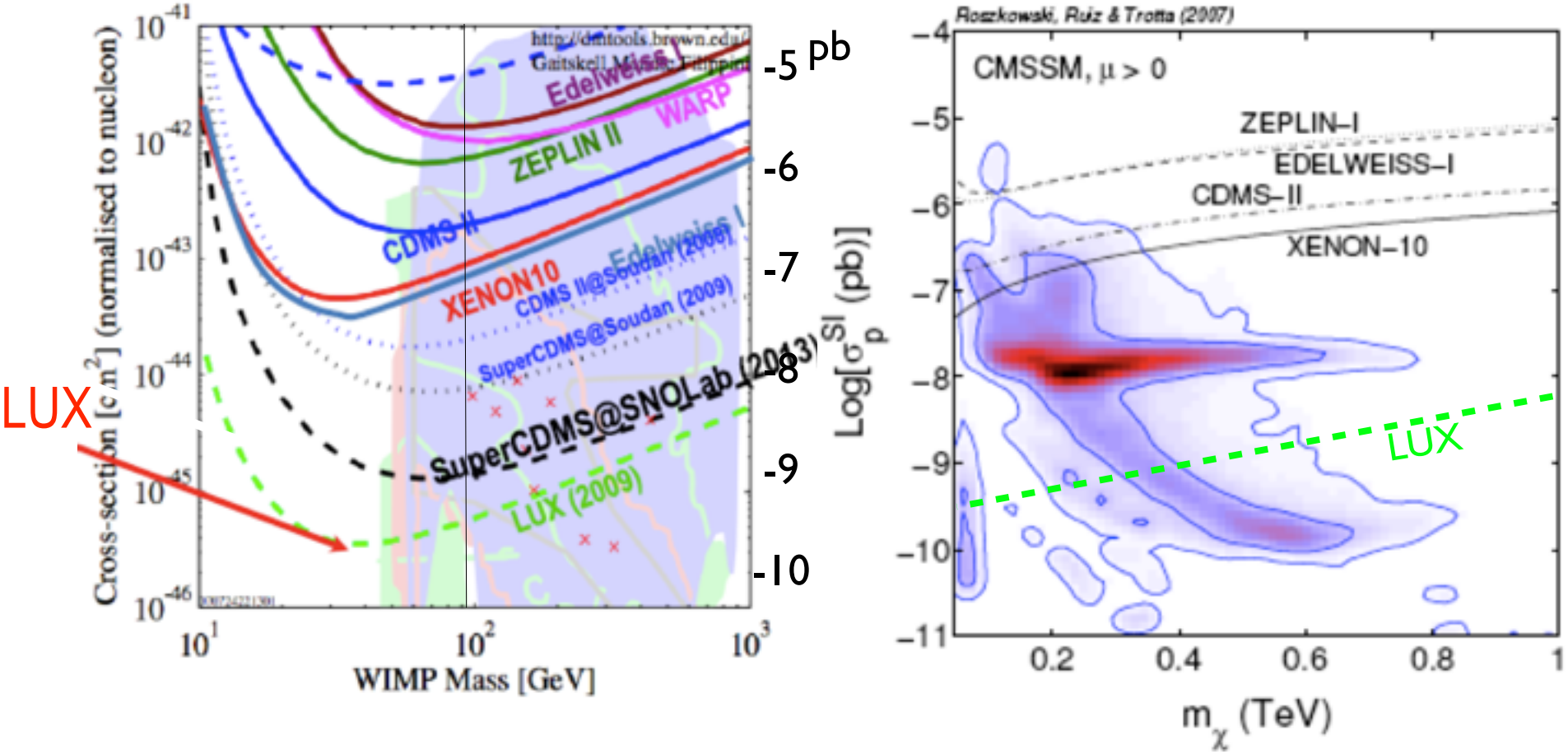

10^{-8} pb = 10^{-44} cm^2 (barn=10^{-24} cm^2, pb = 10^{-12} b = 10^{-36} cm^2)

By ~2015 Direct Detection could probe most of the CMSSM (constrained minimal supersymmetric standard model) and mSUGRA (minimal supergravity) WIMP parameter space!

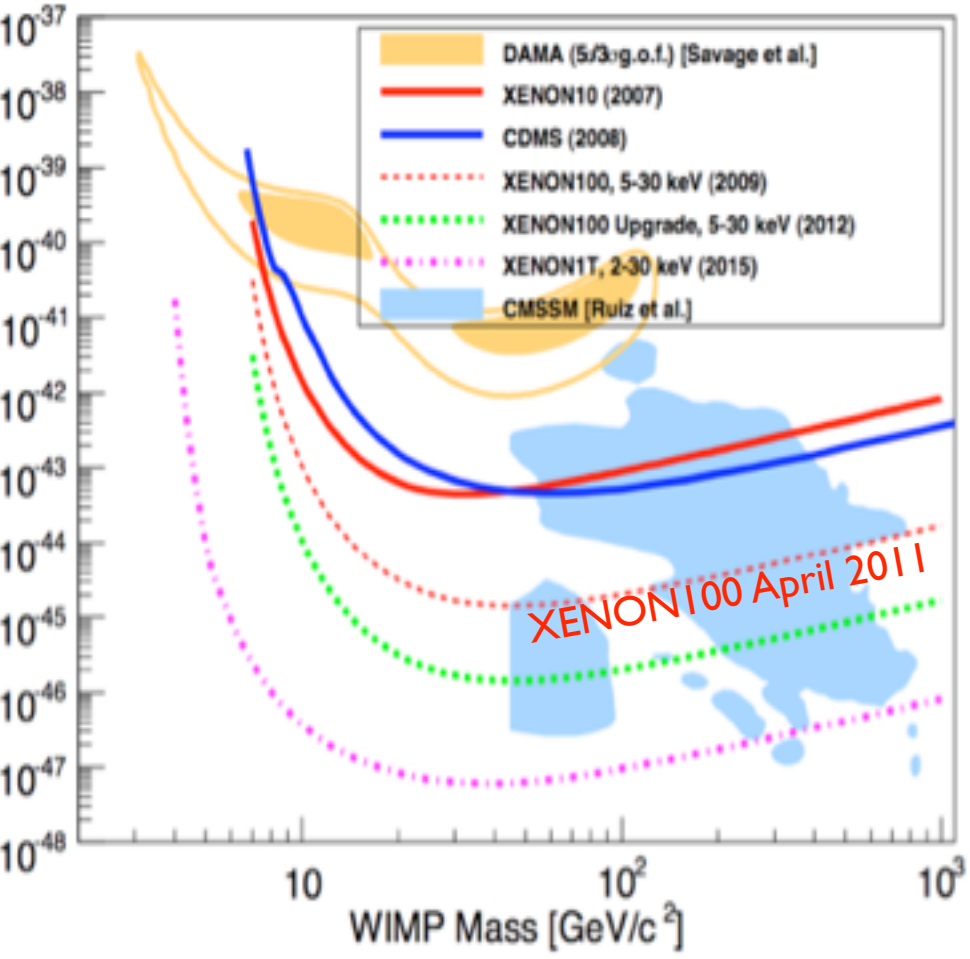

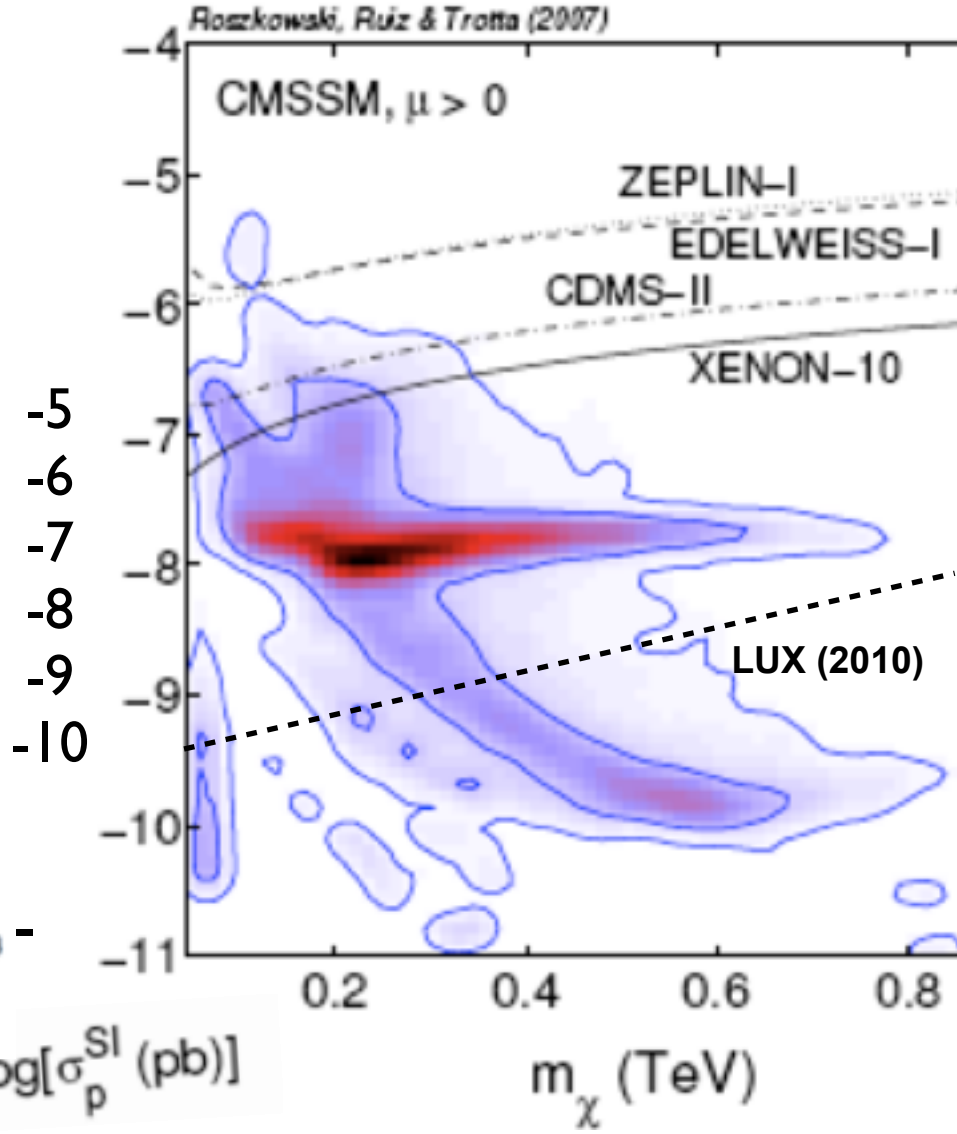

Search for Neutralino Dark Matter

Direct Method (Laboratory Experiments)

Galactic dark matter particle (e.g.neutralino)

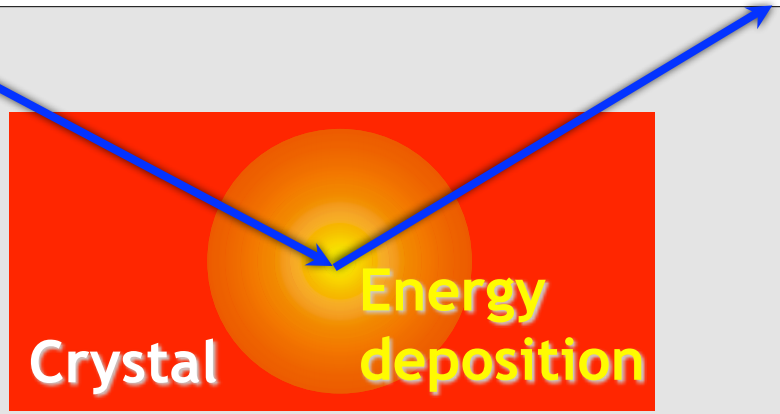

Recoil energy (few keV) is measured by

- Ionisation
- Scintillation
- Cryogenic

Indirect Method (Neutrino Telescopes)

Galactic dark matter particles are accreted

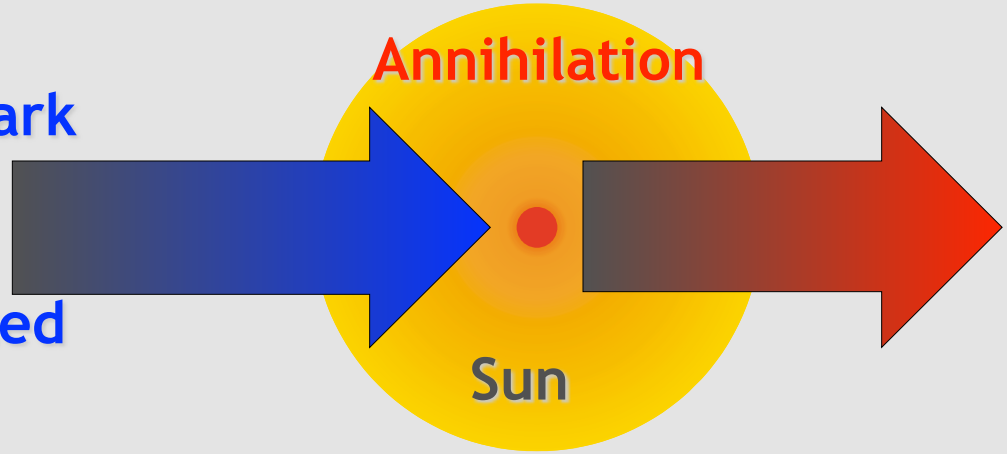

High-energy neutrinos (GeV-TeV) can be measured

DM-Ice Concept

Detector
- 250–500 kg NaI(Tl)
- Closely-packed inside pressure vessel for coincidence veto
- Two PMTs/Crystal

Location
- South Pole, ~ 2500 m deep in the ice
- Near the center of IceCube for additional veto

Pressure vessel
- Withstand > 7000 psi of freeze-back pressure
- Low-background stainless steel
- Low background copper shielding where needed

Electronics
- Pulse digitization inside the vessel
- Power from SP Station or IceCube Counting Lab
- Remotely controllable

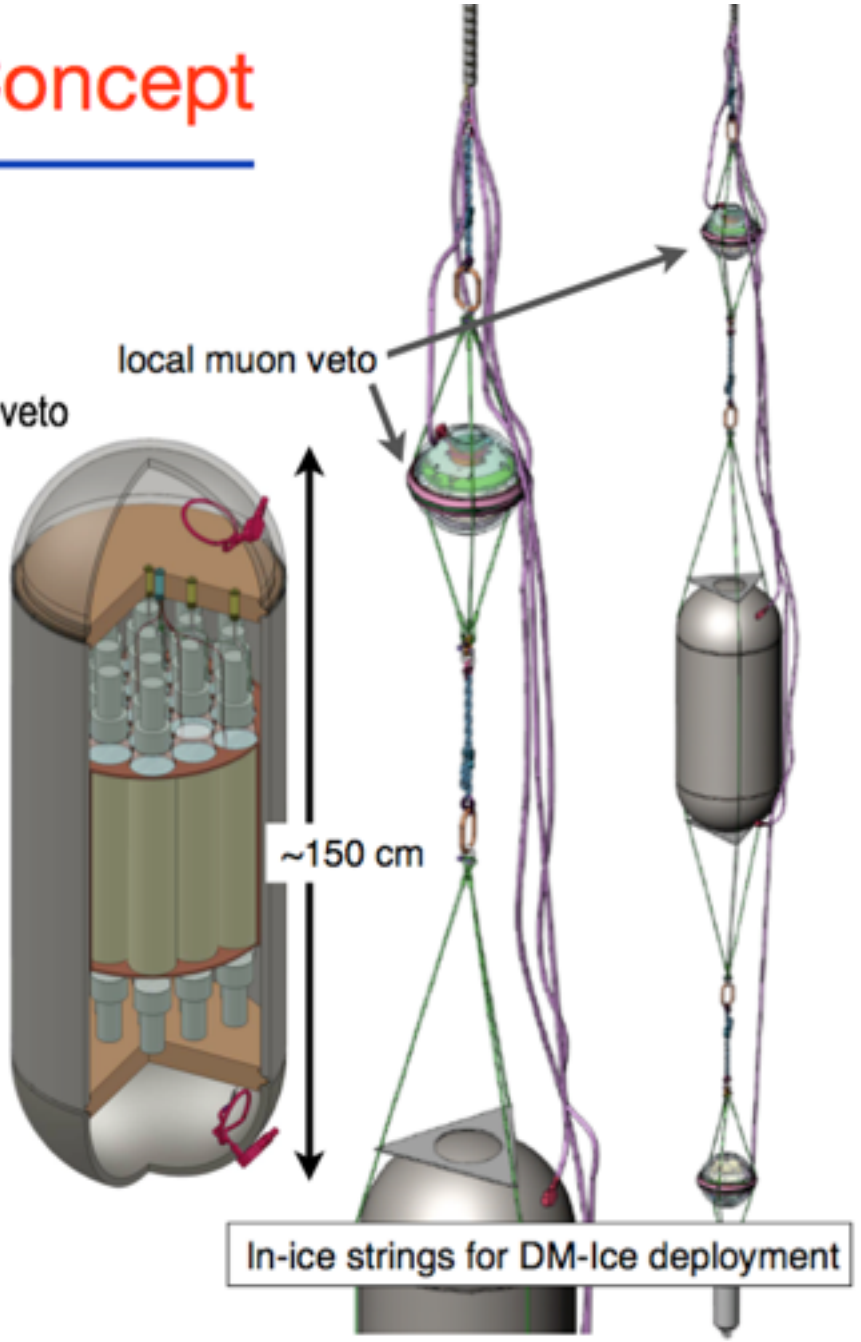

Slide from Reina Maruyma, DM2012

DM-Ice-17 (kg)

Slide reformatted from Reina Maruyma, DM2012

- 17 kg of NaI(Tl) (formerly part of NaIAD) deployed as a feasibility study at the South Pole Dec. 2010
- Continuous operation since Jan. 2011
- Data transmitted via satellite
- Analysis underway